U.PORTO

FMUP FACULDADE DE MEDICINA
UNIVERSIDADE DO PORTO

THE ROLE OF MITOCHONDRIA IN THE NON-TARGETED EFFECT OF IONIZING RADIATION

Silvana Ferreira da Silva Miranda

Mestrado em Medicina e Oncologia Molecular

Porto, 2017

Dissertação de candidatura ao grau de Mestre em Medicina e Oncologia Molecular, apresentada à Faculdade de Medicina da Universidade do Porto

The role of mitochondria in the non-targeted effect of ionizing radiation

Silvana Ferreira da Silva Miranda

Orientadora:
Professora Doutora Paula Boaventura
Investigadora Pós-Doutoramento Ipatimup/i3S

Co-orientadores:
Professor Doutor Valdemar de Jesus Conde Máximo
Professor Auxiliar, Faculdade de Medicina da Universidade do Porto
Investigador Principal. Ipatimup/i3S

Professora Doutora Anabela Dias
Professora convidada na Faculdade de Ciências da Universidade do Porto
Investigadora no Grupo de Física Médica, Radiobiologia & Protecção Radiológica (GFMRPR)

“The essence of life is not the atoms and small molecules that go into us, it’s the way, the ordering, that those molecules are put together.”

- Carl Sagan

Agradecimentos

''Caminhando se faz caminho'' e o meu fez-se com a ajuda de muitos caminhantes. Desta forma, gostaria de agradecer:

À actual direcção do programa de Mestrado em Medicina e Oncologia Molecular, na pessoa do Professor Doutor Henrique Almeida, por toda a disponibilidade demonstrada para comigo, ao longo destes dois anos.
Estendo o agradecimento à Professora Doutora Paula Soares por ter me ter acolhido no grupo de investigação, proporcionando-me todas as condições necessárias para a realização deste trabalho.
À minha orientadora, Professora Doutora Paula Boaventura, por ter aceitado trilhar este percurso comigo, por toda a disponibilidade que teve para me orientar, e por toda a ajuda que me deu no decorrer deste ano de trabalho.
Ao Professor Doutor Valdemar Máximo, meu co-orientador, que apontou o caminho a seguir e me disponibilizou as condições necessárias para este projecto.
À Professora Doutora Anabela (Bela), minha co-orientadora, por toda a ajuda dada neste demanda, todas as tardes perdidas e ensinamentos fornecidos.
Ao Serviço de Radioterapia do IPO do Porto, a todos os meus colegas de profissão.
À Lili, ao André, à Cristina e à Marina, por me pouparem as pernas (e a carteira) com as boleias para o i3S.
Ao Novalis da tarde, que soube sempre arranjar uma 'vaga' na agenda para as minhas células. Em especial, à minha Claudinha, à Ana e ao Lourenço, por toda a ajuda.
Aos meus amigos, por toda a força que sempre me deram e todas as lamúrias que ouviram.
Ao grupo Cancer Signalling and Metabolism, porque não podia estar melhor entregue. Todos os momentos, todos os ataques de riso, todas as histórias, à Cirstina, ao Jõao, ao Rui e em particular à Ana Pestana, ao Pedro (volta, estás perdoado), à Raquel e à Helena pelos ensinamentos.
Ao Marcelo, por tudo o que me ensinou sobre trabalho experimental e laboratorial; pela amizade e paciência; pela Orientação. Por ser um exemplo a seguir. Sem ele estariam, na melhor das hipóteses, a ler estas linhas em 2027.
Ao bando dos 4. Não vou ter palavras que cheguem. Sofia, obrigada por tudo. Tiago, obrigada principalmente por me teres (re)lembrado que nunca mais quero ir aos Passadiços do Paiva.
Às minhas companheiras de bancada, tese, minis, momentos de descompensação, minis, momentos de desespero ('vai ficar tudo bem!'), minis... Ana, Lili. Sem vocês isto não seria a mesma coisa, não podia ter sido melhor.
Aos meus avós pelo carinho, em especial à minha avó, que demonstra o seu afecto através da comida, obrigada por todas as 'marmitas'.
Ao Wolfgang pelo apoio e preocupação.
À minha mãe, que é e será sempre a minha inspiração na vida.

Abstract

Radiotherapy is a clinical modality dealing with the use of ionizing radiation (IR) for the treatment of cancer patients. It aims delivering a precisely measured dose to a defined volume with minimal damage to the surrounding healthy tissue. In radiobiology, the classical view of DNA as the target for radiation has been changing with emerging evidence showing radiobiological effects in cells not traversed by ionizing radiation. These effects have been described as bystander effects and the term comprises a variety of changes which emerge in cells which were not directly irradiated. These effects seem to be more relevant in low dose scenarios. Mitochondria are essential organelles for cellular homeostasis, not only for ATP production but also as intermediaries in several signalling pathways. Some authors have raised the veil of the role of mitochondria in bystander signalling by showing that the production of a bystander effect in bystander cells was not observed when the irradiated counterparts did not have mitochondrial DNA (mtDNA).

We proposed to investigate the role of mitochondria in the production of a bystander signal using an osteosarcoma cell line (143B) manipulated in order to obtain cybrids with different mitochondrial status. The cell lines used were: normal mtDNA cybrid (Cy143Bwt); a cell line with mtDNA mutated in the A3243T $tRNA^{Leu(UUR)}$ gene, characteristic of the hereditary syndrome MELAS, and a cell line without mtDNA (143B- ρ0).

We irradiated cells (with 0.2 Gy and 2.0 Gy) and characterized their response to direct IR through cellular growth, ROS production, mitochondrial membrane potential alterations, DNA double strand breaks and apoptosis. To induce a bystander effect in non-irradiated cells, we used media from irradiated cells to treat bystander non-irradiated cells, analysing DNA double strand breaks and apoptosis.

Irradiation induced an increased DNA damage in all three cell lines but increased apoptosis was not observed. Conditioned media increased DNA damage but the effect of the damage was different according to the cell line it derived: Cy143bwt irradiated with 0.2 Gy conditioned media induced more damage in Cy143Bwt, but in Cy143BMELAS, 2.0 Gy conditioned media induced more damage. Cy143Bwt conditioned media induced similar amounts of apoptosis in all cell lines. Cy143BMELAS 2.0 Gy increased damage in Cy143Bwt but it did not induce an increase in apoptosis. The response of cells to conditioned media was also different, for Cy143BMELAS showed little response to conditioned media from Cy143Bwt. No effect was observed when 143B- ρ0 conditioned media was used

These results point to a possible role of mitochondria in the radiation-induced bystander effect which upon better characterized, may be an interesting modulator of the response to Radiotherapy.

Keywords: Radiotherapy, Radiobiology, Bystander effect, Mitochondria

Resumo

A Radioterapia é uma área clínica especializada no uso da radiação ionizante no tratamento do cancro. Tem como principal objectivo a administração de uma determinada dose de radiação a um volume alvo, minimizando ao máximo a dose nos tecidos normais adjacentes. Em radiobiologia, a visão clássica do DNA como alvo primordial da radiação tem vindo a mudar, com novas evidências que mostram a existência de efeitos da radiação em células que não foram atravessadas por esta. Estes efeitos denominam-se efeitos *bystander* e compreendem uma variedade de alterações que ocorrem em células que não são directamente irradiadas, mas que de alguma forma recebem factores libertados por células irradiadas. Aparentemente, o efeito *bystander* é mais evidente no espectro das doses baixas. A mitocôndria é um organelo essencial para a homeostasia celular, não só indispensável para a produção de energia na forma de ATP, mas também como intermediária nas diversas vias de sinalização celular. Alguns autores demostraram que a mitocôndria poderá estar envolvida na transmissão de um sinal *bystander* pelas células irradiadas, uma vez que, quando estas não têm DNA mitocondrial, não são capazes de induzir um efeito *bystander* em células não irradiadas.

Propusemo-nos a estudar o papel da mitocôndria na produção do sinal *bystander* usando uma linha celular de osteossarcoma (143B), manipulada para a obtenção de cíbridos com diferentes estados mitocondriais. Foram usadas as seguintes linhas celulares: uma linha celular com DNA mitocondrial normal (Cy143Bwt), uma linha com DNA mitocondrial com a mutação A3243T $tRNA^{Leu(UUR)}$, característica da síndrome hereditária MELAS (Cy143BMELAS), e uma linha sem DNA mitocondrial (143B- ρ0).

Irradiámos as células (com 0,2 Gy e 2,0 Gy) e caracterizámos a sua resposta à radiação directa, analisando o crescimento celular, a produção de espécies reactivas de oxigéno, alterações do potencial de membrana, quebra da cadeia dupla do DNA e morte celular por apoptose. Para provocar o efeito *bystander* em células não irradiadas, irradiámos as células e retirámos o meio de cultura que foi posteriormente usado para tratar células não irradiadas (meio condicionado). Nestas células não irradiadas avaliámos a ocorrência de quebras da cadeia dupla de DNA e morte celular por apoptose.

A irradiação directa provocou dano no DNA das células, mas não induziu um aumento na apoptose. O meio condicionado aumentou o dano no DNA de forma diferente, dependendo da linha celular que lhe deu origem. O meio de Cy143Bwt irradiadas com 0,2 Gy provocou mais dano no DNA de Cy143Bwt, mas, nas Cy143BMELAS, foi o meio de Cy143Bwt irradiadas com 2,0 Gy que provocou este efeito. Os níveis de apoptose foram semelhantes aos do dano no DNA para o meio das células Cy143Bwt. Na apoptose, a resposta das células foi diferente, uma vez que o meio de Cy143Bwt não provocou alterações nas Cy143BMELAS.

O meio condicionado de Cy143BMELAS provocou uma resposta diferente nas 3 linhas celulares. Com o meio de células irradiadas com 2,0 Gy, houve mais dano no DNA relativamente às outras linhas. Com o meio condicionado de Cy143BMELAS não houve diferenças na indução da apoptose.
Células sem DNA mitocondrial não foram capazes de produzir factores que provocassem efeitos nas células não irradiadas.
Estes resultados apontam para um papel da mitocôndria no efeito *bystnander* que, quando melhor caracterizado, poderá representar um mecanismo de modulação da resposta à radioterapia.

Palavras-chave: Radioterapia; Radiobiologia; efeito *bystander*; mitocôndria;

Table of Contents

Abbreviations

53BP1	p53 binding protein 1
ADP	adenosine diphosphate
AL	Alabama
AntA	Antimycin A
ATM	ataxia-telangiectasia mutated
ATP	adenosine tryphosphate
ATR	ataxia-telangiectasia Rad3-related
Bcl2	B-cell lymphoma 2 protein
BRCA1	breast cancer type 1 susceptibility protein
BSA	bovine serum albumine
c-PTIO	2-(4-carboxyphenyl)-4,4,5,5-tetramethylimidazoline-1-oxyl-3-oxide
Ca^{2+}	Calcium ion
CDC25	cell division cycle 25
cm	centimetre
cNOS	constitutive nitric oxide synthetase
CO_2	carbon dioxide
CT	computerized tomography
CTV	clinical tumour volume
DAPI	4',6-diamidino-2-phenylindole
DDR	DNA damage response
DHE	dihydroethidium
DMEM	Dulbecco's modified Eagle's medium
DNA	Deoxyribonucleic acid
dNTP	deoxynucleotide
Drp1	dynamin-related protein
DSB	double strand break
EcoRI	*E. coli* originated endonuclease I
EMR	electromagnetic radiation
ER	endoplasmic reticulum
FBS	fetal bovine serum
FW	forward
G1	Cell cycle growth phase 1
G2	Cell cycle growth phase 2
GTV	gross tumour volume

Gy	Gray
H2AX	Histone H2A family X
HRR	homologous recombination repair
i3S	Instituto de Investigação e Inovação em Saúde
ICCM	irradiated cells conditioned media
IAEA	International Atomic Energy Agency
IgG	Immunoglobulin G
IL	interleukins
IMRT	intensity modulated radiotherapy
iNOS	inducible nitric oxide synthetase
IPO	Instituto Português de Oncologia
IR	ionizing radiation
keV	kiloelectron volt
Km	Kilometre
LDRB	low dose radiobiology
LET	linear energy transfer
Leu	Leucine
M	Mitosis
MDC1	mediator of DNA–damage checkpoint protein 1
MELAS	mitochondrial encephalomyopathy, lactic acidosis, and stroke-like episodes
min	minutes
MRI	magnetic resonance imaging
MRN	Mre11-Rad50-Nbs1
mtDNA	mitochondrial DNA
mRNA	messenger RNA
MU	Monitor Units
MV	megavoltage
NF-kB	nuclear factor k B
NHEJ	non-homologous end joining
NIH/3T3	3-day transfer, inoculum 3×105 cells
NO	Nitric oxide
NTE	non-targeted effects
$O^{\cdot -}$	superoxide
OAR	organs at risk
OF	output factor

$OH^{\cdot}$	Hydroxide ion
OXPHOS	oxidative phosphorilation
PBS	phosphate buffered saline
PCR	polymerase chain reaction
PDD	percentage depth dose
PES	polyethersulfone
PET	positron emission tomography
PFA	paraformaldehyde
PI	propidium iodine
PI3K	phosphatidylinositol 3-kinase
PIKK	protein kinases
PTV	planning target volume
RB	radiobiology
RBE	Relative Radiobiological Effectiveness
RIBE	radiation-induced bystander effects
RNA	ribonucleic acids
RNS	reactive nitrogen species
ROS	reactive oxygen species
rRNA	ribossomic RNA
RT	radiotherapy
RV	reverse
S	Cell cycle DNA synthesis phase
SOD	superoxide dismutase
SSB	single strand break
SSD	source-surface distance
TLR-9	Toll-like receptor family
tRNA	transfer DNA
UAB	University Alabama Birmingham
UL12.5	Herpes Simplex protein
USA	United States of America
VMAT	volumetic arc therapy
WT	wild type
µm	micrometre
ρ0	Rho 0

Figures index

Tables index

Chapter 1

Introduction

1. Introduction

Throughout the course of time, bits and pieces of answers to the infinite number of questions man has been asking since the dawn of time rise to the surface. As each piece of a puzzle is added to the whole, patterns slowly begin to emerge. A single piece grows into multiple pieces, multiple pieces grow into entire sections, revealing previously unseen or unknown possibilities. And, when enough pieces are connected, a picture is revealed and an answer to an ancient question is found.

1.1 Radiotherapy

1.1.1 Radiotherapy – an Historic perspective

William Conrad Roentgen was a German engineer and physicist. He was interested in the properties of cathode rays and experimented several types of vacuum tube equipment.
As he noticed a fluorescent effect on a small cardboard screen painted with barium platinocyanide, he further tested it with a Hittorf-Crookes tube, completely covered with light-tight cardboard. He continued to observe the flickering light and, to his amazement, the light came from a barium platinocyanide screen which was not even in the apparatus he had set up, but on a bench, a few feet away from the experiment. He wondered if he was in the presence of a new kind of rays and started using the mathematical designation ‘’x’’, for an unknown variable (Bernier, Hall, & Giaccia, 2004).

He continued his work testing various materials for their ability to stop the rays, and concluded that lead was the only viable option. Interestingly, the lead test was the base for the first radiography ever taken: the lead left an impression on a photographic film so he asked his wife to use her hand on a film placed at the end of the tube (Figure 1).

Figure 1 - *The first radiography ever taken.* William Roentgen wife's hand, Anna Bertha Ludwig. Public domain via Wikimedia Commons

Riding the wave of excitement from Roentgen's discovery, Becquerel thought that phosphorescent materials, such as some uranium salts, might emit X-ray-like radiation. In 1896 (Becquerel, 1896) he described that uranium salts emitted radiation with properties very similar to the radiation studied by Roentgen. He stated: '*the uranium salts emitted [phosphorescence] not only when the substances are exposed to light but even when they are kept in darkness, (…) shielded from all the exciting radiation known.*'' He postulated that the effect was due to the presence of uranium and that the metal would have a much stronger effect (Becquerel, 1896).

At the end of 1900, Friedrich Giesel, working with Friedrich Walkoff, at the first German company producer of radium sources, described the strapping of 270 mg of radium salt to his inner forearm for a duration of two hours.

Becquerel's radium burn, often reported as "accidental", was, in fact, an experiment conducted after learning about Walkoff and Giesel's own test. He and Pierre Curie, credited the two Germans in their report of self-exposure measurements with radium (Curie & Becquerel, 1901) (Figure 2). Among other aspects, they described the effects on their hands of handling the tubes or capsules containing radioactive substances.

Interestingly, less than 60 days after the X-rays discovery, clinical radiotherapy (RT) was born – Emil Grubbé treated an advanced breast cancer with X-Rays in January 1896, in Chicago (Grubbé, 1949).

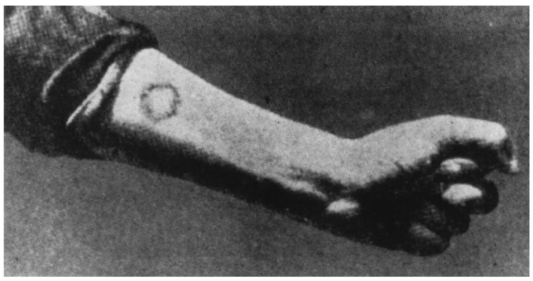

Figure 2 – *Pierre Currie's self-inflicted skin reaction to a radium source exposure* (Curie & Becquerel, 1901; Dutreix, Tubiana, & Pierquin, 1998). Used with permission.

In 1904, Jean Bergonié and Louis Tribondeau studied the effects of radiation on the testis. They observed that irradiation induced azoospermia three weeks after exposure. Additionally, cases of oligospermia and sterility were observed in men who had engaged in work with Roentgen-rays (X-rays) (Upton, 1992).

Claudius Regaud, an experimented histologist who was investigating in the same field, added his interpretation to Bergonié and Tribondeau's findings, stating that the mitotic phase was the point of lesser resistance of the cell. The intensity of the effects was greatest on the spermatogonia and decreased as the cells became more differentiated; thereby, extreme sensitivity of spermatogonias would lead to sterelization. His findings showed the importance of radiation effects in healthy tissues and in malignant tumours. Bergonié and Tribondeau, with Regaud's input, postulated the famous law ''*the Law of Bergonié and Tribondeau"* (Vogin & Foray, 2013) still in use.

Regaud continued to study radio-physiology throughout the first half of the 20th century and his contributions were important to the establishment of RT as a medical speciality (Foray, 2012).

1.1.2 Radiotherapy – Key Concepts

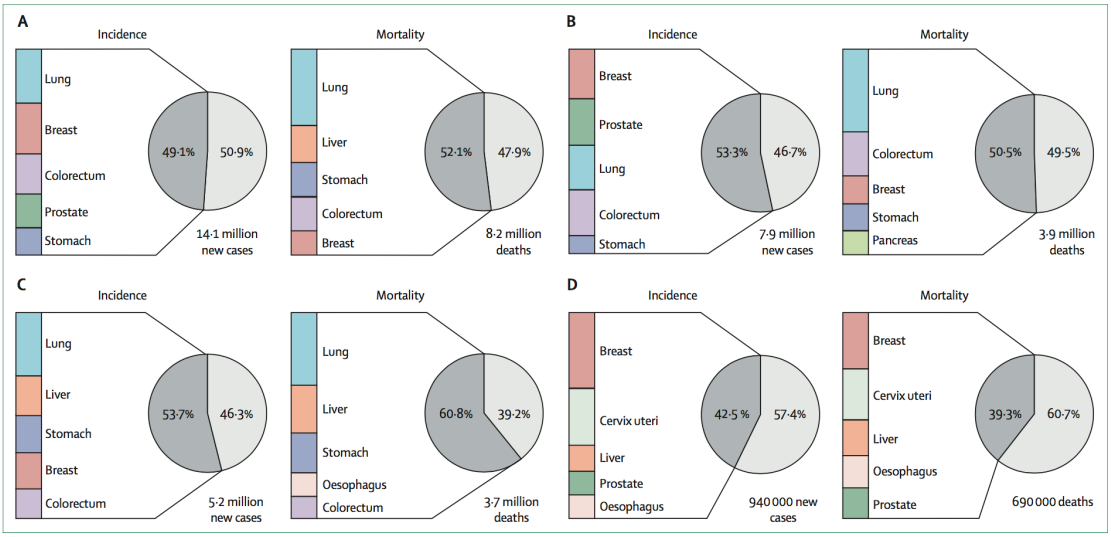

Figure 3 – *Total incidence of cancer and mortality in 2012, worldwide*. A, B, C and D represent the percentage of cancers in the very high, high, medium and low incidence countries according to the Human Development Index (HDI), respectively (Atun et al., 2015). The dark grey portion of the chart represents the top five cancers for each group. Used with permission.

According to several reports (Ferlay et al., 2015; Torre et al., 2015), there were 14.1 million new cases of cancer worldwide in 2012, and this number was projected to reach 24.6 million in 2030. In the same year, 18.2 million cancer deaths were recorded, a figure which was estimated to rise to 13.0 million by 2030 (figure 3).

RT is a comprehensive and integrated part of cancer control, and due to its broad application in several stages of treatment (curative, adjuvant, neoadjuvant, palliative) approximately half of patients with cancer benefit from its use (Barton et al., 2014; Borras et al., 2016) (Table 1).

Table 1 – Radiotherapy utilization rate and outcome benefits for top cancers globally by incidence. Adapted from Atun *et al.* (Atun et al., 2015)

	Radiotherapy utilisation rate (%)	*5-Year local control benefit (%)*	*5-Year overall survival benefit (%)*
Breast	87	15	2
Colorectal	19	5	2
Head & Neck	74	34	20
Lung	77	9	6
Prostate	58	25	1

Generally, the most usual description of Radiotherapy is delivery of a certain dose of radiation to a planned target volume, with minimal consequence to the surrounding tissues, namely critical organs which could be severely damaged by ionizing radiation (IR) (Perez, Carlos;

Bradly, 2008). The irradiation can be delivered using external beams of radiation generated by several types of sources.

The most common sources are linear accelerators (called linacs) which use electricity to accelerate electrons up to a certain velocity and, therefore, energy (Figure 4, box 1). The final IR beam can consist of electrons or, by making them collide into a metallic target (Figure 4, box 2), a beam of X-Rays can be produced (Rosenberg, 2008).

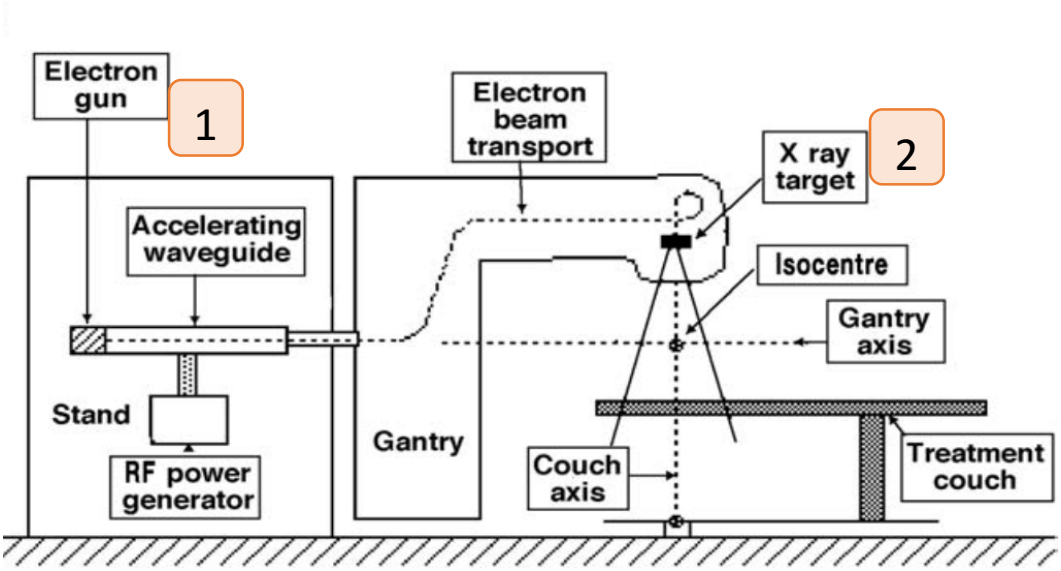

Figure 4 – *Schematic view of a linear accelerator* (linac) depicting its primary beam production mechanisms and treatment conditions. Adapted from Rosenberg (Rosenberg, 2008) © International Atomic Energy Agency (IAEA)

The treatment dose can be delivered in a localized manner with the use of radioactive sources. Brachytherapy (from the Greek *brachy* which means short distance) consists of the application of radioactive seeds directly into the tumour or tumour bed, giving it a high dose while minimizing the dose to the organs at risk (OAR) in its vicinity.

The delineation of volumes, using the computerized tomography (CT) and other complementary diagnostic means (such as functional positron emission tomography – PET or Magnetic Resonance Imaging - MRI) is one of the most important steps in the flowchart of a RT treatment (Figure 5, box 1) (ICRU, 2010).

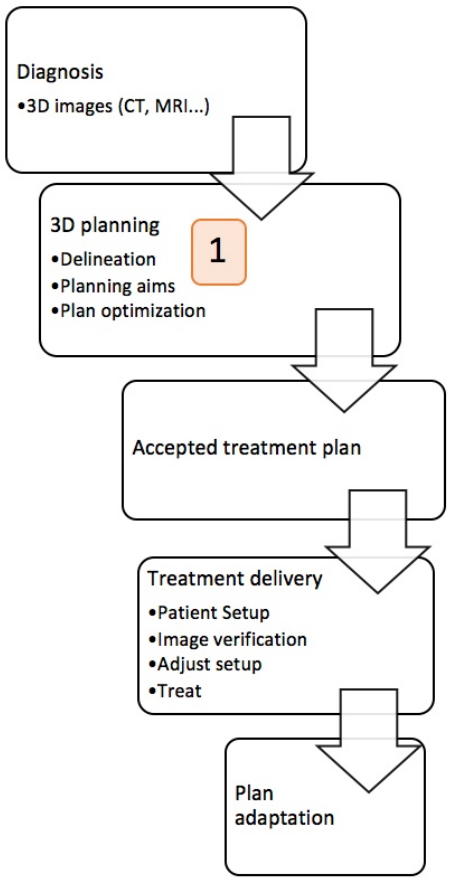

Figure 5 – *Flowchart depicting the major steps of a radiotherapy treatment*. Adapted from ICRU 83 Report (ICRU, 2010). Used with permission.

Firstly, the volume is delineated based on the size of the tumour. A margin is added to this Gross Tumour Volume (GTV) to include any subclinical disease which could be present. GTV gathered with the subclinical margin is considered the Clinical Target Volume (CTV) (Figure 6, box 1). Additional margins are needed to account for any internal movement (Figure 6, boxes 3 and 4). The CTV and these additional margins are the Planning Target Volume (PTV). The treatment planning is thereby optimized around the PTV (Figure 6, scenario A) (Landberg et al., 1999).

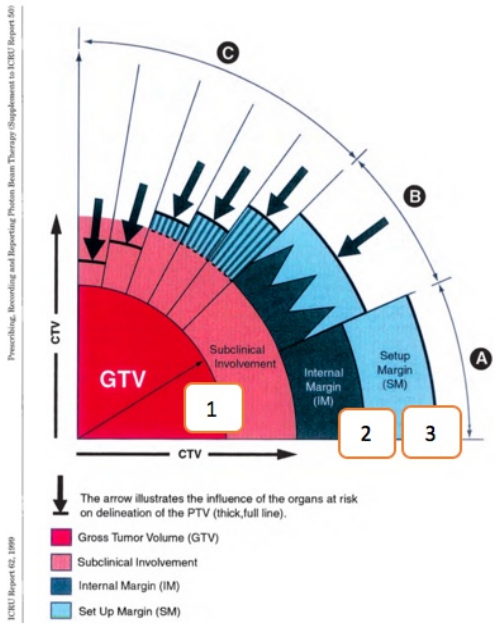

Figure 6 – *Schematic representation of the relations between the different volumes* in different clinical scenarios, from ICRU 62 Report (Landberg et al., 1999). Used with permission.

The objective of a RT treatment can be a radical, adjuvant, neoadjuvant or palliative intervention. Conventionally, the dose delivery is divided into daily amounts, five days a week.

In the last decade, RT suffered a great technological evolution, especially with the introduction of CT imaging, and with the so-called 3D dose planning (Figure 5, box 1).
Dose delivery was also greatly improved with the use of Intensity Modulated Radiation Therapy (IMRT) which consists on the use of physical treatment field conditions (such as position, collimators, dose rate) to create dose gradients within the PTV (Figure 7). It offers the great advantage of dose escalation within the PTV, and lowering the dose in the OAR.

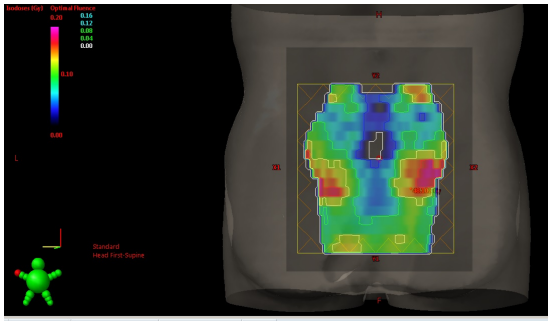

Figure 7 – *Modulation of the dose in a IMRT treatment*. The scale on the left corner represents the colour gradients of the dose observed in the treatment field (yellow square box). Areas in red receive more dose. Courtesy of IPO-Porto Radiotherapy department.

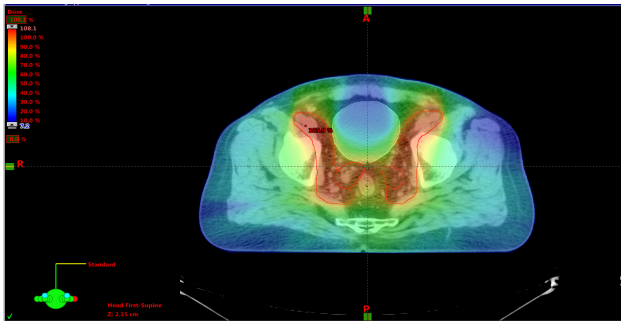

Figure 8 – *Volumetric Arc Therapy (VMAT), and low dose regions.* Axial cut of the planning CT of the pelvis is represented. Delineated in red is the PTV; the scale on the left up-corner represents the percentages of the total dose (in this case 46 Gy) received by the various body regions. Courtesy of IPO-Porto Radiotherapy department.

However, in order to optimize the plan, there is an increase in the volume of the patient that receives lower doses (Figure 8) (Higby et al., 2016). In the past few years there has been a considerable interest in Low Dose Radiobiology (LDRB). Mothersill *et al.* in 2002 (Carmel Mothersill, Seymour, & Joiner, 2002) addressed the hypersensitivity of cell lines used in radiobiology (RB) studies (C. Short, J. Kelly, C. R. Mayes, M., 2001) to investigate the phenomena by which, low doses of IR (below 1 Gy) diminished cells clonogenicity compared with what was to be expected extrapolating from the response to higher doses. More recently, William F Morgan and William J. Bair discussed, in a revision paper, the controversy in LDRB field (for instance, what is considered low dose) (Morgan & Bair, 2013). Sykes acknowledge that the lack of a standardized approach is one of the major issues in LDRB (Sykes, 2016). As Mothersill and Seymor claimed, one of the drawbacks could be that many experiments were focused only in one endpoint at a time, suggesting that a more encompassing methodology, such as system biology, could be an exciting approach (Carmel Mothersill & Seymour, 2013).

1.2 Radiobiology

When a biological material is irradiated it suffers a deposition of energy. This may lead to an *excitation* or to an *ionization.* Briefly, when an electron from an orbital of an atom or a molecule passes to a higher state of energy we are in the presence of an excitation. If the electron is ejected from its orbital, the atom or molecule suffers an ionization. In this scenario, the radiation is an ionization, in other words, it has enough energy to break chemical bonds (Alexander, 1957). IR is considered the most important type of radiation in RB, giving its capacity to damage biomolecules (Hall, Higgins, Giaccia, & Willson, 2012)

IR can directly or indirectly ionize depending on its capacity to produce the chemical/biological damage:

- ◊ It can have such a kinetic force that will *directly* induce damage as it passes through the material, ionizing the atoms in its way.
- ◊ It can be absorbed into the material traversed, giving up energy to particles already present which, *indirectly*, produce the damage.

Most electromagnetic radiation (EMR) ionizes indirectly. In contrast, radiation resulting from particle decay is directly ionizing.

EMR has virtually no mass, behaving both as an electrical and a magnetic wave, with an energy which depends on its wavelength. Interestingly, it can also be considered as a stream of photons which travel in a wavelike manner. The energy of a beam of photons is given by the formula:

$$E = \frac{hc}{\lambda}$$

where h is Planck's Constant, c is the speed of light, and λ is the wavelength of the radiation (Hall et al., 2012).

Photons are absorbed by the material they traverse and this process depends on their energy and on the chemical composition of the absorbing material. For high energy radiation, the photons interact with the electrons of the material which are less bond to their nucleus, giving them energy in the form of kinetic energy. The electron is ejected from its original place and the photon continues moving, defected from its path, interacting with the other atoms on its way. In the end, the result is the production of many fast electrons which can ionize other atoms which in their turn break bonds and produce biological damage (Dunn, Campbell, Fram, & Hutchins, 1948). As will be discussed later, the Deoxyribonucleic Acid (DNA) is considered the primary target of the damage induced by ionizing radiation, as it is essential for the normal functioning of a cell (Lomax, Folkes, & O'Neill, 2013a).

IR damage can be classified as direct or indirect. When IR interacts with biological materials, it can directly ionize the atoms of the critical target (for instance, DNA) and directly initiate the chain of events leading to damage. This is considered the direct action of IR. On the other hand, it can ionize other molecules, most importantly water, producing free radicals such as hydroxyl ($OH^{\bullet}$) or other reactive oxygen species (ROS) that will damage the critical target. In fact, the majority of the damage to DNA, in mammalian cells, is caused by indirect action, via $OH^{\cdot}$ (Desouky, Ding, & Zhou, 2015). The probability of the occurrence via direct or indirect interaction depends on the density of the ionizations – for highly ionizing radiations, the direct mode of interaction predominates over the indirect and *vice versa*. Depending on the damage,

the biological effect has different time scales, ranging from hours to years or even generations (Hall et al., 2012).

When radiation is absorbed, the pattern of occurring ionizations depends on the type of the radiation, if it is EMR or particulate radiation. A unit defined to describe the *average energy* deposited (absorbed) along a length of material is the Linear Energy Transfer (LET), expressed in kilo-electron volt per micrometre (keV/μm). There are high LET radiations and low LET radiations. High LET radiations deposit a large amount of energy over a small distance; on the contrary, low LET radiations deposit less amount of energy along the track, or have infrequent or widely spaced ionizing events (Landberg et al., 1999). A summary of high and low LET examples of radiations is presented in Table 2.

Table 2 – Examples of IR (low and high LET) used in the clinical setting

	Low LET radiations	***High LET radiations***
Examples of ionizing radiations	x-rays γ-Rays	α-particles protons

The *quantity* of radiation is expressed as an absorbed dose, which represents the energy absorbed per unit of mass of the irradiated material; Gray (Gy) is the unit used.
Relative radiobiologic effectiveness (RBE) is the ratio of biological effectiveness of one type of ionizing radiation relative to another, given the same amount of absorbed energy (ICRP, 2003). LET affects the RBE, given that a dose of a high LET radiation has a different biological consequence than the same dose of a low LET radiation (Hall et al., 2012).

1.2.1 DNA damage

As mentioned before, DNA is one critical target for biological effects of radiation. A dose of 1-2 Gy will produce, on average, 1000 single strand breaks (SSBs) and 40 double strand breaks (DSBs) (Hall et al., 2012). DSBs are considered the most important type of lesion caused by radiation as they can lead to cell death or mutations (Jeggo & Löbrich, 2007).
The particle's energy is absorbed by the material in a non-uniform way, creating clusters of damage. These clusters are usually bigger than the diameter of the DNA helix, increasing the probability of occurrence of DSBs. High LET radiations lead to more clusters, closer to each other, and with higher probability to cause damage (Brenner & Ward, 1992; Lomax et al., 2013a).

The DNA Damage Response (DDR)

Cell cycle comprises a sequence of events which lead to the duplication of cellular contents and consequential division in two cells. It is divided in 4 phases: G1, S, G2 and M. Growth period 1 (G1) phase, is the one where cellular growth mainly occurs. At a given point during G1, cells became committed to cell division entering in synthesis (S) phase, which consists on the doubling of DNA content. Cells progress through the cycle moving to a second growth period (G2) phase, which prepares them for the final stage of the cycle, mitosis (M). These events are highly controlled via checkpoints which 'check' if conditions necessary for progression to the next phase are met (Alberts et al., 2007). If these conditions are not fulfilled, cell cycle stops.

DDR involves a complex signalling network which begins with sensing damage, and leads to transmission of signals to transducers which will then signal effectors, with the objective of halting cell cycle and repairing the damage (Hall et al., 2012; Shiloh, 2001).

In the sensors category, we find proteins like Mre11-Rad50-Nbs1 which form the MRN complex, p53 binding protein 1 (53BP1), breast cancer type 1 susceptibility protein (BRCA1), and mediator of DNA–damage checkpoint protein 1 (MDC1) (Canman & Lim, 1998). Briefly, the first sensor arriving at the site is the MRN complex, which binds to chromatin and phosphorylates H2AX histone variant in the 139-serine residue. Phosphorylated H2AX (γH2AX) is fundamental for the binding of other factors, such as MDC1 and 53BP. MDC1 is essential for the maintenance of MRN and 53BP1 bond to the damage site. This supports a more recent view of DDR, which refuses a hierarchy of events and rather considers it as a cyclic, interdependent process, amplifying the damage signal (Shiloh, 2006).

Two of the transducers attracted to the damage foci belong to phosphatidylinositol 3-kinase (PI3K)-like protein kinases (PIKKs) family and possess the PI3K domain motifs: the nuclear protein kinase ataxia-telangiectasia mutated (ATM) and the ataxia-telangiectasia Rad3-related (ATR). The former seems to be more relevant in other types of DNA damage, such as replication errors (Shiloh, 2001). ATM acts as transducer for several downstream effectors (many still being revealed) but, in the DDR context, it triggers the activation of cell cycle checkpoints. It activates the G1/S checkpoint *via* the p53 pathway and the G2/M checkpoint *via* the cell division cycle 25 phosphatases (CDC25), enabling the repair mechanisms to come into action (Figure 9) (Branzei & Foiani, 2008; Shiloh, 2001).

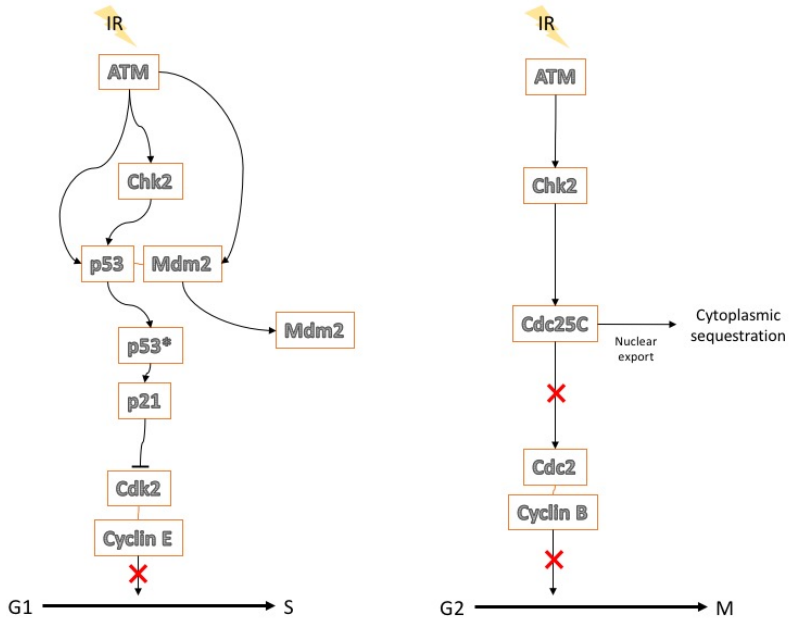

Figure 7 - *Control of cell-cycle checkpoints by ATM following DNA damage*. On the left, The G1/S check point: p53 activation and stabilization in response to DSBs occurs through a series of post-translational modifications mediated directly and indirectly by ATM. ATM-activated Chk2 activates other pathways which lead to additional p53 modifications, and phosphorylates the principal mediator of p53 degradation, Mdm2, thereby achieving tight control of p53 activation and stabilization. On the right, The G2/M checkpoint: activated ATM phosphorylates Chk2. G2 arrest is mediated primarily by subsequent inactivation of Cdc25C, whose phosphatase activity normally activates the cyclin-dependent kinase Cdc2 and enhances entry to mitosis. Adapted from Yosef Shiloh (Shiloh, 2001).

Cell cycle and Radiosensitivity

Following irradiation, DNA damage triggers signalling to activate cell cycle checkpoints, allowing time for repair to occur. G1 checkpoint prevents the replication of damaged DNA, while G2 checkpoint averts segregation of abnormal chromosomes (Hall et al., 2012).

Cells have complex mechanisms of signalling and repairing DNA strand breaks which vary according to the type of the damage and to the stage of the cell cycle.

In eukaryotic cells, DSBs are repaired either by homologous recombination repair (HRR) (Jasin & Rothstein, 2013) or by nonhomologous end-joining (NHEJ) (Hefferin & Tomkinson, 2005). HRR is error free – it uses the sister chromatid as a template for producing a new copy. HRR can occur in S and G2 phases of the cell cycle (Hall et al., 2012). In G1, as there is no sister chromatid to use as template, HRR does not occur. Instead, NHEJ is used – a mechanism prone to error (Figure 10). In M phase, the chromosomes are aligned to be separated making repair difficult. Therefore, M phase is considered the most sensitive phase of the cell cycle (Hall et al., 2012).

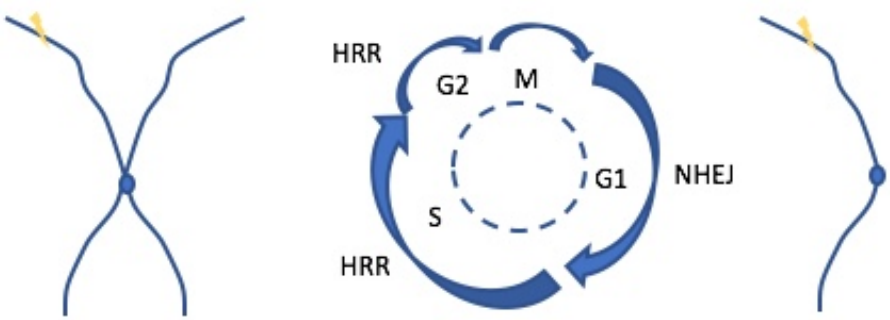

Figure 8 - *Repair mechanisms according to the cell cycle phase*. On the left, during phases S and G2, sister chromatid is available to serve as template for the repair mechanisms. On the right, during G1, damaged DNA has to be repaired without template. Adapted from Eric Hall (Hall et al., 2012).

1.2.2 Non-targeted effects

Other than the targeted effects described above, there is evidence pointing to an 'out-of-field' response to radiation, generally defined as 'non-targeted effects' (NTE).

In the first paper that was considered pivotal in this area, Nagasawa and Little (1992) (Nagasawa & Little, 1992) irradiated a cellular population with α-particles, assuring that only about 1% of the cells were traversed by the radiation. Unexpectedly, they observed that about 30% of the population presented increased chromosomal anomalies. Somehow, cells must have communicated with each other, spreading the restricted expected response (1% of the cells) to a broader one (30% of the cells). This experiment challenged the radiobiology dogma – damage would only occur if the DNA was damaged by the radiation.

Many studies carried out in the field of the NTE have their own definition of effect (Table 3), according to the endpoint tested (Blyth & Sykes, 2011). In broad terms, NTE includes any effect occurring in a cell which was not exposed to radiation but that somehow received a signal from an exposed cell. The unirradiated cells receiving these signals are considered bystander cells and the change observed in them is considered to be a Radiation-Induced Bystander Effect (RIBE) (Carmel Mothersill & Seymour, 2006). In the literature, there is not a clear definition of this phenomena (Baverstock & Belyakov, 2010).

Table 3 – Examples of various definitions for the bystander effect. Adapted from Blyth *et al.* (Blyth & Sykes, 2011)

Definitions of Bystander Effects	***Review that proposes it***
…the induction of biological effects in cells that are not directly traversed by a charged particle, but are in close proximity to cells that are	Ballarini *et al.* (Ballarini, Biaggi, Ottolenghi, & Sapora, 2002)
… biological responses in cells that were not traversed by an ionising radiation track, and, thus, not subject to direct energy deposition; that is, the responses occur in non-irradiated cells. These bystander effects take place in the neighbours of irradiated cells or in other non-irradiated cells that have received signals from neighbouring or distant irradiated cells	Feinendegen *et al.* (Feinendegen, 2003)
…effects occurring in cells that were not traversed by radiation but were induced by signals from irradiated cells. Bystander cells in exposed cell populations can be described as the non-irradiated cells that have received signals from neighbouring or distant irradiated cells	NCRP Report No 136 (National Council on Radiation Protection and Measurements, 2001)
…[a] response, in which non-exposed cells neighbouring an exposed cell respond	John B. Little (J. B. Little, 2006)
… damage that occurs in cells that were not traversed by radiation but were in the same radiation environment; i.e., they were "bystanders" at the time of the irradiation	Carmel Mothersill and Colin Seymour (Carmel Mothersill & Seymour, 2001)
… the detection of responses in unirradiated cells that can reasonably be assumed to have occurred as a result of exposure of other cells to radiation	Lorimore *et al.* (Lorimore, Coates, & Wright, 2003)

In the present work, we decided to use this most common definition of RIBE (Prise & O'Sullivan, 2009):

- When a cell that was not directly irradiated responds to some kind of factor(s) released by irradiated cells (*bystander signals*) it is a *bystander cell* and the response is considered a *bystander effect.*

The implications that RIBE may have on RT and cancer risk remain to be fully determined. LDRB has developed an interest in RIBE, since RIBEs are considered more relevant in the low dose range of IR. Currently, there is the notion that a low dose threshold exists, above which the bystander effects saturate, and the consequences of radiation exposure will be the ones expected with higher doses (Kadhim et al., 2013). This is important for RT, giving the increased areas that receiving low doses of IR following planning optimization, (Figure 8). Radioinduced neoplasias are an important consequence of IR, increasingly relevant in the present therapeutic context, with improved survival for many cancer patients (Newhauser & Durante, 2011).

Nevertheless, RIBE have also been implied in the directly irradiated regions, within the modulated field of treatment (Figure 7). Several reports suggest signalling emerging from high doses region of the PTV which contributes to tumour control (Karl T. Butterworth et al., 2011; Claridge Mackonis et al., 2007). This could have an impact on clinical decision regarding tumour margins, as well as reforcing the innovative notion of a biological margin (K. T. Butterworth, McMahon, Hounsell, O'Sullivan, & Prise, 2013). Moreover, incorporation of this kind of biological data in the planning system may significantly enhance the normal tissue

complication and tumour control predictive models, which usually only take into account the physical constraints of dose distribution.

Radiation effects on health are not strictly limited to carcinogenesis. There are other health implications. Particularly, cardiovascular or ophthalmic co-morbidities are well studied and enhance the importance of bystander signalling and response in the IR exposure context (Morgan & Sowa, 2015).

Bystander effects

It has been relatively well established that the effects occurring in non-irradiated cells receiving signals from irradiated cells mimic those happening in directly irradiated cells.

These have been classified as damaging or protective. Under the damaging category we have effects of genomic instability (Lorimore et al., 2003), micronuclei formation (Morgan, 2012), reduced clonogenic survival (Oth Ersill & Seym R, 1997). In the protective scenario, there are reports of cellular differentiation and apoptosis, where the removal of damaged cells protects the 'system' form carcinogenesis (Lyng, Seymour, & Mothersill, 2002; Najafi, Fardid, Hadadi, & Fardid, 2014).

Bystander signalling

The response to bystander signalling by non-irradiated cells is better characterized than the bystander mechanisms produced by the irradiated cells.

Bystander effects are a response to a stimulus received in the bystander cell. Accumulated proof from *in vitro* studies indicates two modes of transmission of the bystander signals: by direct communication channels between cells (gap junctions) (Calì et al., 2015) or by the secretion of factors by the irradiated cell to the medium – Irradiated Cells Conditioned Medium (ICCM) (Herok et al., 2010; C Mothersill & Seymour, 1997). The nature of the bystander signal or signals is yet to be described. Early investigations used the media transfer method and tried to sieve the possible candidates by physically manipulating the ICCM. By heating, freezing and filtering with different filter sizes a heat sensitive molecule was proposed (C Mothersill & Seymour, 1997; Nagar, Smith, & Morgan, 2003). ROS, reactive nitrogen species (RNS), inflammatory cytokines, calcium, oxidised DNA fragments, exosomes are some examples that fall under these specificities and have, therefore, been proposed as possible bystander signalling factors.

- ROS and RNS

ROS have long been implicated in the radiation induced damage, as previously stated in this work. In fact, Narayanan and colleagues showed that ROS production was an initial biological response of cells when traversed by α-particles (Narayanan, Goodwin, & Lehnert, 1997). Lenhert *et al.* confirmed this using an antioxidant like superoxide dismutase (SOD) which reduced the induction of chromosome damage in cells treated with cell-free medium obtained from irradiated cells (Lehnert & Goodwin, 1997). Yang *et al.* showed the same using X-rays, demonstrating that this phenomena is, apparently, independent of the type of radiation used (Yang, Asaad, & Held, 2005).

Nitric oxide (NO) is an important molecule for several cellular pathways involved in homeostasis, namely in the inflammatory response or in signalling mechanisms in the cardiovascular system (Strijdom, Chamane, & Lochner, 2009). NO is generated by different forms of nitric oxide synthase (NOS), depending on the stimulus. It is lipophilic, relatively stable and can diffuse through plasma membranes and through the cytoplasm (Strijdom et al., 2009). The activity of inducible NOS (iNOS) and constitutive NOS (cNOS) has been demonstrated in the context of radiation response and has also been correlated with the induction of DNA DSBs and genomic instability, both in directly irradiated (Kevin Leach, Black, Schmidt-Ullrich, & Mikkelsen, 2002) and bystander cells (Yakovlev, 2015).
Radiation is known to induce an inflammatory-type response (Gorbunov et al., 2000). With this premise, Shao and collaborators investigated whether NO could be a possible bystander signalling molecule using glioma cells irradiated with microbeams (Shao, Stewart, Folkard, Michael, & Prise, 2003). The levels of NO increased in 40% of the cells when only 1% was directly hit. There was also a cytotoxic effect on non-irradiated cells treated with the medium collected from these irradiated cells. Both events were diminished when the irradiated populations were treated with a NO scavenger, 2-(4-carboxyphenyl)-4,4,5,5-tetramethylimidazoline-1-oxyl-3-oxide (c-PTIO).

- Cytokines chemokines and other inflammatory markers

Cytokines, typical molecules of an inflammatory response, are also involved in NTE.
Irradiated cells not only have increased levels of ROS and RNS, they also release pro-inflammatory interleukins (IL) such as IL-6 and IL-8 (Chia et al., 2007; Narayanan, LaRue, Goodwin, & Lehnert, 1999), which recruit inflammatory cells to the site, like macrophages. On their own, macrophages produce ROS and other IL, leading to an increase of the oxidative pro-inflammatory environment, further increasing the probability of damage (Kidane et al., 2014).

The key pathway connecting the immune-like response to IR seems to be the nuclear factor k B (NF-kB) pathway. NF-kB is a transcription factor, usually found inactive in the cytoplasm. Upon stimulus, NF-kB is activated and enters the nucleus, binding to DNA and triggering the synthesis of messenger ribonucleic acids (mRNA), promoting cell survival, proliferation, angiogenesis and adhesion. Several factors can act as NF-kB inducers, such as inflammatory cytokines, hypoxia, and DNA damage. Consequently, it has also been proposed as a candidate in the bystander signalling.

- Calcium

Calcium (Ca^{2+}) is a very important mineral used by biological systems. It regulates several cellular processes with quick and long-time responses (Berridge, Bootman, & Roderick, 2003). The levels of Ca^{2+} in different cellular compartments are a result of the ratio between the number of bio-reactions which introduce Ca^{2+} into the cytoplasm and its removal by several systems, namely specialized pumps (Santo-Domingo & Demaurex, 2010).

Its role as a bystander signal is not yet clear, but some findings point to the importance of Ca^{2+} fluxes as a radiation response trigger. Shao and colleagues showed that cells receiving ICCM have peaks of Ca^{2+} fluxes as quick as 30s after the addition of the media. Interestingly, this effect was absent when the irradiated cells were treated with a NO scavenger, suggesting a connection with this stress signalling molecule (Shao, Lyng, Folkard, & Prise, 2006). In a similar way, another group proposed a role for both NO and Ca^{2+}: when irradiated cells were treated with NO scavengers and inhibitors of mitochondria calcium uptake, there was a reduced induction of DNA damage in the bystander cells (Chen et al., 2008). These findings point to a correlation between stress signalling by NO, somehow dependent of Ca^{2+}. Thereby, Ca^{2+} is not the signal molecule *per se* but may be an important link in the chain of events inducing the release of signals.

- Oxidative DNA Damage

Cells exposed to a certain degree of damage can undergo apoptosis. Recently, it has been demonstrated that these cells release their oxidized DNA (which becomes extracellular DNA) into the cell media (Ermakov et al., 2013). This oxidized DNA molecules have signalling properties, interacting with the oxidized DNA receptors on bystander cells that sense the oxidized DNA, such as the transmembrane proteins of the Toll-like receptor family (TLR9), responsible for detecting foreign DNA, viral or bacterial, and initiating an inflammatory response (Barber, 2011). The following pathway leads to the activation of NF-kB pathway and, consequently, synthesis of ROS and NO by the cell. Assuming that apoptosis is one of the responses observed in bystander cells, it is conceivable that more oxidized extracellular DNA

will be released, increasing the bystander effect. This has been suggested as a type of body-wide stress signal (Ermakov et al., 2013).

- Exosomes

Exosomes are a type of extracellular vesicles secreted by the majority of cells. They are formed inside the cell and released to the extracellular environment through the fusion of the vesicular bodies into the plasma membrane (Vlassov, Magdaleno, Setterquist, & Conrad, 2012). Their primary function is the transportation of cargo from one cell to others. Therefore, exosomes may contain proteins, micro RNA molecules, and long non-coding RNAs. Due to their cargo, exosomes are able to modify the function of the cell recieving them, and they have been associated with various pathological conditions, such as cancer (Peinado et al., 2012). In the IR setting, it has been suggested that exosomes might modulate the communication of radiation effects between cells irradiated and not irradiated, bringing forth their possible role as a type of bystander signalling (Kumar Jella et al., 2014). Corroborating this, Arscott *et al.*, showed that exosomes from irradiated glioma cells promote the migration of recipient glioma cells (Arscott et al., 2013). Mutschelknaus *et al.* demonstrated that exosomes from irradiated squamous head and neck cancer cells transmit pro-survival factors promoting resistance to IR (Mutschelknaus et al., 2016).

Abscopal effects

Considered in some cases a distinct form of NTE, different from RIBE due to its wide range of action, are the abscopal effects. First described by R. J. Mole (Mole, 1953), abscopal effects stand for the effects in other tumours observed after RT to a localized tumour (for instance, metastasis), distant from the irradiated target.

These effects could have great impact in the clinical outcome in cancer treatment. They are believed to work *via* two main pathways, either eliminating or delaying the growth of out-of-field tumours, or increasing genomic instability in distant normal tissues. These gave rise to two kinds of concerns, either improvement of RT treatments to take advantage of the killing potential of the abscopal effects or the increased risk of secondary malignancies (Siva, MacManus, Martin, & Martin, 2015).

Abscopal effects are believed to be mediated by factors released from the irradiated tumour or normal neighbouring tissues through immune system modulation. Inflammatory cytokine activation has been demonstrated in association with distant organ effects and diminished by the use of SOD or the NO species inhibitor, indicating a role for these signalling molecules (Khan, Van Dyk, Yeung, & Hill, 2003).

It is clear that abscopal effects may be both beneficial in terms of tumour control and harmful in terms of normal tissue toxicity yet the mechanisms of these effects are multifactorial and complex in nature.

Summing up, it seems plausible that the bystander signalling is part of an integrated complex response to stress, which is used to alert and improve adaptation of the cellular population in order to maintain cellular homeostasis.
Radiation therapy for cancer is usually considered to be simply a local treatment modality, however, there is clinical evidence of longer-range effects that render this conceptual simplicity misleading. Further understanding of the mechanisms underlying NTE may lead to novel therapeutic targets taking advantage of the cell signalling mechanisms, and improve radiation response, either in tumour control or in normal tissue side-effects to radiation.

1.3 Mitochondria

Mitochondria are double-membrane organelles with two distinct compartments – mitochondrial matrix and intermembrane space – separated by the inner mitochondrial membrane. The inner mitochondrial membrane is folded into cristae, harbouring the mitochondrial respiratory chain composed by four protein complexes (complexes I-IV) and the ATP synthase which are responsible for the synthesis of adenosine triphosphate (ATP) (Freya & Mannellab, 2000).
Most eukaryotic cells use mitochondria to generate energy as ATP (Lodish, Berk, & Zipursky, 2000). Briefly, in aerobic conditions, this energy generation system consists of the transfer of electrons across the mitochondrial protein complexes from oxidative substrates to oxygen, producing water, a process denominated oxidative phosphorylation (OXPHOS). The movement of the electrons generates an electrochemical gradient which is achieved by pumping protons from the mitochondrial matrix to the intermembrane space, through the respiratory chain complexes I, III and IV. The proton gradient is harnessed by the ATP synthase, which returns protons back to the matrix, using the energy from such flux to produce ATP. One consequence of this process is ROS leakage - mitochondria are known to be the main source of oxidants inside the cell (Nickel, Kohlhaas, & Maack, 2014).

It is believed that mitochondria have originated from aerobic bacteria which were in symbiosis with primordial eukaryotic cells (Lane & Martin, 2010). As they evolved together, genomic content from the bacteria gradually migrated to the host cell and, currently, the vast majority of mitochondrial proteins are encoded by nuclear genome. However, DNA is still present inside mitochondria (mtDNA) in a ring-like form, encoding 37 genes, 13 of which responsible for

synthesising the protein subunits of respiratory complexes I, III, IV and ATP synthase (Taanman, 1999). mtDNA is also responsible for the synthesis of 22 transfer RNAs (tRNA) and 2 ribosomal RNAs (rRNA), important for the translation of the mtDNA genes (Chan, 2006). One mitochondrion has between 2 to 10 mtDNA copies organized in nucleoids; each nucleoid can have one single copy of DNA or small clusters containing several copies (Bogenhagen, 2012).

1.3.1 More than powerhouses

Mitochondria are not only responsible for ATP synthesis, they are also essential for other cellular tasks, like intermediary metabolism (for instance, fatty acid metabolism (Frayn, 2003)), Ca^{2+} homeostasis (Saris & Carafoli, 2005), apoptosis cascades (Guido Kroemer, 2003), among others. Therefore, the idea that mitochondria are simple energy factories has long been replaced by the concept of an organelle that plays key roles in a plethora of cellular functions (Nunnari & Suomalainen, 2012). Structurally, mitochondria are dynamic networks of fused mitochondrion, which separate, move and divide (McBride, Neuspiel, & Wasiak, 2006), and this dynamism is believed to play an important part in their contribution to biological processes (Lomax, Folkes, & O'Neill, 2013b; Soubannier & McBride, 2009).

Cellular signalling circuitry is one of the biological processes, controlled by mitochondria. Generally, this organelle regulates cellular signalling either by serving as place for protein-protein interactions or by regulating the levels of important signalling molecules, such as Ca^{2+} (Berridge et al., 2003) and ROS (D'Autréaux & Toledano, 2007). Although the endoplasmic reticulum (ER) is usually considered the principal intracellular Ca^{2+} stock (Koch, 1990), mitochondria are also a source of Ca^{2+} (Saris & Carafoli, 2005).

Cell death signalling is one of the most established phenomena linked to mitochondria (Guido Kroemer, 2003). Programmed cell death is an essential mechanism for cell homeostasis. Apoptosis is the most common form of programmed cell death, a process which requires the activation of a series of proteases called caspases (cysteine-dependent, aspartate-specific peptidases) (Nicholson & Thornberry, 1997). When apoptosis is initiated, mitochondrial membrane permeabilizes in response to stimulus (such as DNA damage) and cytochrome c (Cyt c) is released from mitochondria. Cyt c is required as a platform for the formation of the apoptosome, a multiprotein structure formed in the apoptotic process (G. Kroemer, Galluzzi, & Brenner, 2007; Reed, 2000).

Another form of programmed cell death is autophagy. It is a degradation route which serves as a method for destroying and/or recycling cellular components, detoxifying the cell, or providing basic constituents when the cell needs them. Proteins, organelles, etc., are engulfed

by a double membrane forming the autophagosome (Mizushima, Levine, Cuervo, & Klionsky, 2008) which carries its cargo, fuses with the lysosome, allowing the cargo destruction (Whelan & Zuckerbraun, 2013). Mitochondria serve as the membrane source for the autophagosome formation (Hailey et al., 2010). Furthermore, regulating ATP/ADP (adenosine diphosphate) ratios, mitochondria are also autophagy regulators, as low ATP levels are one of the autophagy activators (Russell, Yuan, & Guan, 2014).

Mitochondria functions above described show how they are essential for the cell. External stress can disturb mitochondrial function; to counteract this, cells have evolved multiple signalling pathways adapting and protecting mitochondria, and maintaining cellular homeostasis. Facing an insult, mitochondria signal stress by membrane depolarization, ROS production, Ca^{2+} fluxes (Barbour & Turner, 2014), among other mechanisms. These mechanisms seem to be essential to assure cell response and adaptation (Xue & Hua, 2017). One characteristic of cancer cells is their fast proliferation rate. Rapid growth of tumours creates hypoxic regions within them which would usually be toxic to normal cells. However, tumour cells are able to thrive under hypoxia by shifting their metabolism from OXPHOS to glycolysis. This strategy, which also occurs in the presence of oxygen, as Otto Warburg's early described (Liberti & Locasale, 2016), implies that this metabolic shift is not only a matter of environmental adaptation. Tumour cells use glycolysis at high rates (the levels of glucose entering the cell exceeds the consumption demand) to support cellular proliferation. They accumulate pyruvate, essential for lipid synthesis and membrane assembly (Gatenby & Gillies, 2004; M. Vander Heiden, Cantley, & Thompson, 2009).

Mitochondria have also been described to influence other cellular mechanisms, namely cell cycle regulation (Antico Arciuch, Elguero, Poderoso, & Carreras, 2012), being involved in a variety of disease models which will not be further discussed, as they are beyond the scope of the present work.

1.3.2 Radiation and mitochondria

Depending on the cellular type, mitochondria may occupy a considerable portion of the intracellular space (Stuurman & Vale, 2016), making them more exposed to IR. When a cell is irradiated, mtDNA is believed to be more vulnerable as it lacks histone structures to protect it, and mitochondria also lack an efficient repair mechanism (Rogounovitch, Saenko, & Yamashita, 2004). mtDNA damage may lead to mitochondrial dysfunction. It has been assumed that an increase in DNA copy number after IR is a compensatory mechanism for its loss of function. Consequently, an impaired respiratory chain activity and decreased

mitochondrial function leads to an increase in ROS, perpetuating cell injury (Azzam, Jay-Gerin, & Pain, 2012; Nugent et al., 2007), and this oxidative environment may affect the metabolism of the cell (Mikkelsen & Wardman, 2003).

The mtDNA D-Loop region is considered vital for replication and expression of the mitochondrial genome (Taanman, 1999). It holds the leading-strand origin of replication and the main promoters for transcription. Alterations in these regions can alter mtDNA replication and transcription rates and change mitochondrial function (Taanman, 1999). Furthermore, the D310 D-Loop region has been reported to be as more susceptible to damage by oxidative species when compared with other regions of mtDNA (Mambo et al., 2003).
Boaventura *et al.* studied a cohort of patients treated for *tinea* capitis, a skin infection that in the middle of the 20th century was a public health issue (Boaventura, Pereira, Mendes, Teixeira-Gomes, et al., 2014). In order to access the hair follicles of the patients' scalp, epilation was needed and this was achieved with IR. In their study, it was found that the rate of D310 mutation of the D-loop region was 43.0% in the irradiated group comparing with 25% in the non-irradiated group. Furthermore, they observed that this rate was higher when higher doses of radiation were applied (Boaventura, Pereira, Mendes, Batista, et al., 2014). This observation further supports the concept that the radiation exposure potentiates D310 D-Loop instability, as previously postulated by Abdullaev (Abdullaev, Anishchenko, & Gaziev, 2011).

IR can also cause mitochondrial dysfunction through interruption of mitochondrial dynamics, causing accelerated fragmentation of the tubular network (Kobashigawa, Suzuki, & Yamashita, 2011). Kobashigawa *et al.* showed that this event was a consequence of the relocalization of dynamin-related protein (Drp1), responsible for mitochondrial fission, from the cytoplasm to the mitochondria. The authors presumed that Drp1 is dephosphorylated as a consequence of Ca^{2+} increased levels after IR (Heise et al., 2010) through calcineurin (Cribbs & Strack, 2007). This disturbance in mitochondrial dynamics could also explain the increased levels of ROS due to loss of membrane potential (Kobashigawa et al., 2011).

Mitochondria biogenesis is the process by which new mitochondria are produced. It involves mtDNA transcription and translation, as well as incorporation of nuclear encoded transcripts, and the recruitment of other proteins and lipids. Mitochondrial homeostasis within the cell is achieved balancing its production and its elimination. Elimination of mitochondria is designated mitophagy and serves as a mechanism to degrade damaged or excessive mitochondria (Palikaras & Tavernarakis, 2014).
IR can affect mitochondrial biology in several ways, one of them is mitochondrial quantity (Nugent et al., 2007). In a recent report, Yamamori *et al.*, studying the effects of X-Rays on

mouse fibroblasts, (NIH/3T3) cells, have shown that the upregulation of mitochondria abundance after IR was independent of the mitochondrial biogenesis process (Yamamori et al., 2016).

Bystander effects and mitochondria

Mitochondria have an important role in cellular signalling mechanisms and are also involved in IR stress response. It seems plausible that the bystander effect, a response to a stress signal emanated from an irradiated cell, could be mitochondrial dependent.

Several studies approached the role mitochondria in the response to bystander signals.
Apoptosis is one of the effects observed in cells exposed to factors secreted by irradiated cells (Lyng et al., 2002). As mitochondria are important to its initiation, they have been implicated this process. Lyng *et al.* (Lyng, Seymour, & Mothersill, 2000) studied the capacity of ICCM to induce apoptosis in bystander cells. Upon adding ICCM, the non-irradiated group showed less clonogenic survival, increased apoptosis, alteration in the Ca^{2+} fluxes and a late increase in ROS levels (6, 12 and 24 hours after adding the ICCM). Nugent *et al.* also described an increase in mitochondrial mass after cells were treated with ICCM, highlighting mitochondrial sensitivity to bystander signals (Nugent et al., 2007).
Cells lacking mtDNA are a practical model to study mitochondria involvement in various cellular programs (Marchetti et al., 1996) and the response to IR is one of them (van Gisbergen et al., 2017). Radioresistance was observed in mtDNA depleted cells (Cloos et al., 2010) but this is not well established.

In the bystander signalling context, the ability of cells to produce or to release a bystander signal may depend on mitochondria. Cells lacking mitochondrial DNA, when exposed to radiation, are not able to signal this insult to other cells, as shown by Tartier *et al.* (Tartier, Gilchrist, Burdak-Rothkamm, Folkard, & Prise, 2007). However, these cells were able to react to factors released by normal-functioning mitochondria cells (the endpoint evaluated was nuclear DNA damage).
Chen *et al.* studied the bystander signalling capacity of cells without mtDNA, or with normal mtDNA, upon treatment with disrupters of the respiratory chain (Chen et al., 2008). They demonstrated that ICCM from both types of cells was less effective in inducing nuclear DNA damage. Moreover, donor cells treated with Ca^{2+} and NOS inhibitors, produced significantly less damage, showing the need of an uncompromised mitochondria function.
The nature of the signals is still unclear, but mitochondria involvement seems definite.

A more mechanistic view of the phenomena has been proposed in Klammer's review (Klammer, Mladenov, Li, & Iliakis, 2015) who states that the manifestation of a bystander effect seems to be a natural response to damage induced by radiation, with the consequent alteration of the oxidative status. The cell uses these alterations to transmit signals to its neighbour cells, and those cells create alert factors, amplifying the response.

Considering the described premises, a model can be proposed, through which mitochondria may affect the bystander signalling of 'danger' to neighbouring (or distant) bystander cells (Figure 11).

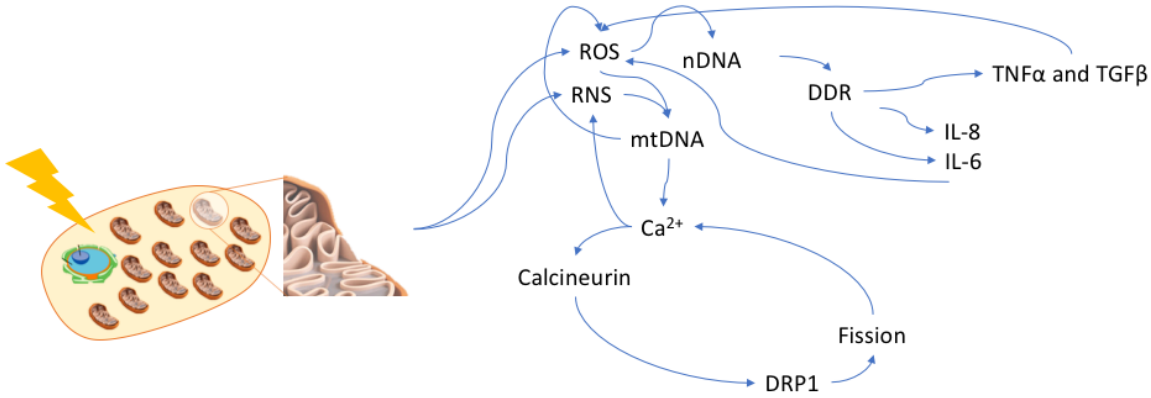

Figure 9 – *Model proposed for mitochondria role in the bystander signalling.* Irradiation causes ROS and RNS increase, which in turn damages nuclear and mitochondrial DNA. Nuclear DNA damage via the DDR response causes inflammatory cytokines release and macrophages recruitment which in turn further increase ROS and RNS production. Damaged mtDNA causes a disruption of Ca^{2+}homeostasis which activates calcineurin and causes relocalization of fission promoting protein DRP1. Mitochondrial fission further increases Ca^{2+}inbalance promoting NO and RNS production, amplifying the loop.

1.3.3 Cybrids

Cytoplasmic hybrid, or cybrid, cell lines were developed as models for studying mtDNA influence in a myriad of cellular processes (H. M. Wilkins, Carl, & Swerdlow, 2014). Cybrids share the same nuclear DNA background but differ in their mitochondrial content, allowing a proper distinction of the effects caused from specific mtDNA alterations. Cybrids are important tools for studying mitochondrial dependent processes as well as diseases that arise from mitochondrial dysfunction.

In order to generate cybrids, cells have to be devoided of their mtDNA content. This mechanism was first discovered in yeast with shifted metabolism towards glycolysis, and the need of genes coding for the proteins of the respiratory chain complexes diminished.

Eventually, generation after generation, mtDNA was no longer replicated (H. M. Wilkins et al., 2014). Since this discovery, several methods for depleting cells from their mtDNA have been developed, such as the use of DNA-intercalating agents, like ethidium bromide (Desjardins, Frost, & Morais, 1985) and 3' dideoxycytidine (Nelson, Hanna, Wood, & Harding, 1997). As these techniques may have consequences for other cellular components, modern methodologies evolved to less disruptive mechanisms, such as the use of endonuclease EcoRI, which cleaves DNA into fragments at specific sites (Robberson, Clayton, & Morrow, 1974).

Cells with no mtDNA are known as Rho Zero (ρ0). Despite having altered function, ρ0 cells maintain mitochondria and mitochondrial membrane potential, proliferate, and receive proteins encoded by the nucleus (Mineri et al., 2009). Nevertheless, they are auxotrophic for pyrimidine, uridine and pyruvate and they need them to be maintained in culture. This represents a practical approach to test/confirm mtDNA depletion, although other techniques are available, such as polymerase chain reaction (PCR).

Briefly, the cybrid production technique consists on fusing enucleated cells harbouring the mtDNA of interest with ρ0 cells (M. G. Vander Heiden, Cantley, & Thompson, 2009) (Figure 12). Cells obtained in this way contain numerous copies of mtDNA and are often heteroplasmic, meaning that a particular mutation in mtDNA can be present in different ratios within the same cell population, with different consequences

for its function (Wallace & Chalkia, 2013). When the mtDNA sequence is the same, we are in the presence of homoplasmy. Thus, there is the need for defining a threshold for the mutational load that is able to cause a consequence (H. M. Wilkins et al., 2014).

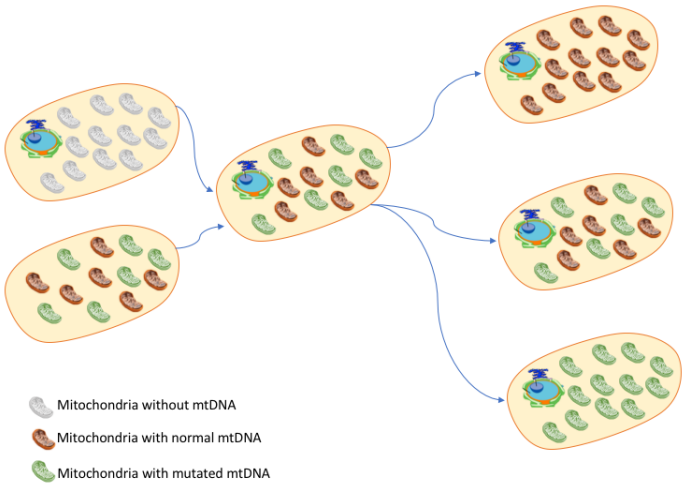

Figure 10 - *Schematic representation of the cybrids production*. A cell line deployed of mtDNA is fused with enucleated cells containing the mtDNA mutation of interest. The resulting cybrid cell line harbours the mutation that can be selected according to the heteroplasmy degree. Homoplasmic cybrids can then be used, for both wild type (WT) mtDNA and mutated mtDNA. Adapted from Máximo *et al.* (Máximo, Lima, Soares, & Sobrinho-Simões, 2009)

Additionally, nuclear background also affects the manifestation of a phenotype. Different ρ0 cells, originated from different parental cell lines, can influence the segregation of mutant and wild-type mitochondrial genomes in cell cybrids (Dunbar, Moonie, Jacobs, & Holt, 1995). This needs to be considered when developing the study model: using the same parental nuclear background for the cybrids production ensures that the differences in the response are only due to the mtDNA content.

1.3.4 MELAS disease

One of the most commonly occurring maternally inherited mitochondrial disorders is Mitochondrial Myopathy, Encephalopathy, Lactic Acidosis with Stroke-like episodes (MELAS) syndrome (El-Hattab, Adesina, Jones, & Scaglia, 2015). As the name indicates, stroke-like episodes are the describing feature of MELAS syndrome. The clinical course of this disorder is highly variable: it can be asymptomatic, present in normal early development, or lead to progressive muscle weakness, lactic acidosis, cognitive dysfunction, seizures, stroke-like episodes, encephalopathy and premature death (DiMauro & Hirano, 1993).

This syndrome is associated with various point mutations in the mitochondrial DNA, the majority of which occurring in the dihydrouridine loop of the mitochondrial tRNA for Leucine (UUR) [$tRNA^{Leu(UUR)}$] gene(Karkos, Waldron, & Johnson, 2004). Several different mechanisms are proposed to contribute to this disease, such as aminoacylation of mitochondrial tRNA resulting in decreased mitochondrial protein synthesis, changes in calcium homeostasis, and alterations in nitric oxide metabolism (Penn et al., 1992).

Considering the aforementioned role these cellular functions have in IR response, MELAS disease is an interesting mitochondrial dysfunction model for radiobiology studies, including RIBE.

1.4 Osteossarcoma

Osteosarcoma is a malignant tumour of the bone with a high mortality rate due to its poor response to therapy (Raymond & Jaffe, 2009).

The cancer rarity and its high genetic heterogeneity makes difficult to define large cohorts of patients according to differences in histologies (Hansen, 2002). Osteosarcoma tumorigenesis is associated with vital genetic alterations, including inactivation of tumour suppressor genes, gain/loss/ rearrangement of chromosomal regions, and misregulated signal transduction pathways (Hansen, 2002). This cancer is considered radioresistant (Luetke, Meyers, Lewis, & Juergens, 2014) and there is still no clear mechanistic insight to explain it, although some

interesting approaches are being presented, like its ability to shut down hypoxia sensing pathways resulting in the promotion of pro-survival responses (Mancuso et al., 2008).

Osteosarcoma-derived cell lines are commonly used as *in vitro* models due to their highly proliferative characteristics and feasible genetic manipulation by transfection (Mohseny et al., 2011). Established osteosarcoma 143B cell lines have been used for several studies and are one of the most frequently used cell lines to generate ρ0 cells and, consequentally, cybrid cell models (H. M. Wilkins et al., 2014).

Chapter 2

Aims

2. Aims

Radiotherapy, as an important therapeutic tool in cancer treatment, can benefit from increasing understanding of the molecular mechanisms underlying interactions between IR and biological systems.

As previously described, mitochondria are important for maintaining cellular equilibrium, especially in a stress/response environment. In an irradiated cell, the communication of factors inducing a reaction in bystander cells may not occur when the irradiated cells have mitochondria without mtDNA (Tartier et al., 2007).

The present project aimed to characterize cell response to direct irradiation or to the media obtained from irradiated cell.

Our primary objectives were to:

1) Investigate the response of cells with different mitochondrial status to IR, and to ICCM;

2) Investigate the bystander effect in cells depleted of mtDNA;

3) Investigate if a cell line with impaired mitochondrial function (mutated A3243T $tRNA^{Leu(UUR)}$ gene) would induce a bystander effect.

Chapter 3

Materials and Methods

3. Materials and Methods

3.1 Cell Culture

The following cell lines were used in this study:

- ◊ 143B-ρ0 cells – 143B osteosarcoma-derived cell line with complete loss of mtDNA. They were derived after transient expression of UL12.5 Herpes Simplex protein, leading to mtDNA degradation (Saffran, Pare, Corcoran, Weller, & Smiley, 2007). Thereby, 143B-ρ0 cells share the nuclear background of 143B cells.
- ◊ Cy143Bwt – cybrid cell line obtained by fusing 143B-ρ0 cells with human enucleated cells harbouring WT mtDNA
- ◊ Cy143BMELAS – obtained by fusing 143B-ρ0 cells with human platelets from a patient with MELAS disease carrying the A3243T mtDNA mutation.

143B-ρ0 were a kind gift from Dr Keshav Singh (University of Alabama at Birmingham (UAB), Alabama (AL), United States of America (USA)). Both cybrid cell lines used were previously established by the group (Nunes et al., 2015).

143B-ρ0 cells are pyrimidine and pyruvate auxotrophs and therefore need special media to grow in. To have consistency, all cell lines were cultured in Dulbecco's modified Eagle's medium (DMEM) high-glucose (Capricorn, Ebsdorfergrund, Germany) supplemented with 10% (v/v) inactivated and filtered fetal bovine serum (FBS), 1% (v/v) penicillin/streptomycin (PenStrep, Biowest, Nuaillé, France), 0.5% fungizone (Biowest), 50µg/ml uridine (Sigma, MO, USA) and 100mM pyruvate (Sigma).

Cells were routinely kept in culture at 37°C, 5% carbon dioxide (CO_2), in a humidified incubator.

3.2 Cell line characterization

3.2.1 Growth Curves

For cellular growth curves determination, $4.0x10^4$ cells were plated in 6 well plates. Every 24 hours, cells were collected and counted in the Z2 Coulter particle counter (Beckman Coulter, Brea, CA). Briefly, cells were washed once with phosphate buffered saline (PBS) 1x and detached using Gibco TrypLE Express (ThermoFisher Scientific®). Cells were then ressuspended in culture media and collected. After a 1:2000 dilution in isotonic buffered diluent

Isoton® solution, cell number was determined in Z2 Coulter particle counter (Beckman Coulter, Brea, CA).

In order to establish a basal cell growth curve, at least three experiments were conducted. The same protocol was applied for counting cells after IR exposure.

3.2.2 Gene sequencing for mtDNA tRNALeu(UUR) mutation

Cell suspension collection

Cells were collected and frozen previously to the DNA extraction protocol. Briefly, sub-confluent cells (approximately 70% confluence) were washed once PBS 1x and detached using Gibco TrypLE Express (ThermoFisher Scientific®). The cell suspension was then centrifuged and the pellet was preserved at -20 ºC prior to DNA extraction.

DNA extraction

DNA extraction was performed using GRS Genomic DNA Kit - Blood & Cultured Cells. The process was done according to the manufacturer's instructions (Grisp research solutions, Portugal) for DNA isolation from cell pellets.

Nucleic acid concentrations were determined using the NanoDrop ND-1000 Spectrophometer (Nanodrop Technologies, Inc., DE, USA).

Polymerase chain reaction (PCR)

mtDNA $tRNA^{Leu(UUR)}$ MELAS mutation was assessed by PCR followed by direct sequencing.

The primers used for amplification covered the region of the A3243T mutation of the $tRNA^{Leu(UUR)}$ gene, forward (FW) primer (5'-ACACCCACCCAAGAACAGGGTTT- 3') and reverse (RV) primer (5'- GTAGAATGATGGCTAGGGTACT-3') (Invitrogen/ThermoFisher, MA, USA).

PCR reactions were performed in total reaction volumes of 25µl using ~100ng of DNA, 0.1µM of each FW and RV primers, 1x PCR Buffer (5x GoTaq Flexi Buffer, Promega), 1.5mM of magnesium chloride solution (Promega), 40mM deoxyribonucleotide triphosphate (dNTP) mix (Bioron GmbH), and 0.5 U of GoTAq DNA polymerase (Promega). PCR reactions were performed on BIO RAD MyCycleTM termal cycler (BIO RAD). PCR conditions were: 1 cycle of 5 minutes at 94°C for initial denaturation, followed by 35 cycles of 30 seconds at 94°C for

denaturation, 30 seconds at 58°C for annealing and an extension step of 30 seconds at 72°C; the final extension consisted of 1 cycle of 5 minutes at 72°C.

DNA purification and sequencing

PCR products were purified using 1U/µl exonuclease I and 0.05U/µl shrimp alkaline phosphatase (Fermentas) at 37°C for 20 minutes, followed by heat inactivation at 80°C for 15 minutes.

The sequencing reaction consisted of 0.5µl of BigDye® Terminator (Perking- Elmer, CA, USA), 3.4µl of sequencing buffer (Perking-Elmer), 0.3µl of primer (FW and RV for tRNALeu(UUR) analysis), 2µl of purified PCR product and DNase/RNase-free distilled water (GIBCO) in a final volume of 10µl. The sequencing reaction was performed in a BIO RAD MyCyclerTM thermal cycle (BIO RAD) with the following conditions: an initial denaturation step of 10 seconds at 94°C, followed by 35 cycles of 10 seconds at 94°C, 30 seconds at 56°C for the annealing and elongation of 2 minutes at 60°C; the final elongation was performed for 10 minutes at 60°C. Before loading on the ABI prism 3130XL Automatic sequencer (Perkin-Elmer), PCR products were purified by precipitation using Sephadex columns (SephadexTM G-50 Fine, GE Healthcare Bioscience AB, Uppsala, Sweden) according to manufacturer's instructions. 15µl of formamide (Applied Biosystems, CT, USA) were added to each pellet in order to maintain the DNA in a single stranded conformation.

3.3 Mitochondrial membrane potential evaluation

Mitochondrial membrane potential was analysed in all three cell lines with MitoTracker™ Red CMXRos (ThermoFisher Scientific®) by flow cytometry. More polarized mitochondria, with more negative interiors, accumulate more cationic dyes, such as MitoTRacker™ Red CMXRos.

Briefly, $1.5x10^5$ cells were plated in 6 well plates, one for each cell line. After 24h incubation, medium was collected and new medium containing 50nM MitoTracker™ was added and incubated for 30 minutes at 37°C. Afterwards, cells were washed once with PBS 1x and detached with Gibco TrypLE Express (ThermoFisher Scientific®). Cells were then ressusspended in DMEM and collected in 1,5mL eppendorfs to centrifuge (1200 rotations per minute – r.p.m; 153 relative centrifugal force – for 5 minutes at room temperature). The pellet obtained was ressuspended in ice-cold PBS, kept on ice, and samples analysed in BD® Accuri C6 flow cytometer (BD Biosciences).

For the evaluation of mitochondrial membrane potential after direct irradiation the same protocol was applied, 20 minutes after exposing cells to radiation.

3.4 Measurement of superoxide levels

The levels of superoxide ($O^{\cdot -}$) were assessed with Dihydroethidium (DHE) from Sigma-Aldrich® by flow cytometry. Briefly, $1.5x10^5$ cells were plated in 6 well plates overnight and incubated with the dye (optimized concentration of 10 µM), in fresh media, for 30 min at 37 ^oC followed by the protocol described in 3.3. In this case, a positive control – Antimycin A (AntA) (Sigma Aldrich), a disrupter of the OXPHOS chain and, therefore, ROS inducer (Spitkovsky, 2004) – was added.
The samples were recorded in BD® Accuri C6 and the fluorescence mean for the respective channel was used as indicative of the $O^{\cdot -}$ level.
For the irradiated cells, the same protocol was used, for the different time-points evaluated.

3.5 Cell transportation

Cells were transported from Instituto de Investigação e Inovação em Saúde (i3S) to Instituto Português de Oncologia (IPO) Porto, where they were irradiated.
Transport was done inside a container that kept optimal culture conditions. Six thermo-accumulators were heated up to maintain an optimal temperature inside the container. A stereofoam box was used for the transportation of cells, filled with the heated thermo-accumulators, was transported by foot through a 1.1 kilometres (Km) distance, 13 minutes (min) each way. For every irradiation, a sham control was included.

3.6 Cell irradiation with EBT3T® radiochromic film dose control

24 hours after platting, cells were irradiated with a 6MV photon beam in a linear accelerator - Novalis Tx from Varian Medical Systems®. The cell culture flasks were irradiated with different doses, ranging from 0.2-10.0 Gy, depending on the experiment. The flasks were centred with the irradiation field, and exposed at a source-surface distance (SSD - cells surface) of 100cm, for a field size of 16x16cm, with a dose rate of 400 cGy/min.
The doses were calculated considering the output factor (OF) for the field size used, the percentage depth dose (PDD) at depth of 2cm for the field size of 16x16 cm and the day dose measured in the accelerator, to eliminate the accelerator dose variation.

In order to ensure a full backscatter condition in the experiment a backscatter correction factor of 1.5% in dose was used for the 6MV megavoltage photon beam, according to Yida Hu et al (Hu & Zhu, 2011) .

The monitor units (MU), used to administered the dose were calculated as follows:

$$MU = [(Dose/PDD_{16x16\ @2cm})/OF_{16x16cm}] \times Dose_{(day\ dose)}$$

3.6.1 Dose verification

In order to validate the cells irradiation, a dose control was performed using EBT3® radiochromic film. The film was placed below the cell culture flask, for each dose used. After irradiation, the films are kept from solar light for 24 hours until processing in EPSON® Expression 10000XL digitalizator (conversion from film to digital image).

The results were obtained relating the film optical density (OD – film darkening) with dose, using for that a DoseLab software (Mobius Medical Systems, LP).

3.7 Media transfer

$2.5x10^5$ cells were plated in T25 cell culture flasks for media transfer experiments. 24 hours after platting, cells were irradiated and kept in the incubator for 60 minutes. The media were then collected and filtered with 0,22 µM polyethersulfone (PES) filters (Frilabo). Cells receiving the ICCM were plated at the same time as cells to be directly irradiated, kept in the incubator and their media was replaced by the filtered ICCM.

3.8 γH2AX evaluation

3.8.1 Immunofluorescence

Cells to be incubated with the γH2AX antibody were plated with 6mm lamellae. The phosphorylated form of the histone H2AX was evaluated in directly irradiated cells (Figure 13) and in cells exposed to ICCM (Figure 14). 60 min after cells were irradiated, media was removed and cells were fixed in a paraformaldehyde (PFA) solution (4%) for 30 min at room temperature. After three washes with PBS 1x, samples were kept at 4 ^{o}C. Cells treated with ICCM were submitted to the same protocol.

The primary antibody used was Human Phospho-Histone H2AX (S139) antibody (affinity-purified polyclonal rabbit immunoglobulin G (IgG)) from R&D Systems and the secondary antibody was goat anti-rabbit IgG H&L with fluorescent dye (Alexa Fluor ® 594) from Abcam.
The lamellae were removed and washed twice in PBS 1x before adding blocking buffer solution (1% Bovine serum albumin – BSA, 0,01% Triton X-100) for 30 min. After new washing with PBS 1x, lamellae were incubated with primary antibody (1:250 in blocking buffer) for 60 min, washed again with PBS and finally incubated with secondary antibody (1:200 in blocking buffer) for 60 min.
After the final washing with PBS, the lamellae were mounted on microscope laminae with Vectashield combined with 4',6-diamidino-2-phenylindole (DAPI) (Vector Laboratories), sealed and stored at -20 ^{o}C for posterior analysis.

Cells were visualized in Zeiss Axio Imager Z1 fluorescent microscope. Images were collected with 63x amplification and analysed with ImageJ Version 1.51 (100), for assessing the number of γH2AX foci, considering at least 10 cells for each condition.

3.9 Annexin V

Annexin V is commonly used to detect apoptotic cells, as it binds to phosphatidylserine (a marker of apoptosis) when it is localized on the outer leaflet of the plasma membrane, a commonly feature of apoptotic cells (Vermes, Haanen, Steffens-Nakken, & Reutellingsperger, 1995).
The percentage of cells in apoptosis was evaluated both for irradiated (Figure 13) and ICCM exposed cells (Figure 14). In either case, cells were collected for the assay 24 hours after exposure (to radiation or ICCM).
The procedure for collecting the cells was as described in 3.3. Cells were centrifuged and ressuspended in Annexin V binding buffer 1x (ApoAlert® Clontech Laboratories, Inc). Cells were kept in ice and Annexin V FITC (ImmunoTools) was added for 10 minutes followed by propidium iodide (PI – Sigma Aldrich) for 5 min (that allowed the distinction of necrotic cells) before the samples were read by flow cytometry (BD Accuri C6).
These experiments were repeated three times.

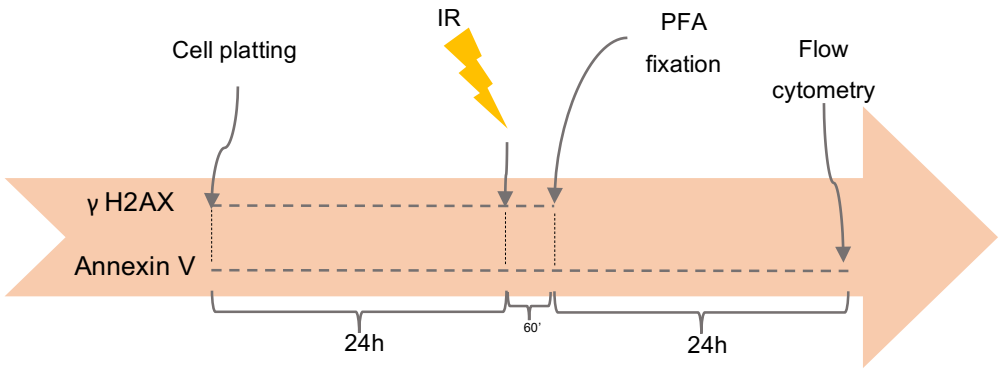

Figure 11 - *Schematic representation of the time-line for the direct IR experiments, DNA damage and apoptosis.* Cells were plated and 24 hours later irradiated. 1 hour after IR, cells are either fixated with PFA for further immunofluorescence assays (first line scenario) or the Annexin V protocol was conducted (second line scenario).

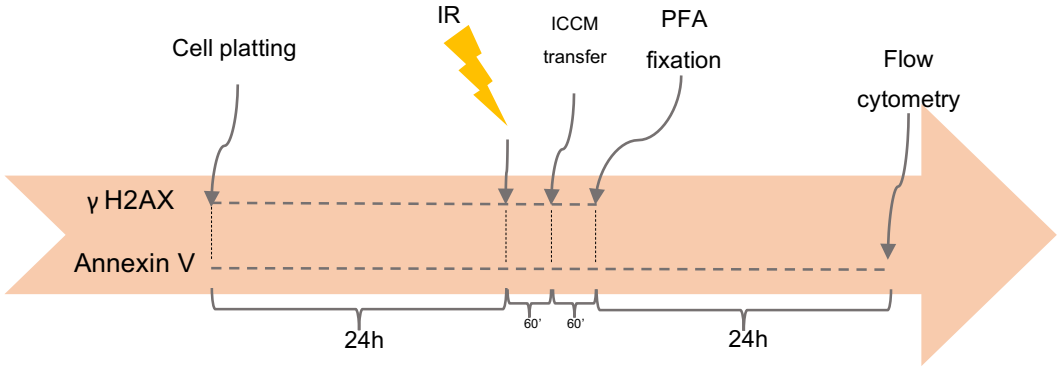

Figure 12 – *Schematic representation of the time-line for the ICCM experiments.* Cells were plated and 24 hours later were irradiated. 1 hour (60 minutes) after IR, ICCM was transferred onto unirradiated cells. ICCM was left on for 60' and cells were either fixated with PFA for further immunofluorescence assays (first line scenario) or the Annexin V protocol was conducted (second line scenario).

3.10 Statistical Analysis

Whenever adequate, the results were presented as mean ± standard error. The data from cell lines experiments were analysed with Two-Way ANOVA followed by the Bonferroni post-test available in Graph Pad Prism software version 5. A p value <0.05 was considered statistically significant.

Chapter 4

Results

4. Results

4.1 Cell line characterization

4.1.1 DNA sequencing results

Sequence analysis was performed to confirm the absence or presence of the $tRNA^{Leu(UUR)}$ gene A3243T mutation in Cy143Bwt and Cy143BMELAS cybrids, respectively. It also served to confirm no mtDNA amplification in 143B-ρ0 cells.

As expected, we confirmed that the Cy143Bwt did not have the $tRNA^{Leu(UUR)}$ (A3243T) mutation (Figure 15, A), while the mutation was present in the Cy143BMELAS, with approximately 60% heteroplasmy (Figure 15, B). The electropherogram of cells without mtDNA, 143B-ρ0, (Figure 15, C) confirms that there was no amplification of the mtDNA region tested.

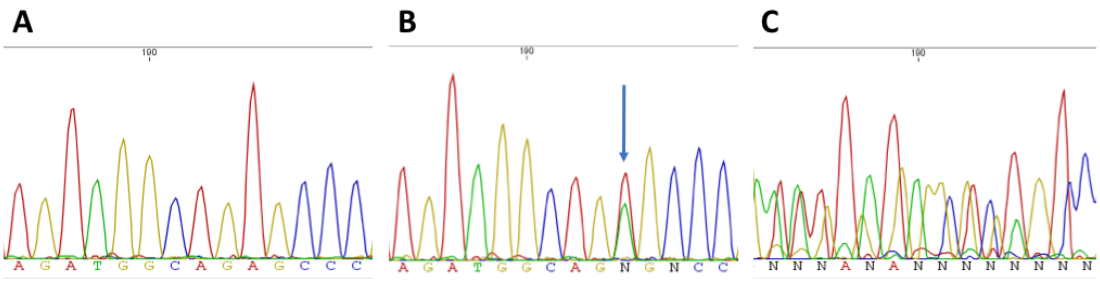

Figure 13 – *DNA sequencing results*. Cy143Bwt, showing the nucleotide Adenine (A) in the 3243 position (**A**). Cy143BMELAS showing an Adenine to Thymine (T) transition at the 3243 position, with approximately 60% of heteroplasmy (blue arrow) (**B**). 143B-ρ0 cells electropherogram showing poor amplification of the region sequenced (**C**).

4.1.2 Cell growth curves under basal conditions

Cellular growth for each cell line was evaluated for a total period of 96 hours after plating $4.0x10^4$ cells (Figure 16). All cell lines grew exponentially although at different rates. The Cy143Bwt was the one with higher increase in total number of cells in culture, followed by Cy143BMELAS.143B-ρ0 cell line had the lowest growth rate.

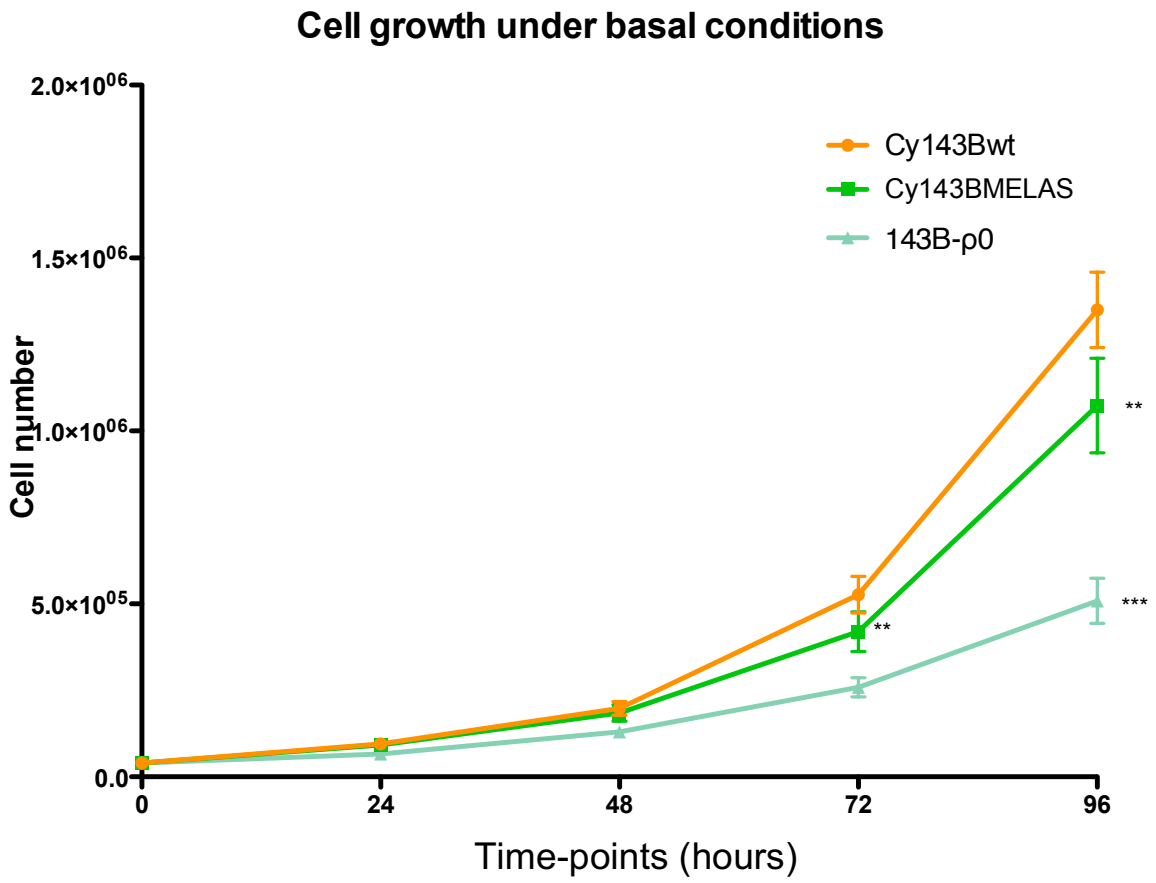

Figure 14 – *Cellular growth curve.* Absolute cell number counted for each cell line; bars represent the standard error. Control Cy143Bwt (orange, circle), Cy143BMELAS (green, square), 143B-ρ0 (light green, triangles) Differences to control statistically significant, with ** for p values <0,01 and *** for p values < 0,001. Data subjected to two-way ANOVA and posterior Bonferroni test.

4.1.3 Mitochondrial membrane potential

Mitochondrial membrane potential assay showed approximately half of the mitochondrial membrane potential in the 143B-ρ0 when compared with the control (Cy143Bwt) and with Cy143BMELAS. There was a slight higher membrane potential in Cy143BMELAS relative to Cy143Bwt (Figure 17).

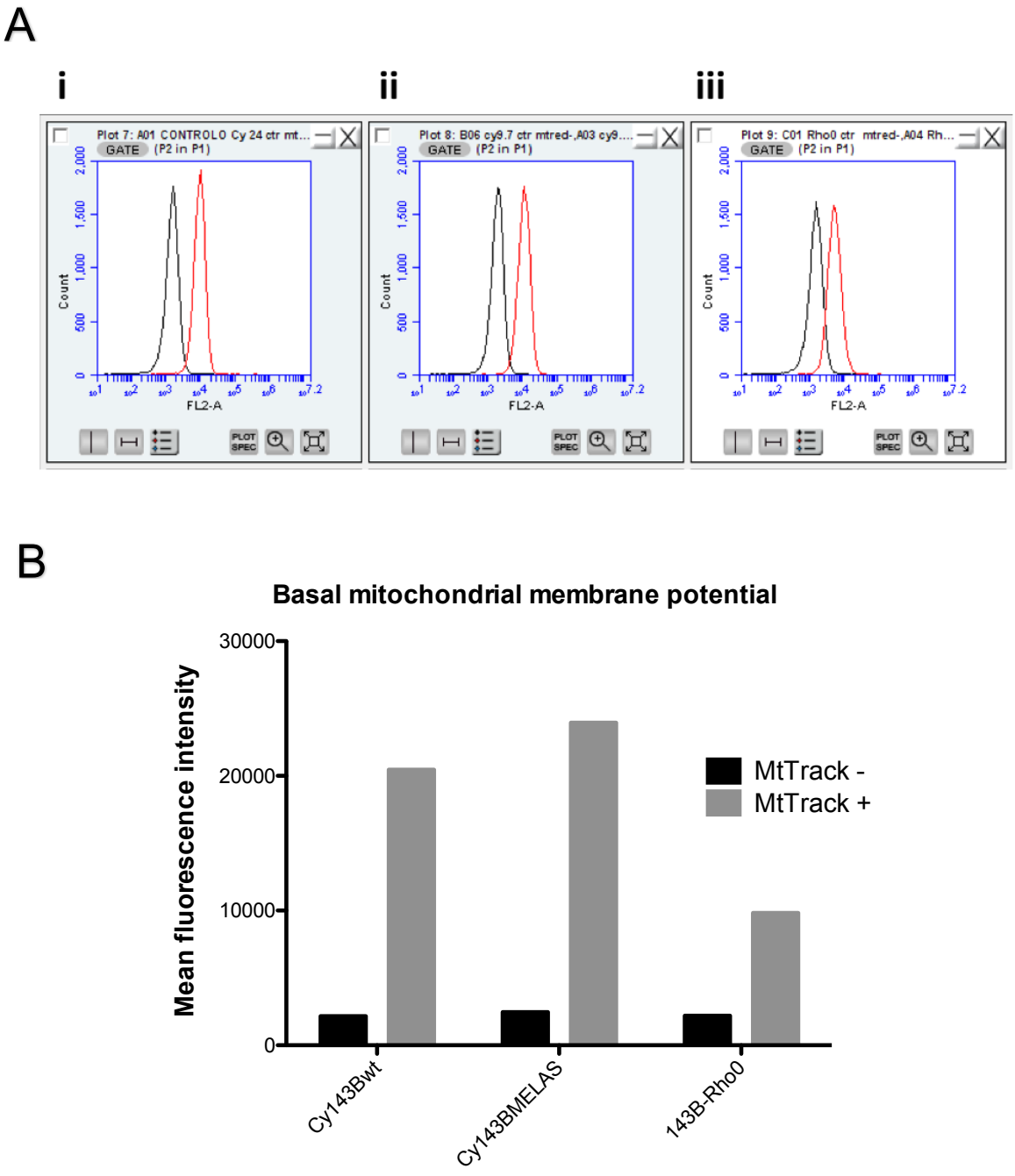

Figure 15 – *Mitochondrial membrane potential.* **A** – The histograms (FL2-A) calculated by BD Accuri C6 software, showed mitochondrial membrane potential observed with Mitotracker (red) and without (black); i) Cy143Bwt, ii) Cy143BMELAS, iii) 143B-ρ0. **B** – comparison of mean fluorescence for the three cell lines (grey bars). The negative control, without MitoTRacker is shown (black bars).

4.1.4 Superoxide levels (basal)

Firstly, we performed a titration assay to choose the best concentration of DHE to be used (Supplementary results, Figure 2). After that, the levels of $O^{\cdot -}$ were assessed in each cell line, using the complex III disrupter AntA (an agent that induces ROS production) as a positive control.

Basal levels of $O^{\cdot -}$ in Cy143BMELAS were higher compared with the ones observed in control Cy143Bwt. In contrast, 143B-ρ0 cell line had very low levels of $O^{\cdot -}$ (Figure 18). AntA, increased $O^{\cdot -}$ levels in Cy143Bwt and Cy143MELAS cell lines, but had no effect in the 143B-ρ0 cell line.

A

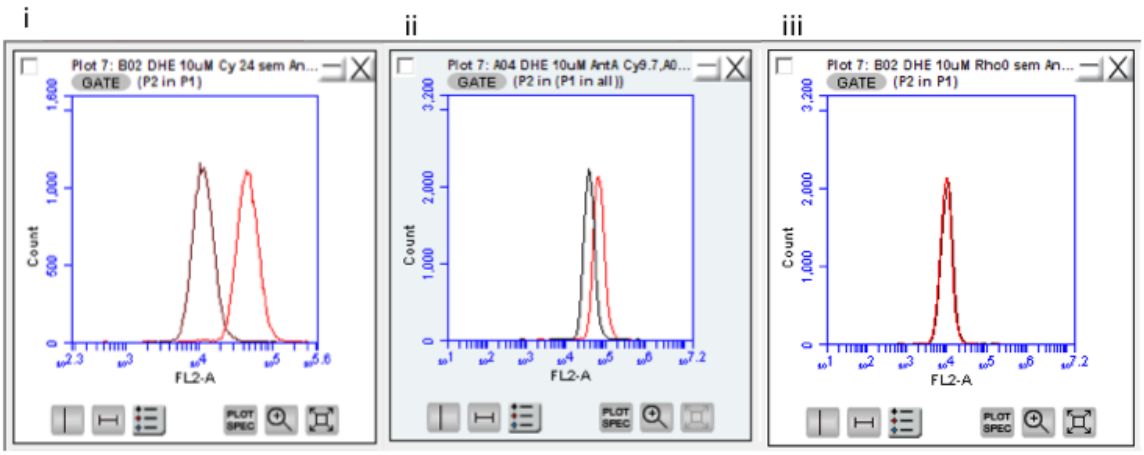

B

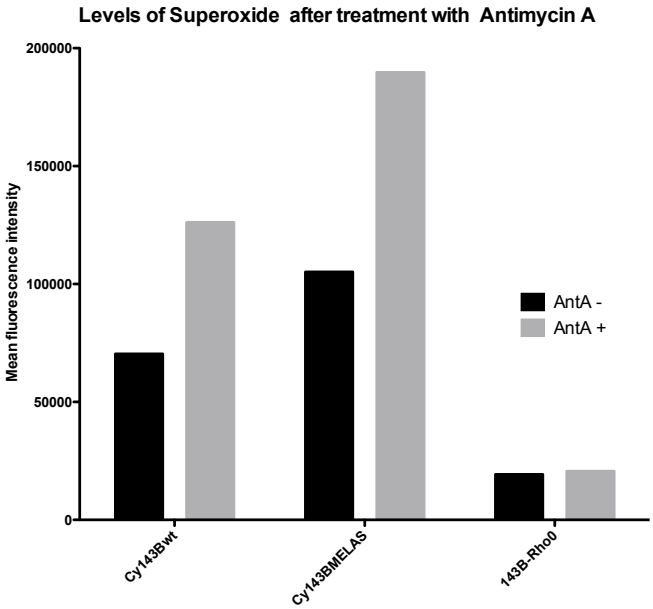

Figure 16 – *Superoxide basal levels.* **A** - The histograms (FL2-A) calculated by BD Accuri C6 software showed the fluorescence intensity of the cells with (red) and without (black) DHE. i) Cy143Bwt; ii) Cy143BMELAS; iii) 143B-ρ0. **B** - $O^{\bullet}_{2}^{-}$ levels are represented with black bars and after AntA treatment (grey bars). Cy143Bwt was the control.

4.2 Dose Verification

Films were irradiated with different doses within the range of 0-10 Gy. The results were obtained relating the film OD with dose, using DoseLab software. We can observe the film darkening with dose increased. The exposure of the films to the IR was compared with the calibration curve previously obtained (Table 4) and the plot relating the dose programmed and the dose read through this method showed a close correlation between dose programed and the dose delivered (r^2=0,99938) (Figure 19).

Table 4 – *Scans of the EBT3® radiochromic film irradiated with the doses used in this work.* According to the calibration curve previously established, the verification of the doses was made with EB3 film and compared to the calibration scans

0 Gy	0.2 Gy	0.5 Gy	1.0 Gy	2.0 Gy	4.0 Gy	6.0 Gy	10.0 Gy
							

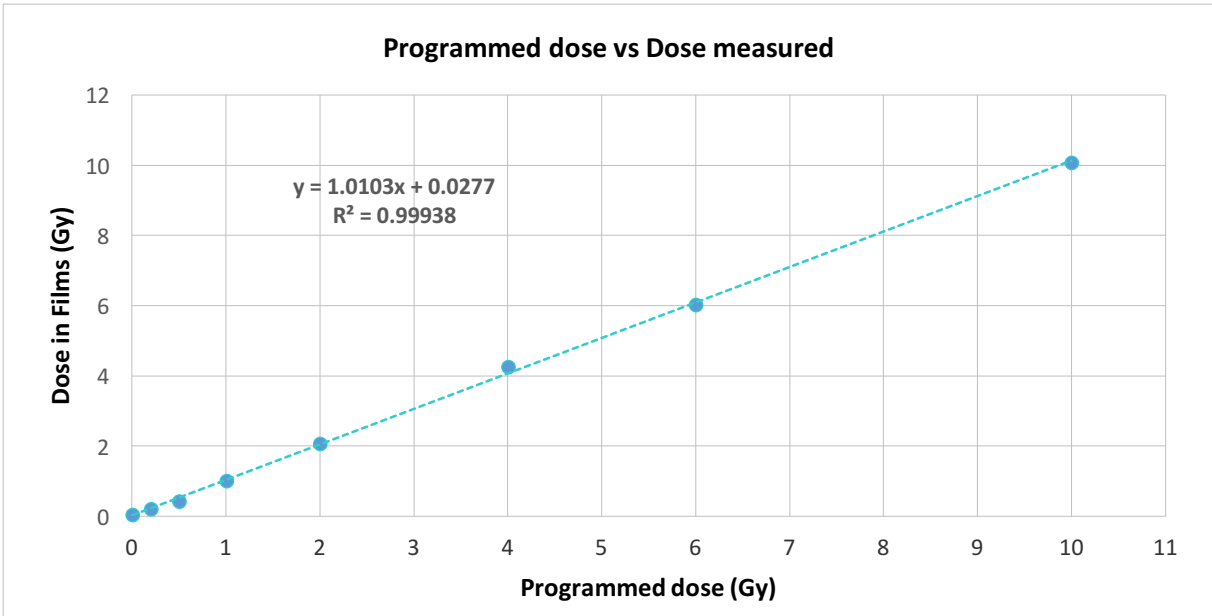

Figure 17 – *Comparison of the dose expected and measured for irradiation.* The relation between the programmed dose and the dose measured with EBT3® films is very close to 1, confirming the accuracy of the irradiation dose used in the experiments.

4.3 Cellular response to direct irradiation

4.3.1 Cell growth curve

Using the same approach previously described (see Section 4.1.3), cellular growth curves were obtained for the three cell lines after irradiation.

a) High doses

Cy143Bwt

Compared with the control, the irradiation caused a decrease in cellular growth for every dose used (Figure 20, A), which was more evident as the dose increased. For higher doses (4.0 Gy, 6.0 Gy and 10.0 Gy) this effect was already evident for the first time-point evaluated, 24 hours after IR (48 hours time-point). 10.0 Gy dose slowed (if not abrograted) exponential growth.

Figure 20 B shows, for 72 hours after IR (96 hours' time-point) the effect of each dose. 10.0 Gy was the dose most affecting cell growth capacity. A decrease in cell number was observed for all IR doses relative to control.

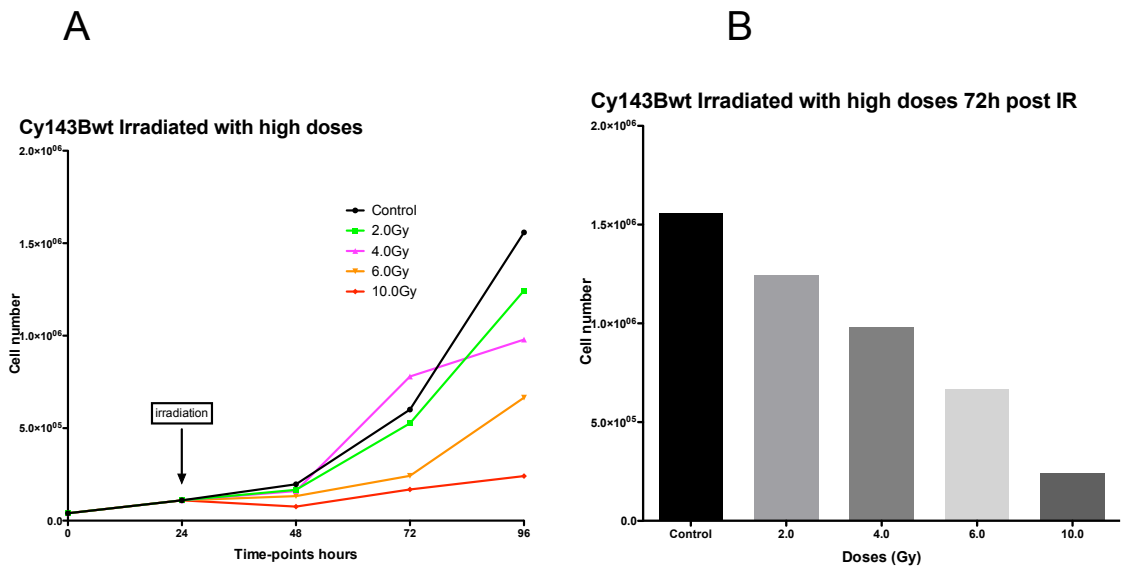

Figure 20 – *High doses Cy143Bwt growth curve*. **A** – Absolute cell number counted for each time-point. Control transported-only (black, circle); transported + irradiated: 2.0 Gy (green, square), 4.0 Gy (pink, upward triangle), 6.0 Gy (orange, downward triangle) and 10.0 Gy (red, diamond). **B** – Absolute cell number assessed at the 96 hours' time-point (72 hours post IR).

Cy143BMELAS

A similar response to IR was observed in the Cy143BMELAS cell line (Figure 21, A) except for 6.0 Gy that showed increased cell number in the 72 hours' time-point (Figure 21, B)

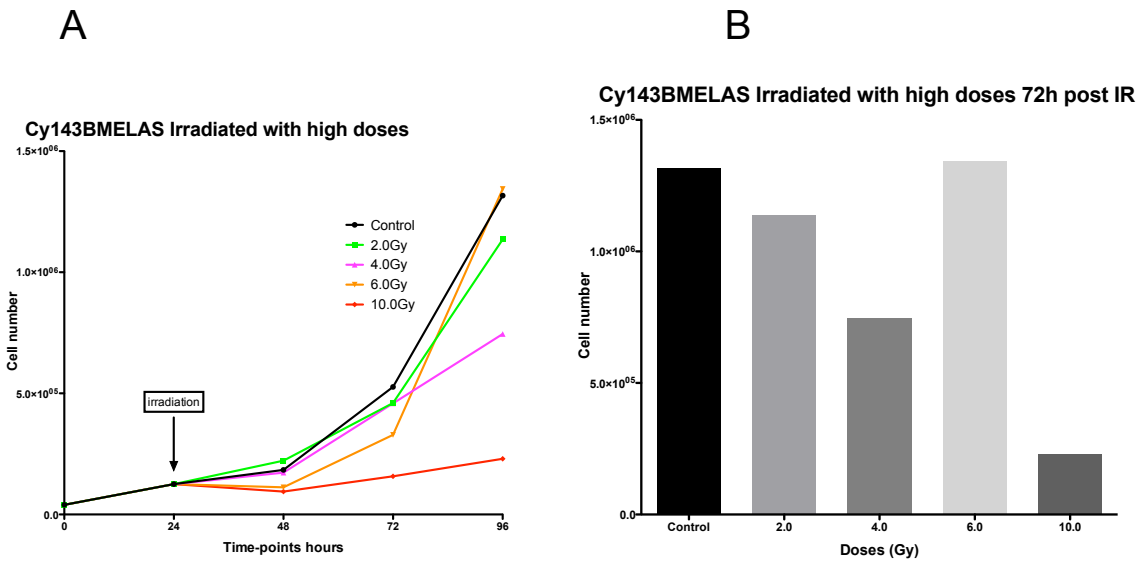

Figure 21 – *High doses Cy143BMELAS growth curve*. **A** – Absolute cell number counted for each time-point. Control transported-only (black, circle); transported + irradiated: 2.0 Gy (green, square), 4.0 Gy (pink, upward triangle), 6.0 Gy (orange, downward triangle) and 10.0 Gy (red, diamond). **B** – Absolute cell number assessed at the 96 hours' time-point (72 hours post IR).

143B-ρ0

Comparing with control, all doses decreased 143B-ρ0 cell number and cell growth in culture (Figure 22).

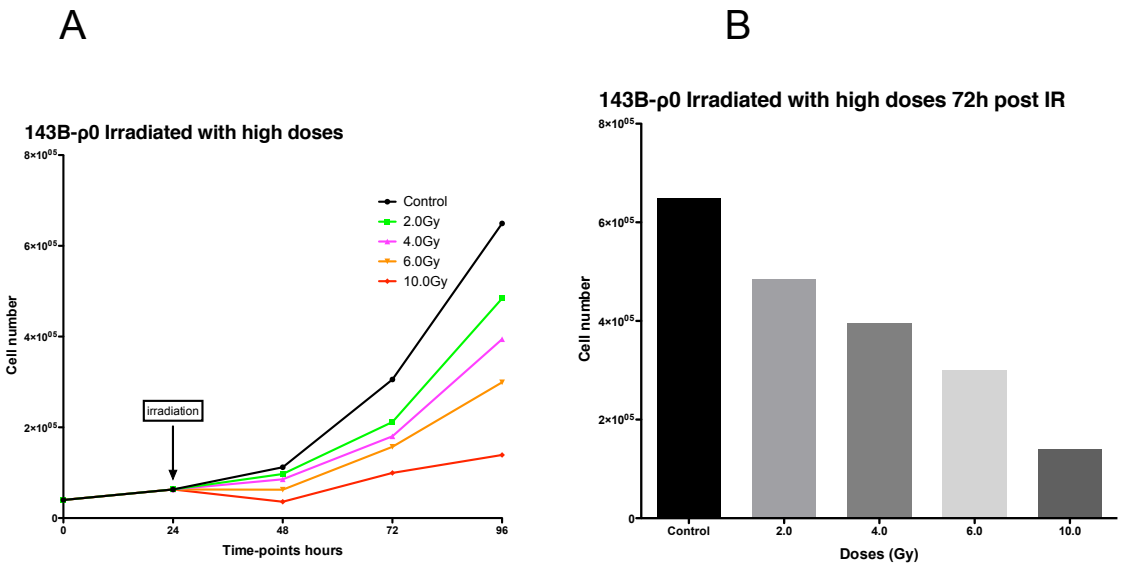

Figure 22 – *High doses 143B-ρ0 growth curve*. **A** – Absolute cell number counted for each time-point. Control transported-only (black, circle); transported + irradiated: 2.0 Gy (green, square), 4.0 Gy (pink, upward triangle), 6.0 Gy (orange, downward triangle) and 10.0 Gy (red, diamond). **B** – Absolute cell number assessed at the 96 hours' time-point (72 hours post IR).

b) Low doses

We were interested in the effects of low IR doses, for their relevance in the issues of RT planning optimization and in the bystander effect context. Therefore, growth curves were obtained for IR doses below 2.0 Gy.

Cy143Bwt

For the studied dose range, cellular growth curves only seem to differ from the 72 hours time-point on (48 hours after IR) (Figure 23, A). Statistical significance was observed with 1.0 Gy and 2.0 Gy, at the 96 hours' time-point (72 hours after IR) (Figure 23, B).

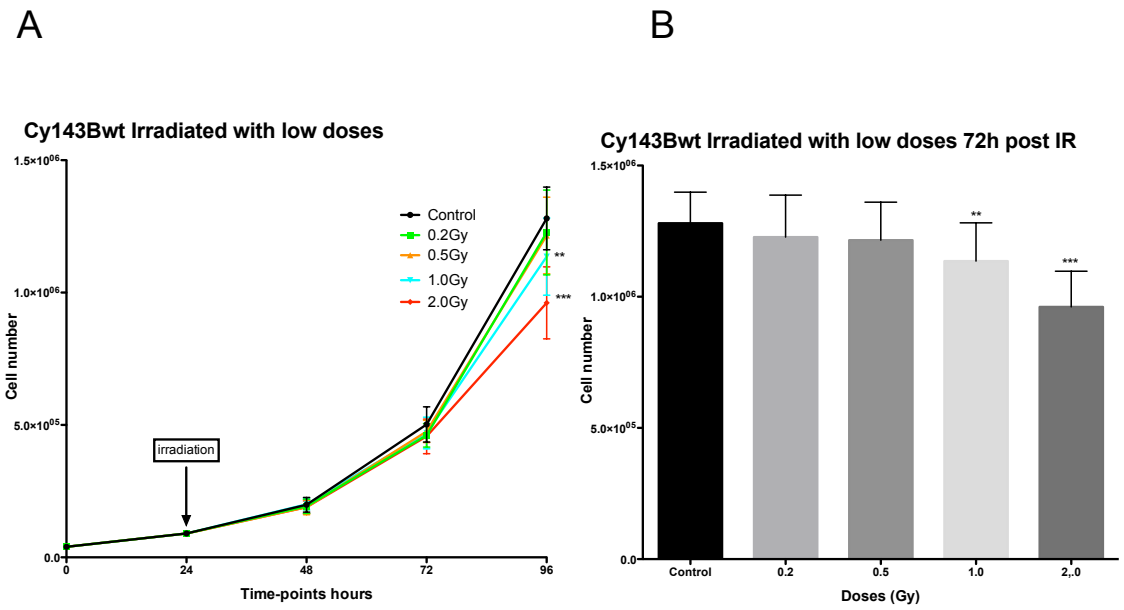

Figure 23 – *Low dose Cy143Bwt growth curve*. **A** – Absolute cell number counted for each time-point. Control transported-only (black, circle); transported + irradiated: 0.2 Gy (green, square), 0.5 Gy (orange, upward triangle), 1.0 Gy (blue, downward triangle) and 2.0 Gy (red, diamond). **B** – Absolute cell number assessed at the 96 hours' time-point (72 hours post IR). Bars correspond to mean ± standard error. Data subjected to two-way ANOVA and posterior Bonferroni test; p values <0,01 (**) and <0,001 (***).

Cy143BMELAS

Similarly, low dose had small effect on the cell count (Figure 24, A) of Cy143BMELAS. For this cell line, a statistical significance was observed for doses ranging from 0.5 Gy to 2.0 Gy at 72 hours time-point after IR (Figure 24, B).

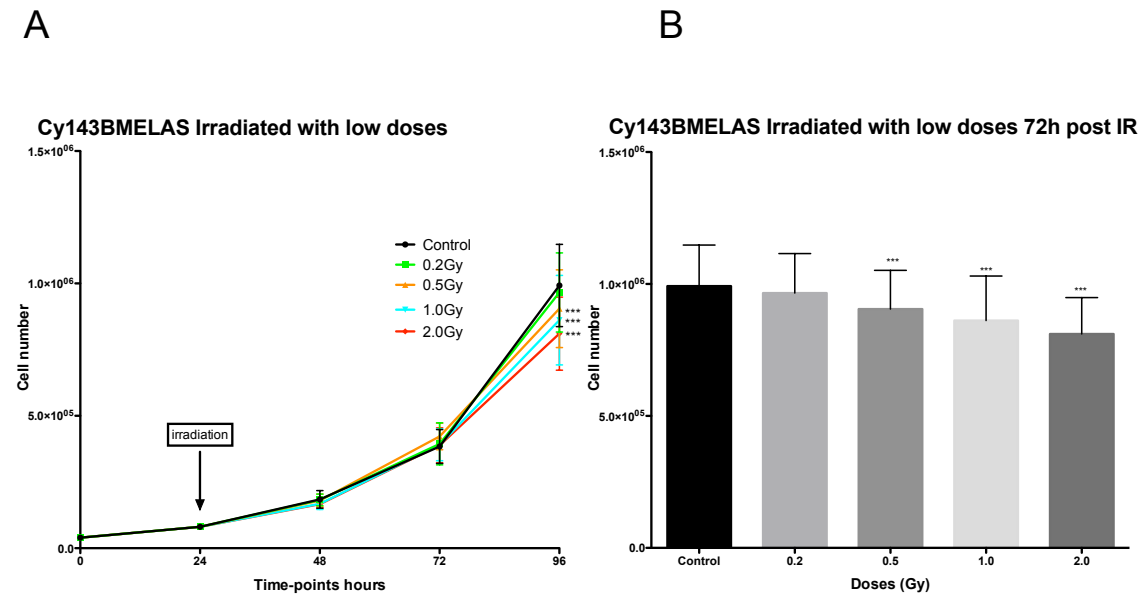

Figure 18 – *Low dose Cy143BMELAS growth curve*. A – Absolute cell number counted for each time-point. Control transported-only (black, circle); transported + irradiated: 0.2 Gy (green, square), 0.5 Gy (orange, upward triangle), 1.0 Gy (blue, downward triangle) and 2.0 Gy (red, diamond). B – Absolute cell number assessed at the 96 hours' time-point (72 hours post IR). Bars correspond to mean ± standard error. Data subjected to two-way ANOVA and posterior Bonferroni test; p values <0,001 (***).

143B-ρ0

143B-ρ0 showed a decreased growth ability upon IR (Figure 25, A). The results for doses 1.0 Gy and 2.0 Gy were statistically significant for the 96 hours time-point (Figure 25, B)

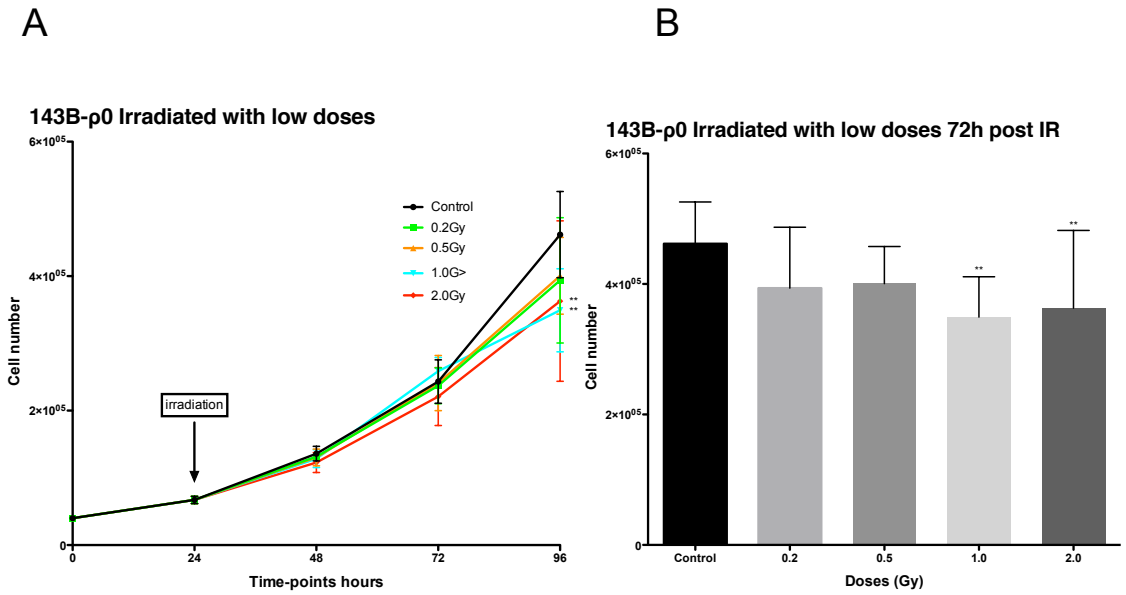

Figure 25 – *Low dose 143B-ρ0 growth curve*. **A** – Absolute cell number counted for each time-point. Control transported-only (black, circle); transported + irradiated: 0.2 Gy (green, square), 0.5 Gy (orange, upward triangle), 1.0 Gy (blue, downward triangle) and 2.0 Gy (red, diamond). **B** – Absolute cell number assessed at the 96 hours' time-point (72 hours post IR). Bars correspond to mean ± standard error. Data subjected to two-way ANOVA and posterior Bonferroni test; p values <0,01 (**).

4.3.2 Levels of superoxide

The effects of IR in ROS cell levels were analysed through $O^{\cdot -}$ production by flow cytometry, using the DHE dye.

Initially, we tested the possible disturbing effects of cell transportation to the place of irradiation (see Chapter 3, section 3.5). An irradiation dose of 2.0 Gy was used and $O^{\cdot -}$ levels measured at 5, 20, 120 minutes and 24 hours after IR.

Cy143Bwt

For the Cy143Bwt cell line, the increase in $O^{\cdot -}$ levels was maximal 20 minutes after IR, comparing with control, decreasing in the 120 minutes time-point. However, the levels of $O^{\cdot -}$ also increased in the control group along the different time-points, what lead to a less evident increase in the $O^{\cdot -}$ levels in the irradiated setting (Figure 26). The 20' time-point seemed to be one where less impact from cell transportation was observed and the increase in $O^{\cdot -}$ levels was due to irradiation effects.

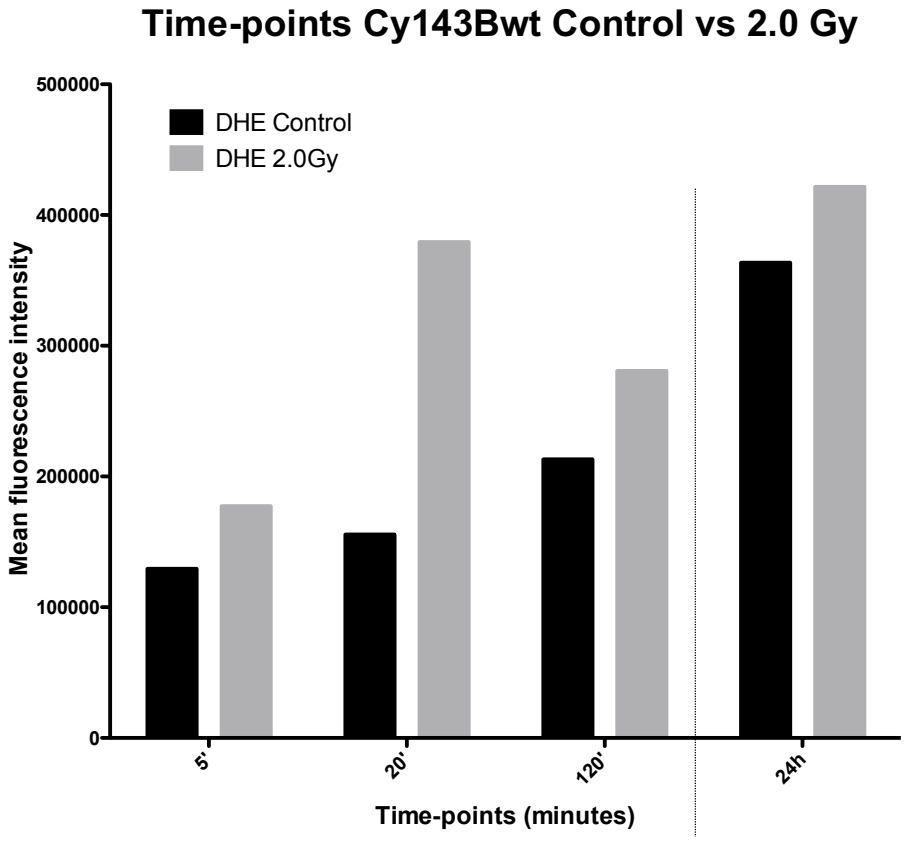

Figure 26 – *Levels of superoxide Cy143Bwt* – Fluorescence mean observed in the FL2-A channel on BD Accuri C6. Comparison between non-irradiated transported-only cells (black bars), and transported + irradiated cells (grey bars), for the time points assessed (5', 20',120' and 24h).

Cy143BMELAS

Similar to what was observed for Cy143Bwt, the levels of $O^{\cdot -}$ for the Cy143BMELAS cell line showed the highest increase at 20 minutes after IR (Figure 27). Again, 24 hours after IR, both the control and irradiated cells had high levels of $O^{\cdot -}$, making this increase less pronounced (with the exception of 5 minutes time-point, where no difference was observed between non-irradiated and irradiated cells).

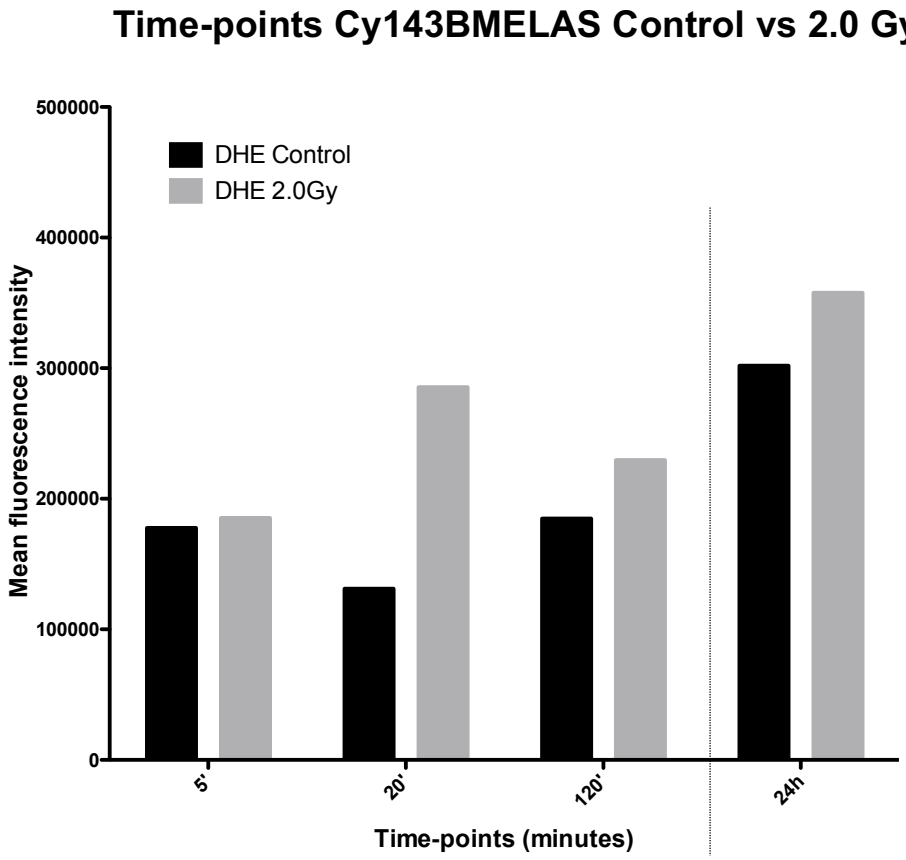

Figure 27 – *Levels of superoxide Cy143BMELAS* – Fluorescence mean observed in the FL2-A channel on BD Accuri C6. Comparison between non-irradiated transported-only cells (black bars), and transported + irradiated cells (grey bars), for the time points assessed.

143B-ρ0

Basal levels of $O^{\cdot -}$ were very low in this cell line and did not change with radiation exposure, as observed in the other cell lines. Analogous to what happened with the other cell lines, there was a slight increase across the time-points.

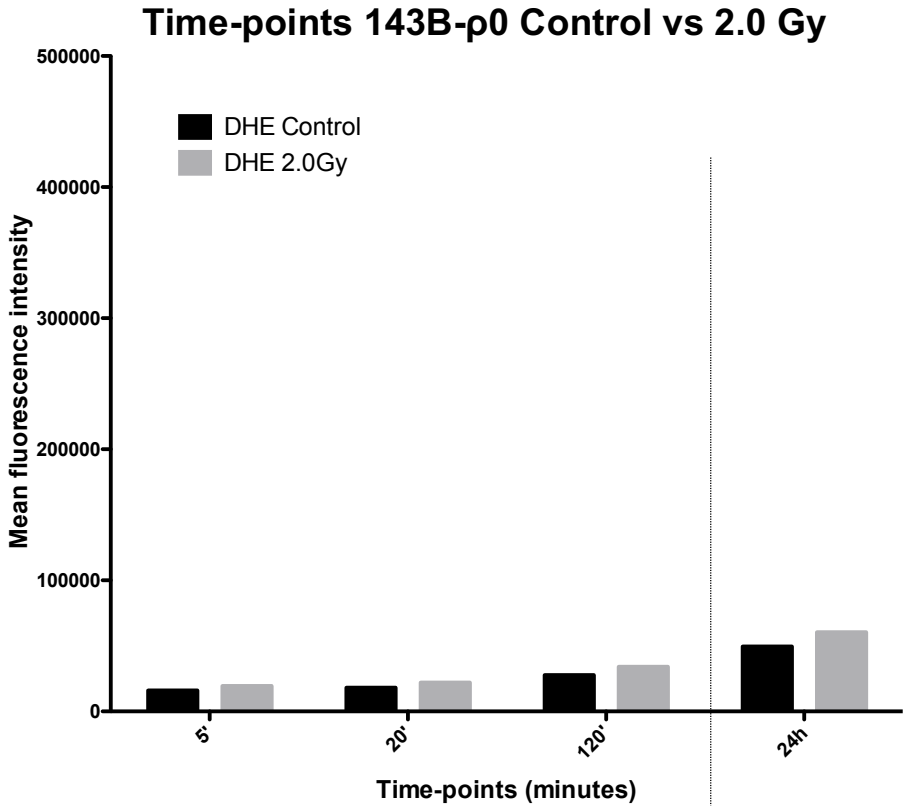

Figure 19 – *Levels of superoxide 143B-ρ0* – Fluorescence mean observed in the FL2-A channel on BD Accuri C6. Comparison between non-irradiated transported-only cells (black bars), and transported + irradiated cells (grey bars), for the time points assessed.

Upon evaluation of the effects after IR overtime, we decided to use the 20' time-point to compare the levels of $O^{\cdot -}$ between cell lines, as it was the one with minimal transportation effects in $O^{\cdot -}$ levels (control group) and maximal changes due to IR.

Comparing the levels of $O^{\cdot -}$ between the three cell lines, at this time-point, (Figure 29), we observed that 2.0 Gy dose induced an increase in $O^{\cdot -}$ levels in both Cy143Bwt and Cy143BMELAS, but no effect was observed for 143B-ρ0 cell line. The effect is slightly more pronounced in Cy143Bwt compared with Cy143BMELAS.

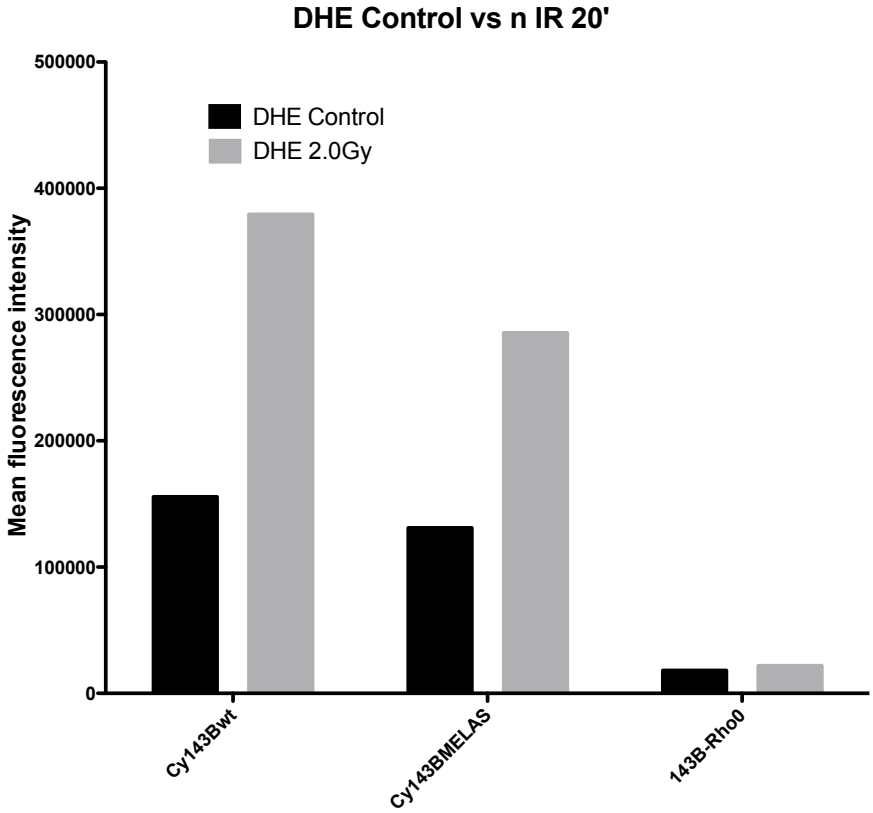

Figure 20 – *Levels of superoxide for the three cell lines, 20 minutes* – Fluorescence mean observed in the FL2-A channel on BD Accuri C6. Comparison between non-irradiated transported-only cells (black bars), and transported + irradiated cells (grey bars) for the three cell lines.

4.3.3 Effects on membrane potential

Membrane potential was evaluated with the MitoTracker™ Red CMXRos by flow cytometry. Irradiation exposure seemed to have little effect on membrane potential, although a slight decrease was observed in the irradiated Cy143Bwt and Cy143BMELAS cell lines. Contrarily, in 143B-ρ0 cell line, whose control group had lower membrane potential comparing with the other control groups, IR seems to slightly increase this parameter (Figure 30).

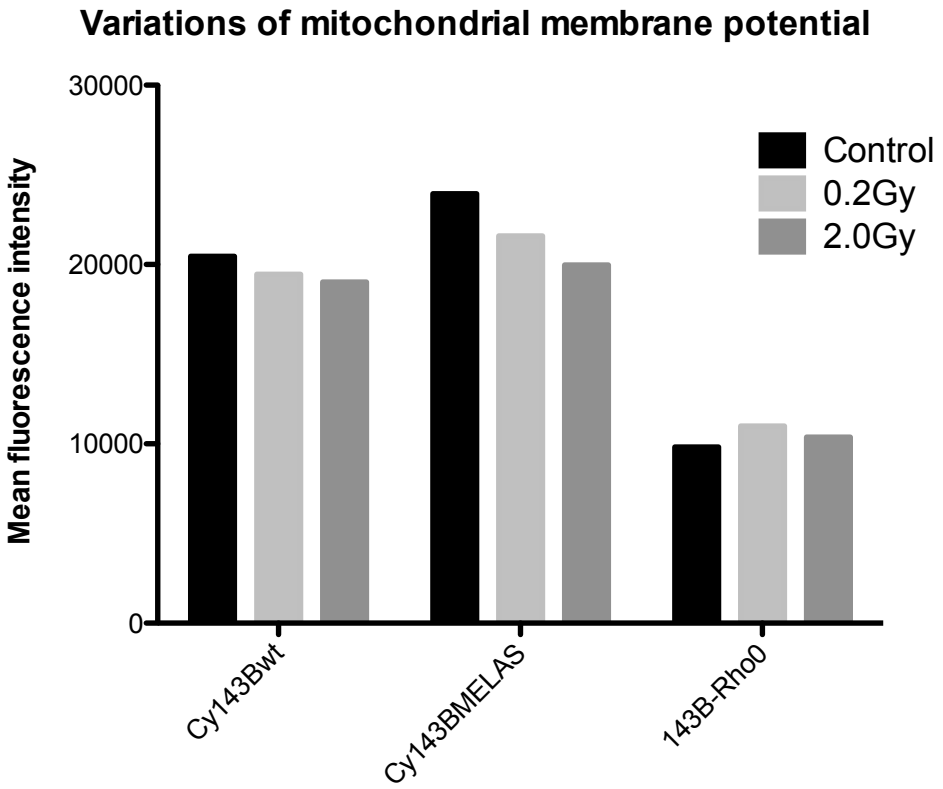

Figure 30 – *Mitochondrial membrane potential 20 minutes after IR* – Fluorescence mean observed in the FL3-A channel on BD Accuri C6. Comparison between non-irradiated, transported-only cells (black bars), and transported + irradiated cells, with 0.2 Gy (light grey bars) and 2.0 Gy (dark grey bars).

4.3.4 DNA evaluated as double strand breaks – γH2AX

Direct IR damage of nuclear DNA was evaluated as DNA DSBs, using the γH2AX assay. Foci number were counted for the doses administered (0.2 Gy and 2.0 Gy). In all cell lines, an increase relative to control was observed in the number of γH2AX foci in IR exposed cells (Figure 31, A).

The Cy143Bwt showed less IR induced γH2AX foci number comparing with the other two cell lines. However, basal levels for this cybrid were already lower, relative to the other cell lines. 143B-ρ0 cell line had the highest increase in DSBs foci number and, for 2,0 Gy this was found to be statistically significant (p value <0,001) (Figure 31, B)

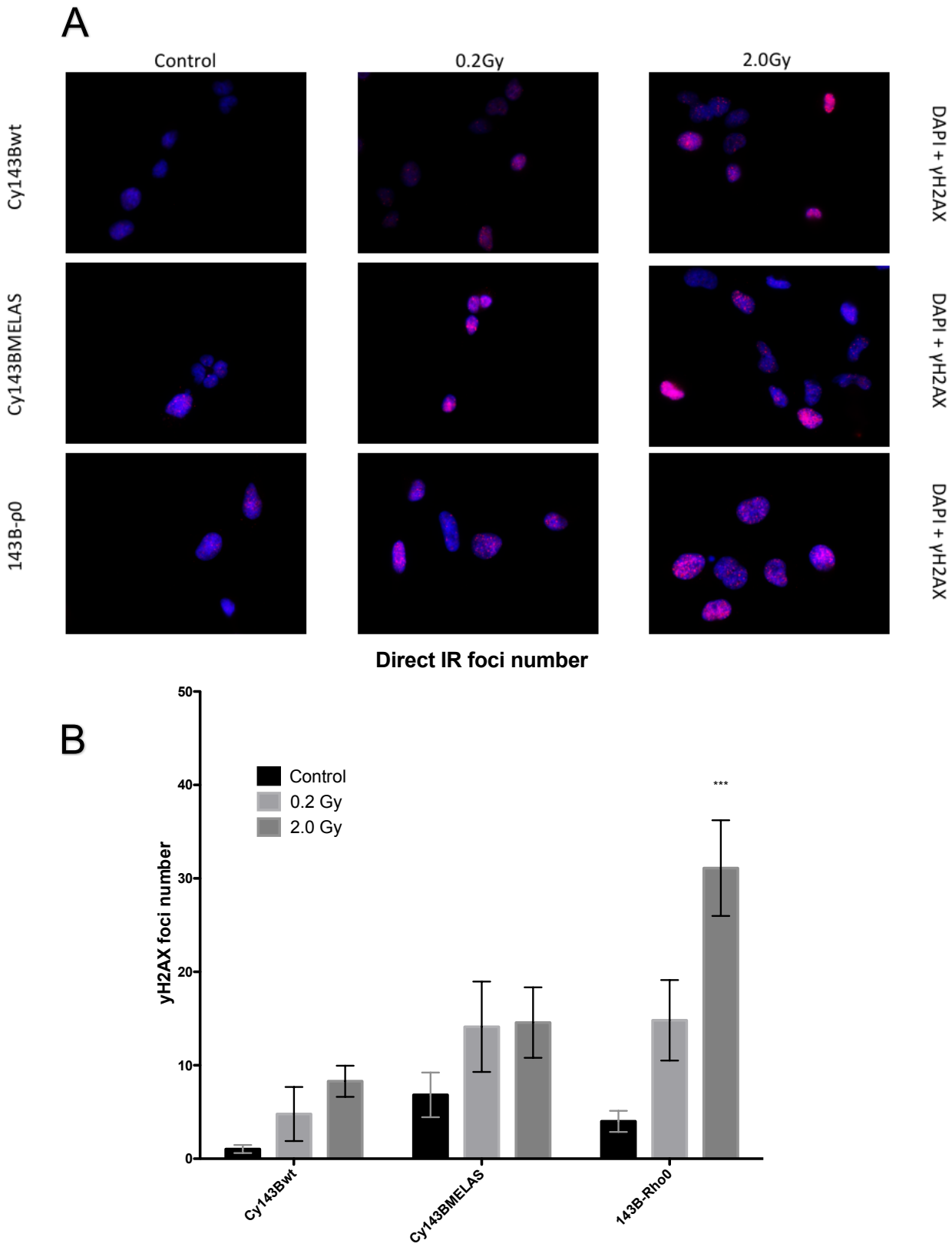

Figure 31 – *Number of γH2AX foci number after IR* – **A** – Images obtained in the fluorescence microscope, showing localization of γH2AX foci (red fluorescence) in the nucleus (blue fluorescence, DAPI). Images were taken with the 63x objective. **B** – After processing the images in Image J software, the number of DSB was counted and a comparison between non-irradiated transported-only cells (black bars), and transported + irradiated cells (grey bars, light grey for 0.2 Gy and dark grey for 2.0 Gy). Bars correspond to mean ± standard error. Data subjected to two-way ANOVA and posterior Bonferroni test; p values <0,001 (***).

4.3.5 Apoptosis induction

Apoptosis induction by IR was assessed by flow cytometry, labelling cells with Annexin V, 24 hours after irradiation (Figure 32, A)

Lower percentage of apoptotic cells was found in irradiated Cy143Bwt, relative to control. For the Cy143BMELAS, which showed lower number of apoptotic cells in the control conditions compared with the other cell lines, IR appeared to have no effect. 143B-ρ0 cell line, which had higher percentage of apoptotic cells in control group, in relation to the other cell lines, IR apparently also had no effect (Figure 32, B).

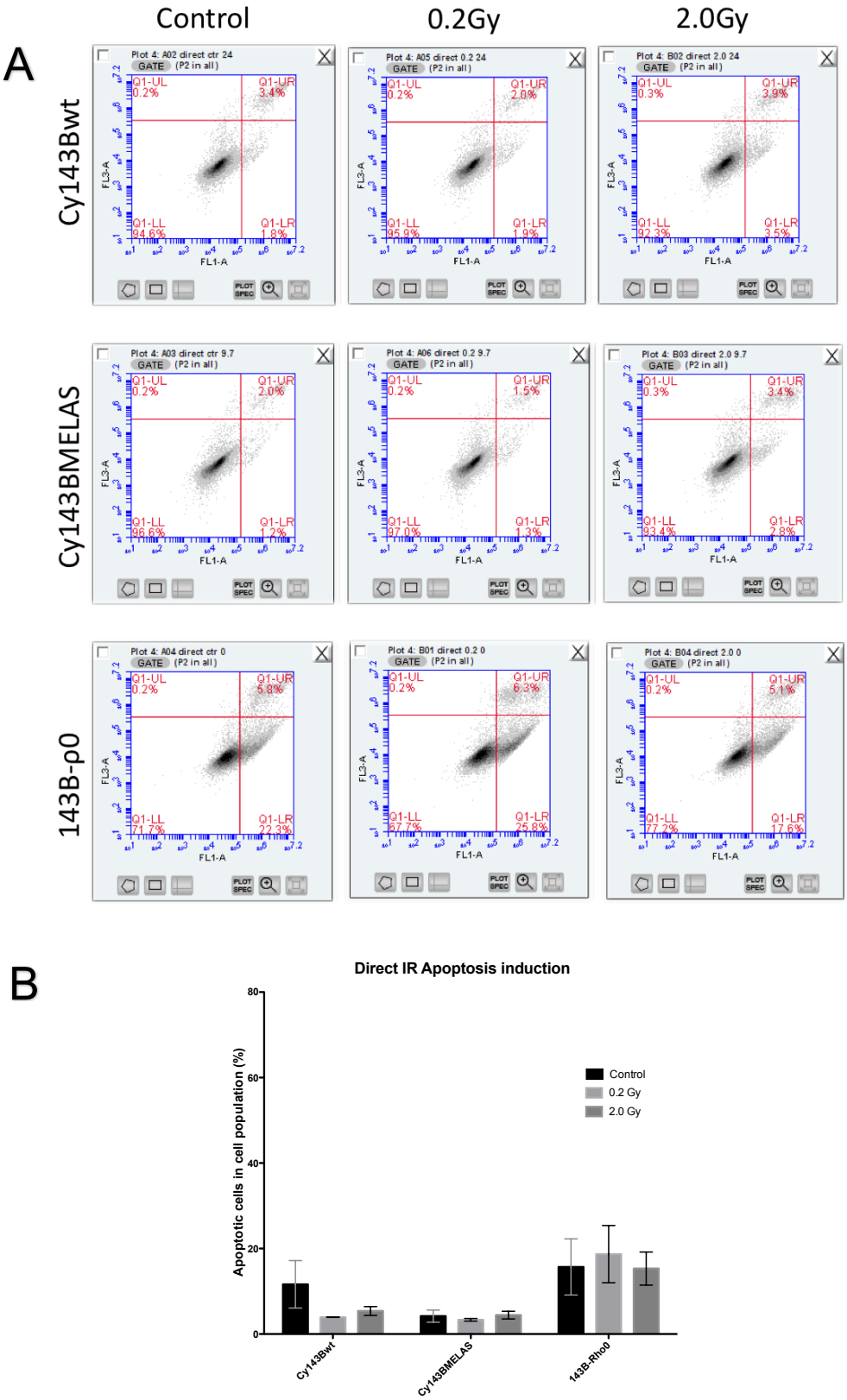

Figure 32 – *Percentage of apoptotic cells after IR* – **A** – Apoptosis was evaluated 24 hours after IR using flow cytometry. The population of was isolated according and the gates chosen to distinguish the percentages of cells viable (Q1-LL) from early apoptotic (Q1-LR), late apoptotic (Q1-UR), and necrotic (Q1-UR). B – From the plots in **A**, the percentages were used to plot a bar graphic, showing non-irradiated transported-only cells (black bars); transported + irradiated cells (grey bars, light grey for 0.2 Gy and dark grey for 2.0 Gy). Bars correspond to mean ± standard error. Data subjected to two-way ANOVA and posterior Bonferroni test.

4.4 Cellular response to irradiated cells conditioned media (ICCM)

The response to ICCM was investigated by testing its capacity to induce nuclear DNA damage and apoptosis. In these assays, the control was the group of cells receiving media from non-irradiated cells.

DNA damage was evaluated using the γH2AX assay, and apoptosis induction using the Annexin V protocol.

4.4.1 DNA damage evaluated as double strand breaks – γH2AX

ICCM from Cy143Bwt

The number of DSBs foci number induced by the Cy143Bwt ICCM was higher for 0.2 Gy in both Cy143Bwt (with statistical significance) and Cy143BMELAS, while 2.0 Gy ICCM induced more DSBs in 143B-ρ0 (Figure 33)

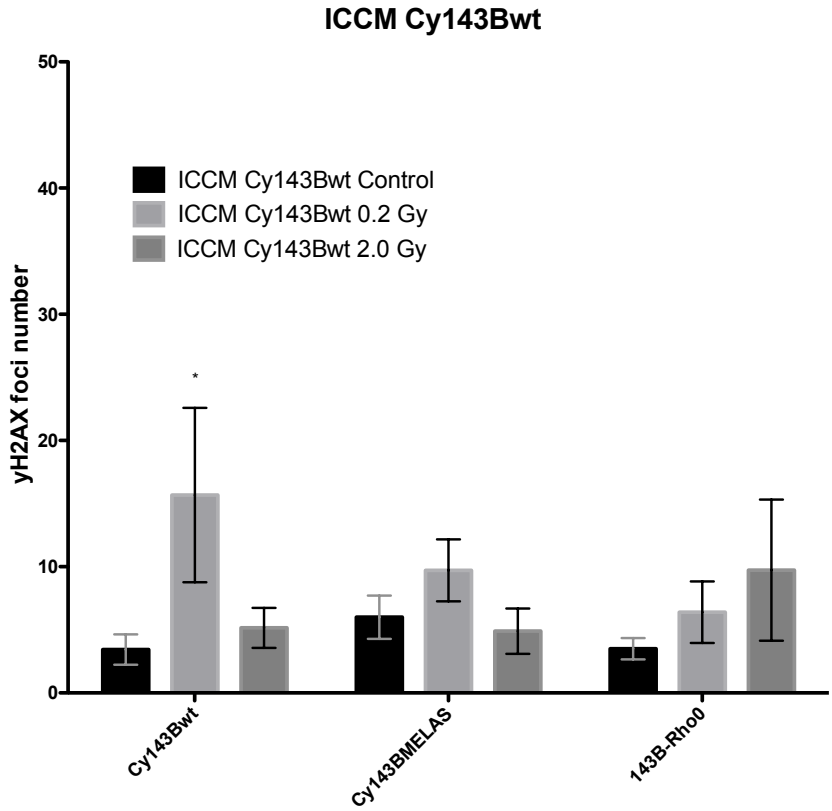

Figure 33 – *Number of γH2AX foci number after treatment with Cy143Bwt ICCM* – After 1 hour with ICCM, cells were stained with γH2AX antibody and the number of DSBs counted. Non-irradiated transported-only cells media (black bars); transported + irradiated cells ICCM (grey bars, light grey for 0.2 Gy and dark grey for 2.0 Gy). Bars correspond to mean ± standard error. Data subjected to two-way ANOVA and posterior Bonferroni test, p value <0,05 (*)

ICCM from Cy143BMELAS

ICCM obtained from Cy143BMELAS cells irradiated with 2.0 Gy caused more DSBs in Cy143Bwt, comparing with 0.2 Gy. In Cy143BMELAS it did not induce any differences, comparing with control. ICCM Cy143BMELAS, both 0.2 Gy and 2.0 Gy, increased the γH2AX foci number in 143B-ρ0, without statistical significance (Figure 34).

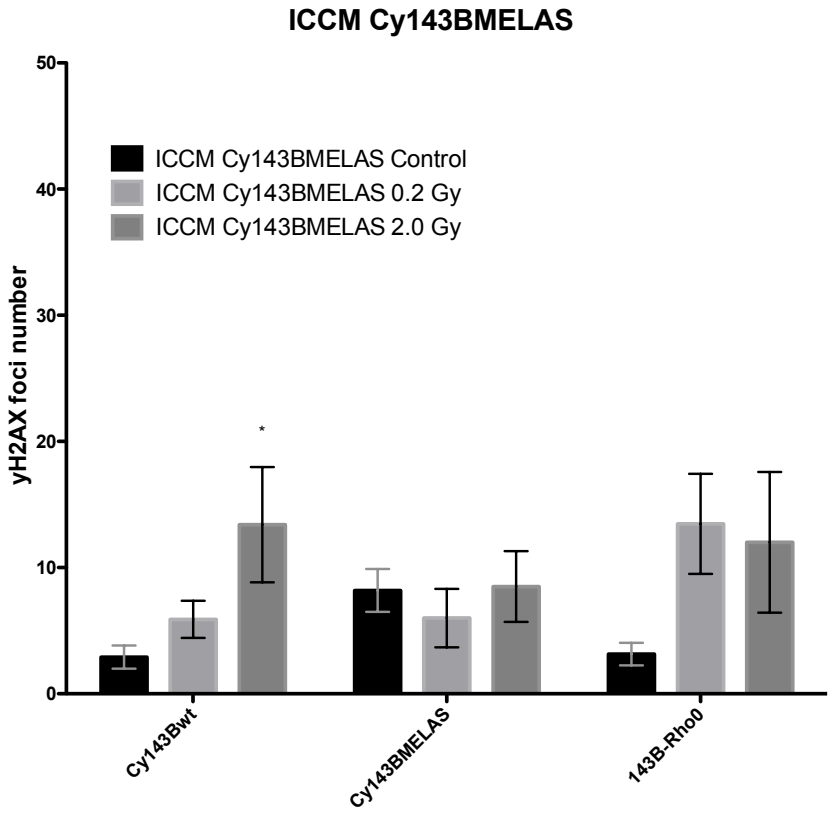

Figure 34 – *Number of γH2AX foci number after treatment with Cy143BMELAS ICCM*. After 1 hour with ICCM, cells were stained with γH2AX antibody and the number of DSBs counted. Non-irradiated transported-only cells media (black bars); transported + irradiated cells ICCM (grey bars, light grey for 0.2 Gy and dark grey for 2.0 Gy). Bars correspond to mean ± standard error. Data subjected to two-way ANOVA and posterior Bonferroni test, p value <0,05 (*)

ICCM from 143B-ρ0

ICCM collected from 143B-ρ0 cells was not able to increase DSBs (Figure 35). Interestingly, when comparing with control, there was a decrease in DSBs in cells incubated with 0.2 Gy ICCM which was statistically significant for Cy143BMELAS and 143B-ρ0 cell lines.

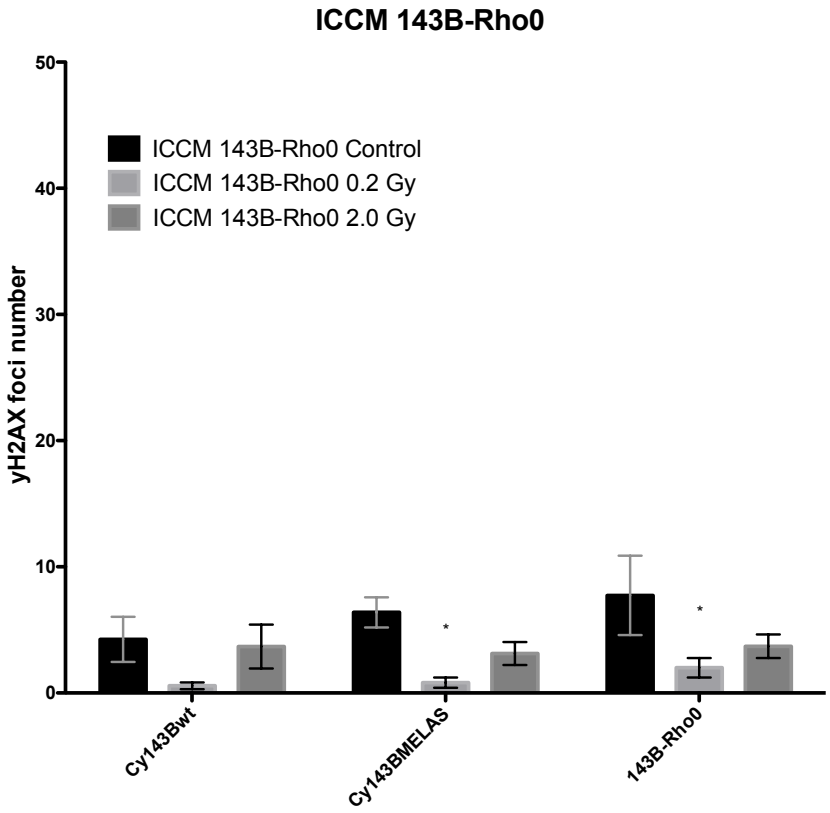

Figure 35 – *Number of γH2AX foci number after treatment with ICCM 143B-ρ0.* After 1 hour with ICCM, cells were stained with γH2AX antibody and the number of DSBs counted. Non-irradiated transported-only cells media (black bars); transported + irradiated cells ICCM (grey bars, light grey for 0.2 Gy and dark grey for 2.0 Gy). Bars correspond to mean ± standard error. Data subjected to two-way ANOVA and posterior Bonferroni test, p value <0,05 (*).

4.4.2 Apoptosis induction

ICCM from Cy143Bwt

ICCM obtained from Cy143Bwt cells irradiated with 0.2 Gy was the only that seemed to slightly affect apoptosis, relative to the cell line cell line control (Figure 36). Apart from this, the other cell lines seemed to not be affected by ICCM.

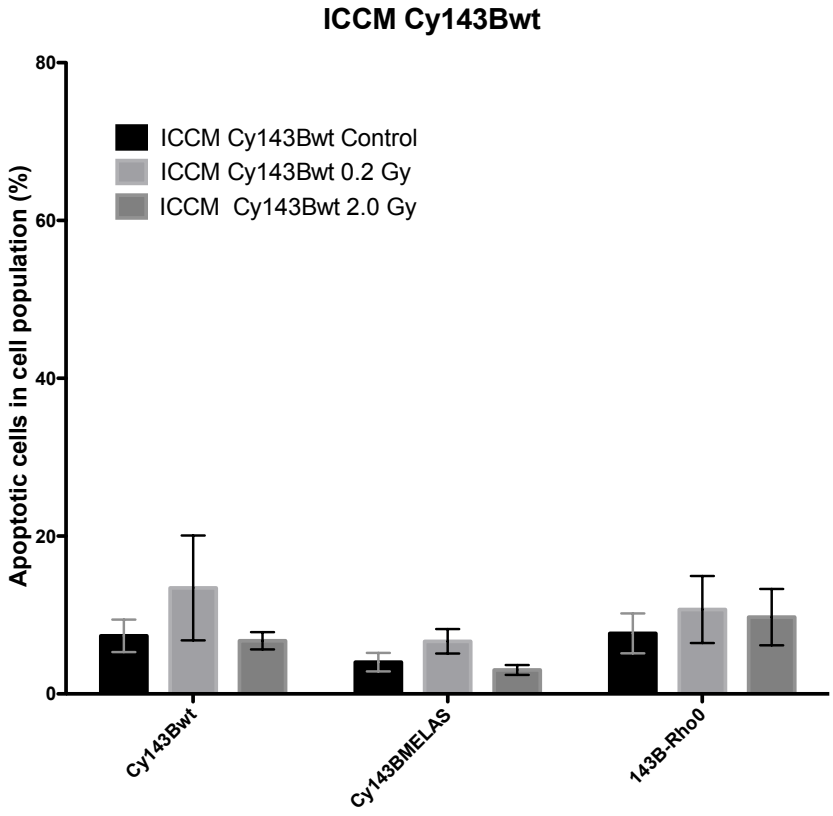

Figure 36 – *Percentage of apoptotic cells after Cy143Bwt ICCM.* After 24 hours with ICCM, apoptosis was evaluated. Non-irradiated transported-only cells media (black bars); transported + irradiated cells ICCM (grey bars, light grey for 0.2 Gy and dark grey for 2.0 Gy). Bars correspond to mean ± standard error. Data subjected to two-way ANOVA and posterior Bonferroni test.

ICCM from Cy143BMELAS

No major differences were observed for ICCM from Cy143BMELAS irradiated with different IR doses (Figure 37).

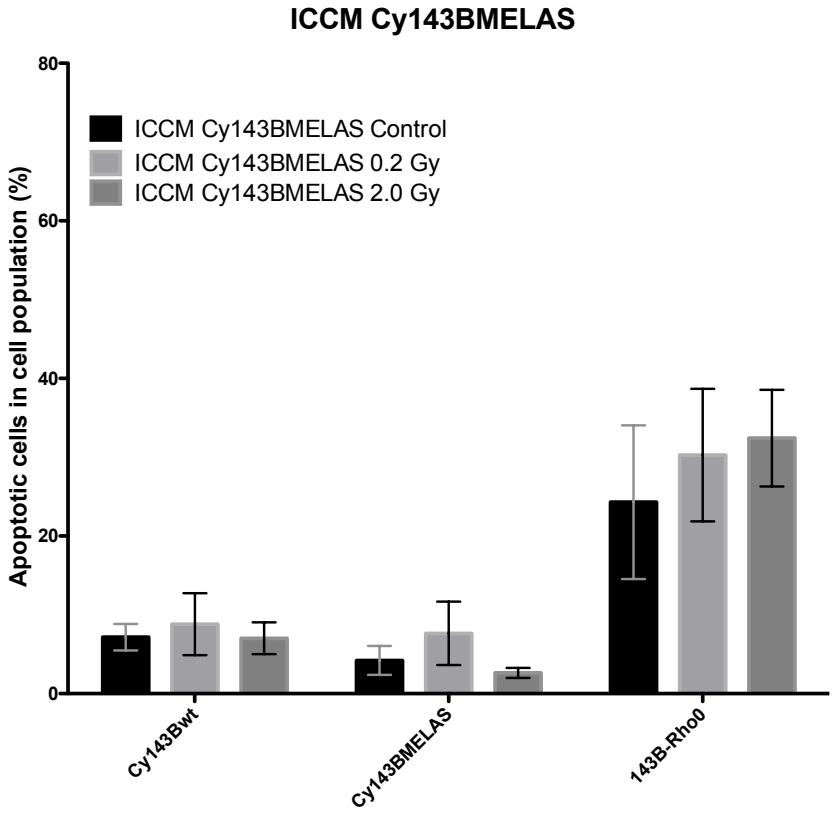

Figure 37 – *Percentage of apoptotic cells after Cy143BMELAS ICCM.* After 24 hours with ICCM, apoptosis was evaluated. Non-irradiated transported-only cells media (black bars); transported + irradiated cells ICCM (grey bars, light grey for 0.2 Gy and dark grey for 2.0 Gy). Bars correspond to mean ± standard error. Data subjected to two-way ANOVA and posterior Bonferroni test.

ICCM from 143B-ρ0

Increased apoptosis induction was not observed with ICCM from the 143B-ρ0 cell line (Figure 38).

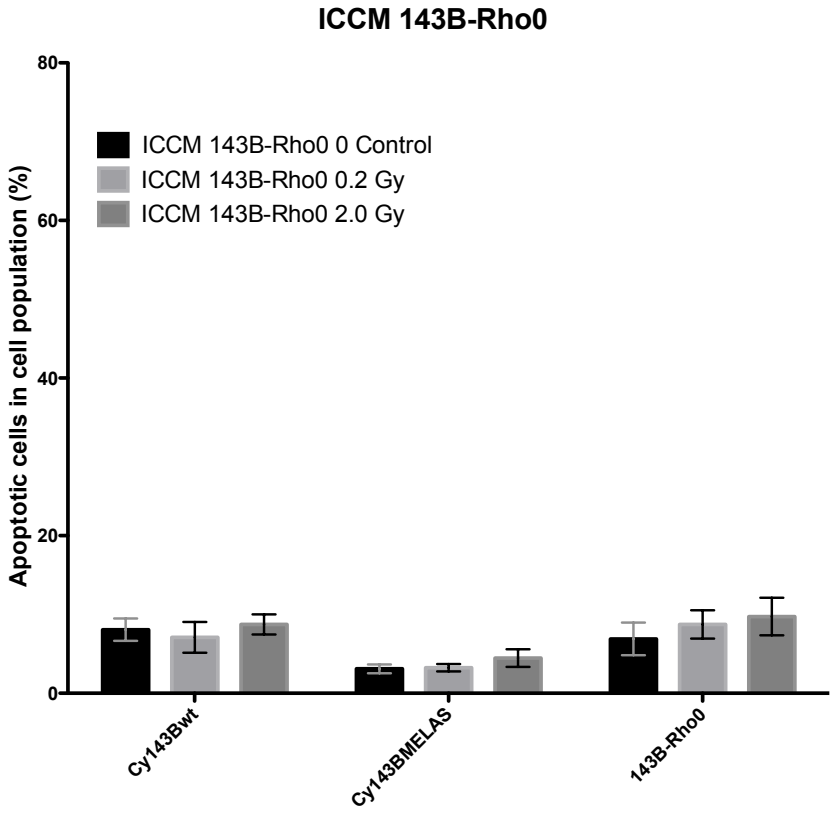

Figure 38 – *Percentage of apoptotic cells after 143B-ρ0 ICCM.* After 24 hours with ICCM, apoptosis was evaluated. Non-irradiated transported-only cells media (black bars); transported + irradiated cells ICCM (grey bars, light grey for 0.2 Gy and dark grey for 2.0 Gy). Bars correspond to mean ± standard error. Data subjected to two-way ANOVA and posterior Bonferroni test.

Chapter 5

Discussion

5. Discussion

RB is a field open to possibilities; with the knowledge that IR may affect cells not directly traversed by it, the molecular aspects of the biological response to radiation are object of renewed interest.

RIBE are not yet well understood and the nature of the signals transmitted after IR inducing a bystander response in cells remains to be elucidated.

Mitochondria are essential organelles in the cells which participate in the regulation of a myriad of cellular functions. Of interest to this study, mitochondria regulate the response to insult. In the RIBE context, cells without mitochondria or with impaired mitochondrial function do not produce, upon irradiation, factors that induce a bystander effect in unirradiated cells. The influence of mitochondria on bystander signalling is not fully understood, so we addressed it in the present work. Cybrid cell lines have been established and are interesting models for studying mitochondrial function and their influence on cellular homeostasis.

One of the cybrids used was Cy143BMELAS. The mechanisms underlying MELAS cytopathy are still being unveiled, however, there is evidence that the A3243Tmutation contributes to respiratory chain enzymes defects, leading to impaired mitochondrial function and increased ROS levels(Flierl, Reichmann, & Seibel, 1997). Finding the effects of such imbalance to bystander signalling and response was another question we tried to address in this project.

Using PCR, we confirmed the presence of the A3243T mutation in Cy143BMELAS; it was present with approximately 60% of heteroplasmy. MELAS syndrome has a mutation threshold below which no phenotypic manifestations are observed (El-Hattab et al., 2015). Considering that Cy143BMELAS is a cancer cell line manipulated to incorporate a certain mtDNA mutation load (Nunes et al., 2015), the threshold for the manifestation of a phenotype typical of the MELAS syndrome could be different from the one observed in the hereditary disease clinical setting. The 60% heteroplasmy observed in our work was considered adequate to study the influence of this mutation on cellular mechanisms, as this mutational load was similar to what was used in other cybrid studies (Moudy et al., 1995).

The confirmation for 143B-ρ0 (mtDNA depleted cells), performed by the same method, showed a background amplification level that did not allow a clear identification of nucleotides in the electropherogram. Since the region amplified by the PCR primers is from mtDNA, ideally, it should not show any genetic material. However, it is believed that nuclear DNA has mtDNA sequences incorporated by transfer of mtDNA to the nucleus, generating nuclear copies of some mtDNA sequences (Hazkani-Covo, Zeller, & Martin, 2010; Ricchetti, Tekaia, & Dujon,

2004), which could explain the background level of nucleotides observed in in Figure 15 (page 40).

In this work, the same parental cell line for deriving the cybrids was used (either for control cybrid with WT mtDNA, or for MELAS cybrid, with mutated mtDNA). This assured that the nuclear DNA was the same and guaranteed that the variations we would observe in the response of the cells would not be not due to different nuclear backgrounds. The depletion of mtDNA, was achieved without the use of DNA disrupters which could impair nuclear DNA, and change the response.

The three cellular lines used, with different mitochondrial contents, may have different metabolic demands, as was previously shown by our group (Nunes et al., 2015). This often translates in diverse growth rates. To overcome this problem and evaluate response to IR, a basal growth curve was included to determine growth differences between the cell lines.

We observed that impaired mitochondrial function resulted into a decreased cellular growth (Figure 16, page 41). 143B-ρ0 cell line had the lowest growth rate compared with the other cybrids (Figure 16). Cells depleted of mitochondrial DNA have downregulated genes involved in the control of cell cycle, for instance, H2AFZ and H2AFX, from the histone family H2A (Mineri et al., 2009) which usually give rise to low doubling rates for these cells. These results seem to support the idea that mitochondria have a significant role in cellular mechanisms related to growth and differentiation (Spitkovsky, 2004).

Mitochondrial membrane potential is an important feature for OXPHOS, as the proton electrochemical gradient potential is used to generate ATP. Additionally, it is a well-coordinated cellular homeostasis control mechanism which works synergistically with others, to an extent not yet fully understood. In this sense, mitochondrial membrane potential assessment in the cell lines used in this work was performed in order to characterize them, considering the Cy143Bwt levels as the control group. 143B-ρ0 cell line showed the lowest membrane potential (Figure 17, page 42), as expected. Cells depleted of mtDNA have impaired OXPHOS, lacking complete electron transport chain complexes, thus obtaining energy (ATP) from glycolysis (Chandel & Schumacker, 1999). Therefore, they do not require high membrane potential to fuel ATP synthase. It is important to note that approximately 13% of the ATP produced by glycolysis is used to maintain a minimal (yet reduced) membrane potential level to sustain other cellular processes, such as protein import from the nucleus, mitochondrial structure and prevention of apoptosis without other extracellular stimuli (Martínez-Reyes et al., 2016). However, Ca^{2+} homeostasis is impaired and may affect cellular functions dependent on Ca^{2+} (Berridge et al., 2003). The same occurs for cellular functions requiring higher membrane potential (Sherer, Trimmer, Parks, & Tuttle, 2000). Giving these considerations, low membrane potential and destabilized signalling mechanisms in cells depleted of mtDNA could explain the absence of bystander signalling arising in these cells.

Cy143BMELAS cybrid cell line did not show a difference in membrane potential relative to Cy143Bwt (Figure 17). Studies using fibroblasts from patients with MELAS syndrome have shown that mitochondrial membrane potential is reduced, which could be caused by an impaired OXPHOS (James, Wei, Pang, & Murphy, 1996; Moudy et al., 1995). Although the mutational load in both studies was similar to the observed in our cell line, the cell type used was different, and the mutations leading to MELAS syndrome were not the same (A3243G instead of A3243T). Furthermore, the method for assessing this feature was not the one used in our project. The differences in the approaches used between the above referred studies and our work could explain the dissimilarities in mitochondrial membrane potential, observed in the present study.

ROS and RNS play an important role in cellular function, as they can act as signalling molecules in several situations. They can also be damaging to biomolecules. Mitochondrial dysfunction is known to increase ROS levels, especially $O^{\cdot -}$ levels, therefore we evaluated them with DHE in the cell lines used.

The normal Cy143Bwt level was considered the control for $O^{\cdot -}$ levels. $O^{\cdot -}$ level of Cy143BMELAS was slightly higher than the control (Figure 18, page 44). MELAS disease pathophysiology is not yet fully elucidated but the metabolic stroke-like episodes may be due to transient OXPHOS dysfunction, with increased production of free radicals which cause an imbalanced NO homeostasis and, consequently, vasoconstriction and stroke; this could explain increased levels of $O^{\cdot -}$ observed in Cy143BMELAS cells (Flierl et al., 1997).

$O^{\cdot -}$ levels were low in 143B-ρ0 cells compared with the other cell lines. Moreover, no increase was observed when the complex III disrupter was added (AntA). ROS are a consequence of OXPHOS respiration (Adam-Vizi & Chinopoulos, 2006), therefore, in cells depleted of mtDNA where the ATP production is conducted by glycolysis, an increase of ROS is not expected.

Having established basal levels of cellular growth, $O^{\cdot -}$ levels, and mitochondrial membrane potential, we evaluated cellular response to IR using the same assays. Firstly, we used high doses, ranging from 2.0 Gy – which is the normal dose used per fraction in a RT setting – to 10.0 Gy. All doses reduced cellular growth in every cell line used. As we were interested in the low dose scenario of RT, we tested low doses (below 2.0 Gy) to infer about their impact on cellular growth. The reduction in cell growth was more evident for high doses, ranging from 1.0 Gy up to 10.0 Gy. This might have occurred as higher doses deposit more energy, increasing the damage inflicted.

Cells have different radiosensitivity to IR damage according to the phase of the cell cycle at the moment of radiation exposure (Hall et al., 2012; Pawlik & Keyomarsi, 2004). In the clinics, irradiation with multiple fractions has the effect of synchronizing cell cycles in the cell

population irradiated, via the cell cycle checkpoints activated by the ATM pathway (Pawlik & Keyomarsi, 2004). Cell cycle synchronization would result in a more homogeneous response to IR and elimination of the radiosensitivity bias of the cell cycle phase. Thereby, it will be a valuable approach for future studies.

We proceeded with the evaluation of $O^{\cdot-}$ levels, known to induce damage after IR. The 143B-ρ0 cells had very low basal levels of $O^{\cdot-}$ and IR did not generate a significant increase in this parameter. Considering that ROS play a role in stress signalling and in the bystander effect, these results could explain the absence of bystander signalling in cells without mtDNA. Cy143Bwt and Cy143BMELAS showed increased levels after irradiation, with a peak at 20 minutes. No difference was found between control and irradiated cells when the measurements were made 5 minutes after IR which could reflect the kinetics of $O^{\cdot-}$ production, consequence of stress. At the 24 hours time-point, the levels for the unirradiated and irradiated groups were higher when compared with the initial measures (Figures 26, 27 and 28, pages 51,52 and 53, respectively), what could be related with the stress induced by transport. In fact, if we look at the levels of the first $O^{\cdot-}$ assay (Figure 18, page 44), when no transportation was performed, the values for the control groups are lower than the ones observed in the first time-point of the irradiation experiments. Interestingly, our measures in 143B-ρ0 also showed a rise in $O^{\cdot-}$ levels at 24 hours, meaning that even for this cell line transportation increased ROS levels.

Mitochondrial membrane depolarisation can be triggered by a number of factors, namely, increased ROS levels, ER stress or high intracellular Ca^{2+} concentrations. Another form of reducing mitochondrial membrane potential seems to be IR as shown by Taneja *et al.* (Taneja, Tjalkens, Philbert, & Rehemtulla, 2001). Since mitochondrial membrane potential is important for several signalling pathways (Tait & Green, 2012), we investigated the effect of IR in this parameter. Our results show a slight decrease, compared with unirradiated controls, in Cy143Bwt and Cy143BMELAS cell lines. The 2.0 Gy dose seemed to decrease membrane potential more than the 0.2 Gy dose, but the difference was not significant, as the results derived from a single experiment, which could explain the lack statistical significance. Nevertheless, we do not exclude that other time-points post IR, beyond the ones investigated, may impact mitochondrial membrane potential. Shonai *et al.* observed a maximal mitochondrial membrane potential breakage at 12 hours post IR (Shonai et al., 2002). Thereby, other timescales for IR effects on mitochondrial membrane potential might be considered in future studies.

Presumably, high $O^{\cdot-}$ levels would lead to more DNA damage, so we evaluated the levels of DNA DSBs after IR. The basal levels of DNA damage varied between the cell lines. DNA damage was slightly higher for the Cy143BMELAS, what could indicate a decreased equilibrium state of these cells due to mitochondrial dysfunction. To the extent of our knowledge, the correlation between mitochondrial dysfunction and DNA damage has not been postulated in the radiation context. However, since cells with impaired mitochondria have persistent oxidative stress (T. Yoshida, Goto, Kawakatsu, Urata, & Li, 2012) and ROS are known to cause DNA damage (Kryston, Georgiev, Pissis, & Georgakilas, 2011), this relationship is plausible. Our results showed, for every cell line, an increase in the number of DSBs in the irradiated cells. In the Cy143BMELAS, γH2AX foci increased in a similar manner for 0.2 Gy and 2.0 Gy IR doses, while only 2.0 Gy IR dose induced DNA damage in Cy143Bwt. mtDNA mutations have been associated with higher sensitivity to IR (Kulkarni, Marples, Balasubramaniam, Thomas, & Tucker, 2010). Our results seem to reflect this, as a low dose (0.2 Gy) caused the same damage of a high dose (2.0 Gy) in Cy143BMELAS. Nevertheless, the increase in the number of DNA DSBs was not statistically significant. Thereby, the results should be interpreted with caution.

The 143B-ρ0 cells had an increase in DSBs foci, which was statistically significant for 2.0 Gy. The radiosensitivity of cells depleted of mtDNA is subjected to controversy, with reports suggesting that these cells would be more sensitive and others suggesting the opposite (Cloos et al., 2010; van Gisbergen et al., 2017; K. Yoshida et al., 2000). Curiously, for the 143B-ρ0 cell line, the increase in DNA damage after IR could not be linked to $O^{\cdot-}$ levels. Donthamsetty *et al.* (Donthamsetty et al., 2014), also using a 143B osteosarcoma derived ρ0 cell line, showed that ρ0 cells were stopped at the G2/M transition of the cell cycle. As previously mentioned, G2 and M are considered the more radiosensitive phases, which could explain why, in our work, 143B-ρ0 cells showed more DSBs after IR.

DSBs could lead to an increase in the number of cells unable to efficiently repair damage and, therefore, undergo apoptosis. Strikingly, no increase in the percentage of cells undergoing apoptosis was observed. Although the results were not statistically significant, Cy143Bwt showed a decreased number of cells undergoing apoptosis after irradiation, for both doses tested (0.2 Gy 2.0 Gy). No changes were observed in Cy143BMELAS after IR. Contrarily, in the 143B-ρ0 cell line, a slight increase in apoptosis was observed after irradiation with 0.2 Gy. However, this effect was no longer apparent for the 2.0 Gy IR dose. These results should be interpreted cautiously, as they are not statistically significant. Furthermore, apoptosis was evaluated 24 hours after IR and DNA damage was evaluated 1 hour after IR. Other time-points after IR may be considered in the future to better explore the relation between DNA damage and programmed cell death.

It might also be noted that osteosarcoma tumours are overall resistant to therapy, namely to radiotherapy (Raymond & Jaffe, 2009). The mechanism behind this resistance is still to be fully revealed, although some investigations have shown that hypoxia mechanisms could be involved, as well as the B-cell lymphoma 2 protein (Bcl2), considered an important anti-apoptotic protein which is found elevated in osteosarcoma tissues (Nedelcu et al., 2008).

So far, our results have shown that there are certain specificities for each cell line regarding the response to IR. Our next goal was to evaluate their capacity of inducing a bystander effect. ICCM is one of the most used methods to emulate a bystander signalling and response. Considering the fact that the response to media from irradiated seems to mirror what occurs in direct response to IR, DNA damage and apoptosis in bystander cells was assessed.
DNA damage was evaluated using γH2AX foci number, 1 hour after contact with ICCM.
We observed that ICCM from the Cy143Bwt and Cy143BMELAS cell lines had the ability to increase the number of DSB sites, compared with control. Nevertheless, differences in the behaviour of the three cell lines were observed, either causing or responding to the bystander effect. 0.2 Gy ICCM from Cy143Bwt cell line induced damage in Cy143Bwt and Cy143BMELAS, comparing with 2.0 Gy ICCM from Cy143Bwt cells. The fact that a low dose causes this type of damage corroborates the notion that low doses of IR seem to cause more damage to cells via the bystander effect (Kadhim et al., 2013). There is not, however, a consensus in this matter (M. P. Little, 2010; Nuta & Darroudi, 2008). In 143B-ρ0 cells, Cy143Bwt 2.0 Gy ICCM induced more γH2AX foci, compared with 0.2 Gy ICCM. This difference in the response to the same ICCM (in this case, 0.2 Gy ICCM from Cy143Bwt) may suggest that mitochondrial function plays a role in the response to bystander signals as these cells are mtDNA depleted.
Cy143BMELAS ICCM induced a slight damage, relative to control, in the Cy143BMELAS cells, comparing to the other two cell lines which showed increased DSBs In Cy143Bwt cell line, 2.0 Gy Cy143BMELAS ICCM induced more DSBs than 0.2 Gy Cy143BMELAS ICCM, but in 143B-ρ0 it was the other way around Considering that Cy143BMELAS cells were not responsive to ICCM, it seems to be reasonable to assume, that an altered mitochondrial function may change the response to ICCM. Additionally, ICCM of the 3 cell lines collected after exposure to the same irradiation dose gave rise to different responses, which could mean that mitochondrial status may affect the ICCM composition. Contrarily to our results, Rajendran *et al.* (Rajendran, Harrison, Thomas, & Tucker, 2011) indicated that mutant mitochondrial DNA impaired bystander effect. Again, the nature of the mutation could be behind the differences in these results.
The 143B-ρ0 ICCM did not increase DNA damage in the three cell lines evaluated. This sustains the premises of our inquiry, in which we hypothesise that the absence of mtDNA

renders irradiated cells incapable of inducing a bystander effect. Interestingly, 0.2 Gy ICCM decreased, relative to control, γH2AX foci number in all cell lines, which was statistically significant in Cy143BMELAS and 143B-ρ0.

To understand if induced DNA damage would translate into apoptosis, Annexin V assay was performed in cells exposed to ICCM for 24 hours. We observed a parallel between DNA damage and apoptosis results. Cy143Bwt 0.2 Gy ICCM caused more apoptosis in Cy143Bwt and Cy143BMELAS. In 143B-ρ0 cells, ICCM from Cy143Bwt 2.0 Gy increased the number of apoptotic cells. Cy143BMELAS ICCM had no effect in Cy 143BMELAS cells but 2.0 Gy ICCM slightly increased apoptosis in Cy143Bwt cells. Cy143BMELAS ICCM, both 0.2 and 2.0 Gy, induced similar levels of apoptosis in 143B-ρ0, which were higher compared with control. Nevertheless, all these were slight differences without statistical significance, suggesting the need for performing more experiments.

It seems that DNA damage caused by ICCM factors is lethal to the unirradiated cells, inducing apoptosis, contrarily to what was observed with direct irradiation. Considering this, the argument for impaired apoptosis suggested for osteosarcoma cells (Nedelcu et al., 2008) does not justify the high apoptosis levels observed after ICCM exposure. A possible explanation for this difference could be that, somehow, IR has the ability to activate repair or protective mechanisms, whereas bystander signals are not able to do so. Ghandhi *et al.* have shown two transcriptional pathways which regulate direct response to IR, implicated in different degrees in the bystander response (Ghandhi, Yaghoubian, & Amundson, 2008). Contrarily to our results, this study showed higher survival of bystander cells (with increased risk of perpetuating genomic defects). Other authors suggested that the response to bystander signals and consequential DDR, arise via different pathways (Burdak-Rothkamm, Short, Folkard, Rothkamm, & Prise, 2007). Burdak-Rothkamm *et al.* showed that γH2AX foci formation in bystander cells was ATR-dependent (instead of ATM dependent, like the DDR after direct irradiation (Burdak-Rothkamm et al., 2007). This may suggest different mechanisms for direct IR and bystander response, justifying the results observed in the present study.

It is also possible that the nature of the damage is different. We considered a quantitative analysis, but not qualitative, for DNA damage. It is possible that, in the case of ICCM experiments, DNA damage observed with the γH2AX assay may not have been on apoptosis related genes. Contrarily, in the direct IR scenario, apoptosis promoting genes could have been damaged and this process blocked.

Our results suggest that DSBs analysis and apoptosis may be used as complementary approaches, to better characterize the response to IR. Moreover, other tests should also be performed in order to better elucidate the nature of the response to both IR and ICCM. For instance, evaluation of apoptotic gene expression.

Additionally, *in vitro* assays have the obvious disadvantage of being poorly related to the biological system reality. In the context of the bystander effect, in a microenvironment scenario, with multiple players modulating the response to IR, the sensing and transducing of factors is certainly much more intricate. More complex experimental models would be preferable, such as 3D cell cultures assemblies or *in vivo* models.

Chapter 6

Conclusions

6. Conclusions

Considering the multiple mechanisms involved in the response to radiation exposure, RB is a study area that would benefit from approaches aiming to study IR interactions at a cellular/molecular level, especially for the low doses which attain healthy tissues adjacent to the targeted tumour.

Mitochondria role in the modulation of several cellular signalling pathways is an interesting topic, linking IR response to 'stress' signals and adaptive responses to IR.

To better clarify the role of mitochondria in the non-targeted effects of radiation exposure, we used the cybrid model approach, with a cell line with mitochondrial dysfunction, and another without mtDNA.

We concluded that mitochondrial dysfunction (mutated DNA or mtDNA absence) may affect the response to IR. Furthermore, mitochondrial impairment could also change the response of cells to bystander signals. We also observed a difference in apoptosis between the directly irradiated cells and the cells exposed to ICCM.

As proof of concept, we observed that absence mtDNA absence prevented irradiated cells from sending factors to their culture media capable of inducing a response in non-irradiated cells. Yet, these cells were still able to respond to factors delivered to the media by irradiated cells lines.

The MELAS mutation A3243T in $tRNA^{Leu(UUR)}$ gene seemed to slightly modify the response to ICCM and its ICCM seemed to induce a different response when compared to ICCM from the wild type cell line (Cy143Bwt).

Our findings point towards an important influence of mitochondria in the IR response. Further investigations should be performed, in order to clarify the results of the present study, namely repetition of the experiments to allow higher statistical power. Additionally, the response of cells to both stimulus (direct IR and ICCM) needs to be better characterized, to account for differences that appear to exist between those two scenarios. This could help reveal one more piece of the puzzle which constitutes the intricate and fine-tuned adaptive mechanisms of organisms.

In a RT context, models that could account for the complexity of a biological system could make interesting additions to these inquiries.

References

References

References

Abdullaev, S. A., Anishchenko, S. E., & Gaziev, A. I. (2011). Mutant copies of mitochondrial DNA in tissues and plasma of mice subjected to X-ray irradiation. *Biophysics*, *55*(5), 840–847. https://doi.org/10.1134/S0006350910050283

Adam-Vizi, V., & Chinopoulos, C. (2006, December 1). Bioenergetics and the formation of mitochondrial reactive oxygen species. *Trends in Pharmacological Sciences*. Academic Press. https://doi.org/10.1016/j.tips.2006.10.005

Alberts, B., Johnson, A., Lewis, J., Raff, M., Roberts, K., & Walter, P. (2007). *Molecular Biology of the Cell*. *Molecular Biology of the Cell*. Garland Science. https://doi.org/10.1002/1521-3773(20010316)40:6<9823::AID-ANIE9823>3.3.CO;2-C

Alexander, P. (1957). *Atomic radiation and life*. Retrieved from https://books.google.pt/books?hl=en&lr=&id=Zf9NDAAAQBAJ&oi=fnd&pg=PP1&dq=excitation+or+ionization+of+materials+by+irradiation&ots=SVd0vNlbPj&sig=gcsYsH0a-qq7UXhnB1iHTReMpME&redir_esc=y#v=onepage&q=excitation or ionization of materials by irradiation&f=fal

Antico Arciuch, V. G., Elguero, M. E., Poderoso, J. J., & Carreras, M. C. (2012). Mitochondrial Regulation of Cell Cycle and Proliferation. *Antioxidants & Redox Signaling*, *16*(10), 1150–1180. https://doi.org/10.1089/ars.2011.4085

Arscott, W. T., Tandle, A. T., Zhao, S., Shabason, J. E., Gordon, I. K., Schlaff, C. D., … Camphausen, K. A. (2013). Ionizing Radiation and Glioblastoma Exosomes: Implications in Tumor Biology and Cell Migration. *Translational Oncology*, *6*(6), 638–IN6. https://doi.org/10.1593/tlo.13640

Atun, R., Jaffray, D. A., Barton, M. B., Bray, F., Baumann, M., Vikram, B., … Gospodarowicz, M. (2015). Expanding global access to radiotherapy. *The Lancet Oncology*. https://doi.org/10.1016/S1470-2045(15)00222-3

Azzam, E. I., Jay-Gerin, J. P., & Pain, D. (2012, December 31). Ionizing radiation-induced metabolic oxidative stress and prolonged cell injury. *Cancer Letters*. https://doi.org/10.1016/j.canlet.2011.12.012

Ballarini, F., Biaggi, M., Ottolenghi, A., & Sapora, O. (2002). Cellular communication and bystander effects: a critical review for modelling low-dose radiation action. *Mutation Research*, *501*(1–2), 1–12. https://doi.org/10.1016/S0027-5107(02)00010-6

Barber, G. N. (2011). Cytoplasmic DNA innate immune pathways. *Immunological Reviews*, *243*(1), 99–108. https://doi.org/10.1111/j.1600-065X.2011.01051.x

Barbour, J. A., & Turner, N. (2014, January 22). Mitochondrial stress signaling promotes cellular adaptations. *International Journal of Cell Biology*. Hindawi.

https://doi.org/10.1155/2014/156020

Barton, M. B., Jacob, S., Shafiq, J., Wong, K., Thompson, S. R., Hanna, T. P., & Delaney, G. P. (2014). Estimating the demand for radiotherapy from the evidence: A review of changes from 2003 to 2012. *Radiotherapy and Oncology*, *112*(1), 140–144. https://doi.org/10.1016/j.radonc.2014.03.024

Baverstock, K., & Belyakov, O. V. (2010). Some important questions connected with non-targeted effects. *Mutation Research - Fundamental and Molecular Mechanisms of Mutagenesis*, *687*(1–2), 84–88. https://doi.org/10.1016/j.mrfmmm.2010.01.002

Becquerel, H. (1896). Emission de Radiations Nouvelles par l'Uranium Metallique. *Compt Ren*, *122*(Received), 1086.

Bernier, J., Hall, E. J., & Giaccia, A. (2004). Timeline: Radiation oncology: a century of achievements. *Nature Reviews Cancer*, *4*(9), 737–747. https://doi.org/10.1038/nrc1451

Berridge, M. J., Bootman, M. D., & Roderick, H. L. (2003). Calcium: Calcium signalling: dynamics, homeostasis and remodelling. *Nature Reviews Molecular Cell Biology*, *4*(7), 517–529. https://doi.org/10.1038/nrm1155

Blyth, B. J., & Sykes, P. J. (2011). Radiation-induced bystander effects: what are they, and how relevant are they to human radiation exposures? *Radiation Research*, *176*(2), 139–157. https://doi.org/10.1667/RR2548.1

Boaventura, P., Pereira, D., Mendes, A., Batista, R., da Silva, A. F., Guimarães, I., … Soares, P. (2014). Mitochondrial D310 D-Loop instability and histological subtypes in radiation-induced cutaneous basal cell carcinomas. *Journal of Dermatological Science*, *73*(1), 31–39. https://doi.org/10.1016/j.jdermsci.2013.09.002

Boaventura, P., Pereira, D., Mendes, A., Teixeira-Gomes, J., Sobrinho-Simões, M., & Soares, P. (2014). Thyroid and parathyroid tumours in patients submitted to X-ray scalp epilation during the tinea capitis eradication campaign in the North of Portugal (1950???1963). *Virchows Archiv*, *465*(4), 445–452. https://doi.org/10.1007/s00428-014-1644-0

Bogenhagen, D. F. (2012). Mitochondrial DNA nucleoid structure. *Biochimica et Biophysica Acta - Gene Regulatory Mechanisms*. https://doi.org/10.1016/j.bbagrm.2011.11.005

Borras, J. M., Lievens, Y., Barton, M., Corral, J., Ferlay, J., Bray, F., & Grau, C. (2016). How many new cancer patients in Europe will require radiotherapy by 2025? An ESTRO-HERO analysis. *Radiotherapy and Oncology*, *119*(1), 5–11. https://doi.org/10.1016/j.radonc.2016.02.016

Branzei, D., & Foiani, M. (2008). Regulation of DNA repair throughout the cell cycle. *Nature Reviews Molecular Cell Biology*, *9*(4), 297–308. https://doi.org/10.1038/nrm2351

Brenner, D. J., & Ward, J. F. (1992). Constraints on Energy Deposition and Target Size of Multiply Damaged Sites Associated with DNA Double-strand Breaks. *International Journal of Radiation Biology*, *61*(6), 737–748.

https://doi.org/10.1080/09553009214551591

Burdak-Rothkamm, S., Short, S. C., Folkard, M., Rothkamm, K., & Prise, K. M. (2007). ATR-dependent radiation-induced gamma H2AX foci in bystander primary human astrocytes and glioma cells. *Oncogene*, *26*(7), 993–1002. https://doi.org/10.1038/sj.onc.1209863

Butterworth, K. T., McGarry, C. K., Trainor, C., O'Sullivan, J. M., Hounsell, A. R., & Prise, K. M. (2011). Out-of-field cell survival following exposure to intensity-modulated radiation fields. *International Journal of Radiation Oncology Biology Physics*, *79*(5), 1516–1522. https://doi.org/10.1016/j.ijrobp.2010.11.034

Butterworth, K. T., McMahon, S. J., Hounsell, A. R., O'Sullivan, J. M., & Prise, K. M. (2013). Bystander signalling: Exploring clinical relevance through new approaches and new models. *Clinical Oncology*, *25*(10), 586–592. https://doi.org/10.1016/j.clon.2013.06.005

C. Short, J. Kelly, C. R. Mayes, M., S. (2001). Low-dose hypersensitivity after fractionated low-dose irradiation in vitro. *International Journal of Radiation Biology*, *77*(6), 655–664. https://doi.org/10.1080/09553000110041326

Calì, B., Ceolin, S., Ceriani, F., Bortolozzi, M., Agnellini, A. H. R., Zorzi, V., … Mammano, F. (2015). Critical role of gap junction communication, calcium and nitric oxide signaling in bystander responses to focal photodynamic injury. *Oncotarget*. Retrieved from www.impactjournals.com/oncotarget

Canman, C. E., & Lim, D. S. (1998). The role of ATM in DNA damage responses and cancer. *Oncogene*, *17*(25), 3301–3308. https://doi.org/10.1038/sj.onc.1202577

Chan, D. C. (2006). Mitochondria: Dynamic Organelles in Disease, Aging, and Development. *Cell*, *125*(7), 1241–1252. https://doi.org/10.1016/j.cell.2006.06.010

Chandel, N. S., & Schumacker, P. T. (1999, July 9). Cells depleted of mitochondrial DNA (??0) yield insight into physiological mechanisms. *FEBS Letters*. https://doi.org/10.1016/S0014-5793(99)00783-8

Chen, S., Zhao, Y., Han, W., Zhao, G., Zhu, L., Wang, J., … Wu, L. (2008). Mitochondria-dependent signalling pathway are involved in the early process of radiation-induced bystander effects. *British Journal of Cancer*, *98*(11), 1839–44. https://doi.org/10.1038/sj.bjc.6604358

Chia, H. C., Chen, P. J., Lee, P. H., Cheng, A. L., Hsu, H. C., & Cheng, J. C. H. (2007). Radiation-induced hepatitis B virus reactivation in liver mediated by the bystander effect from irradiated endothelial cells. *Clinical Cancer Research*, *13*(3), 851–857. https://doi.org/10.1158/1078-0432.CCR-06-2459

Claridge Mackonis, E., Suchowerska, N., Zhang, M., Ebert, M., McKenzie, D. R., & Jackson, M. (2007). Cellular response to modulated radiation fields. *Physics in Medicine and Biology*, *52*(18), 5469–5482. https://doi.org/10.1088/0031-9155/52/18/001

Cloos, C. R., Daniels, D. H., Kalen, A., Matthews, K., Du, J., Goswami, P. C., & Cullen, J. J.

(2010). Mitochondrial DNA Depletion Induces Radioresistance by Suppressing G2 Checkpoint Activation in Human Pancreatic Cancer Cells. *Radiation Research*, *171*(5), 581–587. https://doi.org/10.1667/RR1395.1.Mitochondrial

Cribbs, J. T., & Strack, S. (2007). Reversible phosphorylation of Drp1 by cyclic AMP-dependent protein kinase and calcineurin regulates mitochondrial fission and cell death. *EMBO Reports*, *8*(10), 939–944. https://doi.org/10.1038/sj.embor.7401062

Curie, P., & Becquerel, H. (1901). *Action physiologique des rayons du radium* (Vol. 132).

D'Autréaux, B., & Toledano, M. B. (2007). ROS as signalling molecules: mechanisms that generate specificity in ROS homeostasis. *Nature Reviews Molecular Cell Biology*, *8*(10), 813–824. https://doi.org/10.1038/nrm2256

Desjardins, P., Frost, E., & Morais, R. (1985). Ethidium bromide-induced loss of mitochondrial DNA from primary chicken embryo fibroblasts. *Molecular and Cellular Biology*, *5*(5), 1163–9. https://doi.org/10.1128/MCB.5.5.1163.Updated

Desouky, O., Ding, N., & Zhou, G. (2015). Targeted and non-targeted effects of ionizing radiation. *Journal of Radiation Research and Applied Sciences*, *8*(2), 247–254. https://doi.org/10.1016/j.jrras.2015.03.003

DiMauro, S., & Hirano, M. (1993). *MELAS*. *GeneReviews(®)*. University of Washington, Seattle. Retrieved from http://www.ncbi.nlm.nih.gov/pubmed/20301411

Donthamsetty, S., Brahmbhatt, M., Pannu, V., Rida, P. C. G., Ramarathinam, S., Ogden, A., … Aneja, R. (2014). Mitochondrial genome regulates mitotic fidelity by maintaining centrosomal homeostasis. *Cell Cycle*, *13*(13), 2056–2063. https://doi.org/10.4161/cc.29061

Dunbar, D. R., Moonie, P. A., Jacobs, H. T., & Holt, I. J. (1995). Different cellular backgrounds confer a marked advantage to either mutant or wild-type mitochondrial genomes. *Proceedings of the National Academy of Sciences of the United States of America*, *92*(14), 6562–6. https://doi.org/10.1073/pnas.92.14.6562

Dunn, C. G., Campbell, W. L., Fram, H., & Hutchins, A. (1948). Biological and Photo-Chemical Effects of High Energy, Electrostatically Produced Roentgen Rays and Cathode Rays. *Journal of Applied Physics*, *19*(7), 605–616. https://doi.org/10.1063/1.1698179

Dutreix, J., Tubiana, M., & Pierquin, B. (1998). The hazy dawn of brachytherapy. *Radiotherapy and Oncology*, *49*(3), 223–232. https://doi.org/10.1016/S0167-8140(98)00137-6

El-Hattab, A. W., Adesina, A. M., Jones, J., & Scaglia, F. (2015). MELAS syndrome: Clinical manifestations, pathogenesis, and treatment options. *Molecular Genetics and Metabolism*. https://doi.org/10.1016/j.ymgme.2015.06.004

Ermakov, A. V, Konkova, M. S., Kostyuk, S. V, Izevskaya, V. L., Baranova, A., & Veiko, N. N. (2013, March 6). Oxidized extracellular DNA as a stress signal in human cells. *Oxidative Medicine and Cellular Longevity*. Hindawi. https://doi.org/10.1155/2013/649747

References

Feinendegen, L. E. (2003). Relative implications of protective responses versus damage induction at low dose and low-dose-rate exposures, using the microdose approach. *Radiation Protection Dosimetry*, *104*(4), 337–46. https://doi.org/10.1093/oxfordjournals.rpd.a006197

Ferlay, J., Soerjomataram, I., Dikshit, R., Eser, S., Mathers, C., Rebelo, M., … Bray, F. (2015). Cancer incidence and mortality worldwide: Sources, methods and major patterns in GLOBOCAN 2012. *International Journal of Cancer*, *136*(5), E359–E386. https://doi.org/10.1002/ijc.29210

Flierl, A., Reichmann, H., & Seibel, P. (1997). Pathophysiology of the MELAS 3243 transition mutation. *Journal of Biological Chemistry*, *272*(43), 27189–27196. https://doi.org/10.1074/jbc.272.43.27189

Foray, N. (2012, July). Claudius Regaud (1870-1940) : Relecture des archives d'un pionnier de la radiobiologie et de la radioth??rapie. *Cancer/Radiotherapie*. https://doi.org/10.1016/j.canrad.2012.05.006

Frayn, K. N. (2003). The glucose–fatty acid cycle: a physiological perspective. *Biochemical Society Transactions*, *31*(6). Retrieved from http://www.biochemsoctrans.org/content/31/6/1115

Freya, T. G., & Mannellab, C. A. (2000, July). The internal structure of mitochondria. *Trends in Biochemical Sciences*. https://doi.org/10.1016/S0968-0004(00)01609-1

Gatenby, R. A., & Gillies, R. J. (2004). Why do cancers have high aerobic glycolysis? *Nature Reviews Cancer*, *4*(11), 891–899. https://doi.org/10.1038/nrc1478

Ghandhi, S. A., Yaghoubian, B., & Amundson, S. A. (2008). Global gene expression analyses of bystander and alpha particle irradiated normal human lung fibroblasts: Synchronous and differential responses. *BMC Medical Genomics*, *1*(1), 63. https://doi.org/10.1186/1755-8794-1-63

Gorbunov, N. V., Pogue-Geile, K. L., Epperly, M. W., Bigbee, W. L., Draviam, R., Day, B. W., … Greenberger, J. S. (2000). Activation of the Nitric Oxide Synthase 2 Pathway in the Response of Bone Marrow Stromal Cells to High Doses of Ionizing Radiation. *Radiation Research*, *154*, 73–86. https://doi.org/10.2307/3580019

Grubbé, E. H. (1949). *X-ray treatment; its origin, birth and early history.* Saint Paul: Bruce Pub. Co.

Hailey, D. W., Rambold, A. S., Satpute-Krishnan, P., Mitra, K., Sougrat, R., Kim, P. K., & Lippincott-Schwartz, J. (2010). Mitochondria Supply Membranes for Autophagosome Biogenesis during Starvation. *Cell*, *141*(4), 656–667. https://doi.org/10.1016/j.cell.2010.04.009

Hall, E., Higgins, F., Giaccia, A. J., & Willson, S. (2012). *Radiobiology for the radiologist* (Seventh Ed). Lippincott Williams & Wilcons.

References

Hansen, M. F. (2002). Genetic and molecular aspects of osteosarcoma. *Journal of Musculoskeletal Neuronal Interactions*. Retrieved from http://webcache.googleusercontent.com/search?q=cache:vFJz942oL5gJ:www.ismni.org/jmni/pdf/10/19Hansen.pdf+&cd=1&hl=en&ct=clnk&gl=pt&client=firefox-b-ab

Hazkani-Covo, E., Zeller, R. M., & Martin, W. (2010, February 12). Molecular poltergeists: Mitochondrial DNA copies (numts) in sequenced nuclear genomes. (H. S. Malik, Ed.), *PLoS Genetics*. https://doi.org/10.1371/journal.pgen.1000834

Hefferin, M. L., & Tomkinson, A. E. (2005, June 8). Mechanism of DNA double-strand break repair by non-homologous end joining. *DNA Repair*. https://doi.org/10.1016/j.dnarep.2004.12.005

Heise, N., Palme, D., Misovic, M., Koka, S., Rudner, J., Lang, F., … Henke, G. (2010). Non-selective cation channel-mediated Ca2+-entry and activation of Ca2+/calmodulin-dependent kinase II contribute to G2/M cell cycle arrest and survival of irradiated leukemia cells. *Cellular Physiology and Biochemistry*, *26*(4–5), 597–608. https://doi.org/10.1159/000322327

Herok, R., Konopacka, M., Polanska, J., Swierniak, A., Rogolinski, J., Jaksik, R., … Rzeszowska-Wolny, J. (2010). Bystander Effects Induced by Medium From Irradiated Cells: Similar Transcriptome Responses in Irradiated and Bystander K562 Cells. *International Journal of Radiation Oncology Biology Physics*, *77*(1), 244–252. https://doi.org/10.1016/j.ijrobp.2009.11.033

Higby, C., Khafaga, Y., Al-Shabanah, M., Mousa, A., Ilyas, M., Nazer, G., & Khalil, E. M. (2016). Volumetric-modulated arc therapy (VMAT) versus 3D-conformal radiation therapy in supra-diaphragmatic Hodgkin's Lymphoma with mediastinal involvement: A dosimetric comparison. *Journal of the Egyptian National Cancer Institute*, *28*(3), 163–168. https://doi.org/10.1016/j.jnci.2016.04.007

Hu, Y., & Zhu, T. C. (2011). Backscatter correction factor for megavoltage photon beam. *Medical Physics*, *38*(10), 5563–5568. https://doi.org/10.1118/1.3633903

ICRP. (2003). 2003 Annual Report International Commission on Radiological Protection. Retrieved from http://www.icrp.org/docs/2003_Ann_Rep_52_249_04a.pdf

ICRU. (2010). Report 83. *Journal of the ICRU*, *10*(1), 1–106. https://doi.org/10.1093/jicru/10.1.Report83

James, A. M., Wei, Y. H., Pang, C. Y., & Murphy, M. P. (1996). Altered mitochondrial function in fibroblasts containing MELAS or MERRF mitochondrial DNA mutations. *The Biochemical Journal*, *318 (Pt 2*(2), 401–7. https://doi.org/10.1042/bj3180401

Jasin, M., & Rothstein, R. (2013, November 1). Repair of strand breaks by homologous recombination. *Cold Spring Harbor Perspectives in Biology*. Cold Spring Harbor Laboratory Press. https://doi.org/10.1101/cshperspect.a012740

Jeggo, P. A., & Löbrich, M. (2007). DNA double-strand breaks: their cellular and clinical impact? *Oncogene*, *26*(56), 7717–7719. https://doi.org/10.1038/sj.onc.1210868

Kadhim, M., Salomaa, S., Wright, E., Hildebrandt, G., Belyakov, O. V., Prise, K. M., & Little, M. P. (2013). Non-targeted effects of ionising radiation--implications for low dose risk. *Mutation Research*, *752*(2), 84–98. https://doi.org/10.1016/j.mrrev.2012.12.001

Karkos, P. D., Waldron, M., & Johnson, I. J. (2004, February 1). The MELAS syndrome. Review of the literature: The role of the otologist. *Clinical Otolaryngology and Allied Sciences*. Blackwell Science Ltd. https://doi.org/10.1111/j.1365-2273.2004.00769.x

Kevin Leach, J., Black, S. M., Schmidt-Ullrich, R. K., & Mikkelsen, R. B. (2002). Activation of constitutive nitric-oxide synthase activity is an early signaling event induced by ionizing radiation. *Journal of Biological Chemistry*, *277*(18), 15400–15406. https://doi.org/10.1074/jbc.M110309200

Khan, M. A., Van Dyk, J., Yeung, I. W. ., & Hill, R. P. (2003). Partial volume rat lung irradiation; Assessment of early DNA damage in different lung regions and effect of radical scavengers. *Radiotherapy and Oncology*, *66*(1), 95–102. https://doi.org/10.1016/S0167-8140(02)00325-0

Kidane, D., Chae, W. J., Czochor, J., Eckert, K. A., Glazer, P. M., Bothwell, A. L. M., & Sweasy, J. B. (2014). Interplay between DNA repair and inflammation, and the link to cancer. *Critical Reviews in Biochemistry and Molecular Biology*, *49*(2), 116–139. https://doi.org/10.3109/10409238.2013.875514

Klammer, H., Mladenov, E., Li, F., & Iliakis, G. (2015). Bystander effects as manifestation of intercellular communication of DNA damage and of the cellular oxidative status. *Cancer Letters*. https://doi.org/10.1016/j.canlet.2013.12.017

Kobashigawa, S., Suzuki, K., & Yamashita, S. (2011). Ionizing radiation accelerates Drp1-dependent mitochondrial fission, which involves delayed mitochondrial reactive oxygen species production in normal human fibroblast-like cells. *Biochemical and Biophysical Research Communications*, *414*(4), 795–800. https://doi.org/10.1016/j.bbrc.2011.10.006

Koch, G. L. (1990). The endoplasmic reticulum and calcium storage. *BioEssays : News and Reviews in Molecular, Cellular and Developmental Biology*, *12*(11), 527–31. https://doi.org/10.1002/bies.950121105

Kroemer, G. (2003). Mitochondrial control of apoptosis: An introduction. *Biochemical and Biophysical Research Communications*, *304*(3), 433–435. https://doi.org/10.1016/S0006-291X(03)00614-4

Kroemer, G., Galluzzi, L., & Brenner, C. (2007). Mitochondrial Membrane Permeabilization in Cell Death. *Physiological Reviews*, *87*(1), 99–163. https://doi.org/10.1152/physrev.00013.2006

Kryston, T. B., Georgiev, A. B., Pissis, P., & Georgakilas, A. G. (2011, June 3). Role of

oxidative stress and DNA damage in human carcinogenesis. *Mutation Research - Fundamental and Molecular Mechanisms of Mutagenesis*. https://doi.org/10.1016/j.mrfmmm.2010.12.016

Kulkarni, R., Marples, B., Balasubramaniam, M., Thomas, R. A., & Tucker, J. D. (2010). Mitochondrial gene expression changes in normal and mitochondrial mutant cells after exposure to ionizing radiation. *Radiation Research*, *173*(5), 635–644. https://doi.org/10.1667/RR1737.1

Kumar Jella, K., Rani, S., O'Driscoll, L., McClean, B., Byrne, H. J., & Lyng, F. M. (2014). Exosomes Are Involved in Mediating Radiation Induced Bystander Signaling in Human Keratinocyte Cells. *Radiation Research*, *181*(2), 138–145. https://doi.org/10.1667/RR13337.1

Landberg, T., Chavaudra, J., Dobbs, J., Gerard, J.-P., Hanks, G., Horiot, J.-C., … Svensson, H. (1999). Report 62. *Journal of the International Commission on Radiation Units and Measurements*, *os32*(1), NP-NP. https://doi.org/10.1093/jicru/os32.1.Report62

Lane, N., & Martin, W. (2010). The energetics of genome complexity. *Nature*, *467*(7318), 929–934. https://doi.org/10.1038/nature09486

Lehnert, B. E., & Goodwin, E. H. (1997). Extracellular Factor(s) following Exposure to alpha Particles Can Cause Sister Chromatid Exchanges in Normal Human Cells. *Cancer Research*, *57*(11), 2164–2171. Retrieved from http://cancerres.aacrjournals.org/content/57/11/2164?ijkey=f0406403980009d71389aa6348ea3e577023458b&keytype2=tf_ipsecsha

Liberti, M. V, & Locasale, J. W. (2016). The Warburg Effect: How Does it Benefit Cancer Cells? *Trends in Biochemical Sciences*. https://doi.org/10.1016/j.tibs.2015.12.001

Little, J. B. (2006). Cellular radiation effects and the bystander response. *Mutation Research/Fundamental and Molecular Mechanisms of Mutagenesis*, *597*(1–2), 113–118. https://doi.org/10.1016/j.mrfmmm.2005.12.001

Little, M. P. (2010). Do non-targeted effects increase or decrease low dose risk in relation to the linear-non-threshold (LNT) model? *Mutation Research/Fundamental and Molecular Mechanisms of Mutagenesis*, *687*(1–2), 17–27. https://doi.org/10.1016/j.mrfmmm.2010.01.008

Lodish, H., Berk, A., & Zipursky, S. (2000). Electron Transport and Oxidative Phosphorylation. In *Molecular Cell Biology* (4th Editio). New York: W. H. Freeman. Retrieved from https://www.ncbi.nlm.nih.gov/books/NBK21528/

Lomax, M. E., Folkes, L. K., & O'Neill, P. (2013a). Biological Consequences of Radiation-induced DNA Damage: Relevance to Radiotherapy. *Clinical Oncology*, *25*(10), 578–585. https://doi.org/10.1016/j.clon.2013.06.007

Lomax, M. E., Folkes, L. K., & O'Neill, P. (2013b). Biological Consequences of Radiation-

induced DNA Damage: Relevance to Radiotherapy. *Clinical Oncology*, *25*(10), 578–585. https://doi.org/10.1016/j.clon.2013.06.007

Lorimore, S. A., Coates, P. J., & Wright, E. G. (2003). Radiation-induced genomic instability and bystander effects: inter-related nontargeted effects of exposure to ionizing radiation. *Oncogene*, *22*(45), 7058–7069. https://doi.org/10.1038/sj.onc.1207044

Luetke, A., Meyers, P. A., Lewis, I., & Juergens, H. (2014). Osteosarcoma treatment – Where do we stand? A state of the art review. *Cancer Treatment Reviews*, *40*(4), 523–532. https://doi.org/10.1016/j.ctrv.2013.11.006

Lyng, F. M., Seymour, C. B., & Mothersill, C. (2000). Production of a signal by irradiated cells which leads to a response in unirradiated cells characteristic of initiation of apoptosis. *British Journal of Cancer*, *83*(9), 1223–1230. https://doi.org/10.1054/bjoc.2000.1433

Lyng, F. M., Seymour, C. B., & Mothersill, C. (2002). Initiation of apoptosis in cells exposed to medium from the progeny of irradiated cells: a possible mechanism for bystander-induced genomic instability? *Radiation Research*, *157*(4), 365–70. https://doi.org/10.1667/0033-7587(2002)157[0365:IOAICE]2.0.CO;2

Mambo, E., Gao, X., Cohen, Y., Guo, Z., Talalay, P., & Sidransky, D. (2003). Electrophile and oxidant damage of mitochondrial DNA leading to rapid evolution of homoplasmic mutations. *Proceedings of the National Academy of Sciences*, *100*(4), 1838–1843. https://doi.org/10.1073/pnas.0437910100

Mancuso, M., Pasquali, E., Leonardi, S., Tanori, M., Rebessi, S., Di Majo, V., … Saran, A. (2008). Oncogenic bystander radiation effects in Patched heterozygous mouse cerebellum. *Proceedings of the National Academy of Sciences*, *105*(34), 12445–12450. https://doi.org/10.1073/pnas.0804186105

Marchetti, P., Susin, S. A., Decaudin, D., Gamen, S., Castedo, M., Hirsch, T., … Kroemer, G. (1996). Apoptosis-associated derangement of mitochondrial function in cells lacking mitochondrial DNA. *Cancer Research*, *56*(9), 2033–8. Retrieved from http://www.ncbi.nlm.nih.gov/pubmed/8616847

Martínez-Reyes, I., Diebold, L. P., Kong, H., Schieber, M., Huang, H., Hensley, C. T., … Chandel, N. S. (2016). TCA Cycle and Mitochondrial Membrane Potential Are Necessary for Diverse Biological Functions. *Molecular Cell*, *61*(2), 199–209. https://doi.org/10.1016/j.molcel.2015.12.002

Máximo, V., Lima, J., Soares, P., & Sobrinho-Simões, M. (2009). Mitochondria and cancer. *Virchows Archiv*, *454*(5), 481–495. https://doi.org/10.1007/s00428-009-0766-2

McBride, H. M., Neuspiel, M., & Wasiak, S. (2006). Mitochondria: More Than Just a Powerhouse. *Current Biology*, *16*(14), R551–R560. https://doi.org/10.1016/j.cub.2006.06.054

Mikkelsen, R. B., & Wardman, P. (2003). Biological chemistry of reactive oxygen and nitrogen

and radiation-induced signal transduction mechanisms. *Oncogene*, *22*(37), 5734–5754. https://doi.org/10.1038/sj.onc.1206663

Mineri, R., Pavelka, N., Fernandez-Vizarra, E., Ricciardi-Castagnoli, P., Zeviani, M., & Tiranti, V. (2009). How Do Human Cells React to the Absence of Mitochondrial DNA? *PLoS ONE*, *4*(5), e5713. https://doi.org/10.1371/journal.pone.0005713

Mizushima, N., Levine, B., Cuervo, A. M., & Klionsky, D. J. (2008). Autophagy fights disease through cellular self-digestion. *Nature*, *451*(7182), 1069–1075. https://doi.org/10.1038/nature06639

Mohseny, A. B., Machado, I., Cai, Y., Schaefer, K.-L., Serra, M., Hogendoorn, P. C. W., … Cleton-Jansen, A.-M. (2011). Functional characterization of osteosarcoma cell lines provides representative models to study the human disease. *Laboratory Investigation*, *91*(8), 1195–1205. https://doi.org/10.1038/labinvest.2011.72

Mole, R. H. (1953). Whole Body Irradiation—Radiobiology or Medicine? *The British Journal of Radiology*, *26*(305), 234–241. https://doi.org/10.1259/0007-1285-26-305-234

Morgan, W. F. (2012). Non-targeted and Delayed Effects of Exposure to Ionizing Radiation: I. Radiation-Induced Genomic Instability and Bystander Effects In Vitro. *Radiation Research*, *178*(2), AV223-AV236. https://doi.org/10.1667/RRAV19.1

Morgan, W. F., & Bair, W. J. (2013). Issues in Low Dose Radiation Biology: The Controversy Continues. A Perspective. *Radiation Research*, *179*(5), 501–510. https://doi.org/10.1667/RR3306.1

Morgan, W. F., & Sowa, M. B. (2015). Non-targeted effects induced by ionizing radiation: Mechanisms and potential impact on radiation induced health effects. *Cancer Letters*, *356*(1), 17–21. https://doi.org/10.1016/j.canlet.2013.09.009

Mothersill, C., & Seymour, C. (1997). Medium from irradiated human epithelial cells but not human fibroblasts reduces the clonogenic survival of unirradiated cells. *International Journal of Radiation Biology*, *71*(4), 421–7. https://doi.org/10.1080/095530097144030

Mothersill, C., & Seymour, C. (2001). Radiation-Induced Bystander Effects: Past History and Future Directions. *Source: Radiation Research*, *155*(6), 759–767. https://doi.org/10.1667/0033-7587(2001)155[0759:RIBEPH]2.0.CO;2

Mothersill, C., & Seymour, C. (2006). Radiation-Induced Bystander and other Non-Targeted Effects: Novel Intervention Points in Cancer Therapy? *Current Cancer Drug Targets*, *6*(5), 447–454. https://doi.org/10.2174/156800906777723976

Mothersill, C., & Seymour, C. (2013). Uncomfortable issues in radiation protection posed by low-dose radiobiology. *Radiation and Environmental Biophysics*, *52*(3), 293–298. https://doi.org/10.1007/s00411-013-0472-y

Mothersill, C., Seymour, C. B., & Joiner, M. C. (2002). Relationship between radiation-induced low-dose hypersensitivity and the bystander effect. *Radiation Research*, *157*(5), 526–32.

https://doi.org/10.1667/0033-7587(2002)157[0526:RBRILD]2.0.CO;2

Moudy, A. M., Handran, S. D., Goldberg, M. P., Ruffin, N., Karl, I., Kranz-Eble, P., … Rothman, S. M. (1995). Abnormal calcium homeostasis and mitochondrial polarization in a human encephalomyopathy. *Proceedings of the National Academy of Sciences of the United States of America*, *92*(3), 729–33. https://doi.org/10.1073/pnas.92.3.729

Mutschelknaus, L., Peters, C., Winkler, K., Yentrapalli, R., Heider, T., Atkinson, M. J., & Moertl, S. (2016). Exosomes derived from squamous head and neck cancer promote cell survival after ionizing radiation. *PLoS ONE*, *11*(3). https://doi.org/10.1371/journal.pone.0152213

Nagar, S., Smith, L. E., & Morgan, W. F. (2003). Characterization of a Novel Epigenetic Effect of Ionizing Radiation : The Death-Inducing Effect Characterization of a Novel Epigenetic Effect of Ionizing Radiation : The Death-Inducing Effect 1. *Cancer Research*, *63*(2), 324–328. Retrieved from http://cancerres.aacrjournals.org/content/63/2/324.long

Nagasawa, H., & Little, J. B. (1992). Induction of sister chromatid exchanges by extremely low doses of alpha-particles. *Cancer Research*, *52*(22), 6394–6. Retrieved from http://www.ncbi.nlm.nih.gov/pubmed/1423287

Najafi, M., Fardid, R., Hadadi, G., & Fardid, M. (2014). The mechanisms of radiation-induced bystander effect. *Journal of Biomedical Physics & Engineering*, *4*(4), 163–172. Retrieved from www.jbpe.org

Narayanan, P. K., Goodwin, E. H., & Lehnert, B. E. (1997). α Particles Initiate Biological Production of Superoxide Anions and Hydrogen Peroxide in Human Cells. *Cancer Research*, *57*(18). Retrieved from http://cancerres.aacrjournals.org/content/57/18/3963.long

Narayanan, P. K., LaRue, K. E., Goodwin, E. H., & Lehnert, B. E. (1999). Alpha particles induce the production of interleukin-8 by human cells. *Radiation Research*, *152*(1), 57–63. https://doi.org/10.2307/3580049

National Council on Radiation Protection and Measurements. (2001). Report No. 136 - Evaluation of the Linear-Nonthreshold Dose-Response Model for Ionizing Radiation. *Health Physics*, 287. Retrieved from https://www.ncrppublications.org/Reports/136

Nedelcu, T., Kubista, B., Koller, A., Sulzbacher, I., Mosberger, I., Arrich, F., … Toma, C. D. (2008). Livin and Bcl-2 expression in high-grade osteosarcoma. *Journal of Cancer Research and Clinical Oncology*, *134*(2), 237–244. https://doi.org/10.1007/s00432-007-0276-z

Nelson, I., Hanna, M. G., Wood, N. W., & Harding, A. E. (1997). Depletion of mitochondrial DNA by ddC in untransformed human cell lines. *Somatic Cell and Molecular Genetics*, *23*(4), 287–90. Retrieved from http://www.ncbi.nlm.nih.gov/pubmed/9542530

Newhauser, W. D., & Durante, M. (2011). Assessing the risk of second malignancies after modern radiotherapy. *Nature Reviews Cancer*, *11*(6), 438–448.

https://doi.org/10.1038/nrc3069

Nicholson, D. W., & Thornberry, N. A. (1997). Caspases: killer proteases. *Trends in Biochemical Sciences*, *22*(8), 299–306. Retrieved from http://www.ncbi.nlm.nih.gov/pubmed/9270303

Nickel, A., Kohlhaas, M., & Maack, C. (2014). Mitochondrial reactive oxygen species production and elimination. *Journal of Molecular and Cellular Cardiology*, *73*, 26–33. https://doi.org/10.1016/j.yjmcc.2014.03.011

Nugent, S. M. E., Mothersill, C. E., Seymour, C., McClean, B., Lyng, F. M., & Murphy, J. E. J. (2007). Increased Mitochondrial Mass in Cells with Functionally Compromised Mitochondria after Exposure to both Direct γ Radiation and Bystander Factors. *Radiation Research*, *168*(1), 134–142. https://doi.org/10.1667/RR0769.1

Nunes, J. B., Peixoto, J., Soares, P., Maximo, V., Carvalho, S., Pinho, S. S., … Lima, J. (2015). OXPHOS dysfunction regulates integrin- 1 modifications and enhances cell motility and migration. *Human Molecular Genetics*, *24*(7), 1977–1990. https://doi.org/10.1093/hmg/ddu612

Nunnari, J., & Suomalainen, A. (2012). Mitochondria: In Sickness and in Health. *Cell*, *148*(6), 1145–1159. https://doi.org/10.1016/j.cell.2012.02.035

Nuta, O., & Darroudi, F. (2008). The impact of the bystander effect on the low-dose hypersensitivity phenomenon. *Radiation and Environmental Biophysics*, *47*(2), 265–274. https://doi.org/10.1007/s00411-007-0145-9

Oth Ersill, C. M., & Seym R, C. O. (1997). M edium from irradiated hum an epithelial cells but not hum an ®broblasts reduces the clonogenic survival of unirradiated cells. *Int. J. Radiat. Biol Int J Radiat Biol Downloaded*, *7125*(4), 421–42714.

Palikaras, K., & Tavernarakis, N. (2014). Mitochondrial homeostasis: The interplay between mitophagy and mitochondrial biogenesis. *Experimental Gerontology*, *56*, 182–188. https://doi.org/10.1016/j.exger.2014.01.021

Pawlik, T. M., & Keyomarsi, K. (2004). Role of cell cycle in mediating sensitivity to radiotherapy. *International Journal of Radiation Oncology*Biology*Physics*, *59*(4), 928–942. https://doi.org/10.1016/j.ijrobp.2004.03.005

Peinado, H., Alečković, M., Lavotshkin, S., Matei, I., Costa-Silva, B., Moreno-Bueno, G., … Lyden, D. (2012). Melanoma exosomes educate bone marrow progenitor cells toward a pro-metastatic phenotype through MET. *Nature Medicine*, *18*(6), 883–891. https://doi.org/10.1038/nm.2753

Penn, A. M. W., Lee, J. W. K., Thuillier, P., Wagner, M., Maclure, K. M., Menard, M. R., … Kennaway, N. G. (1992). MELAS syndrome with mitochondrial tRNA Leu[UUR] mutation: Correlation of clinical state, nerve conduction, and muscle 31P magnetic resonance spectroscopy during treatment with nicotinamide and riboflavin. *Neurology*, *42*(11), 2147–

2147. https://doi.org/10.1212/WNL.42.11.2147

Perez, Carlos; Bradly, L. (2008). *Principles and Practice of Radiation Oncology*. (L. W. & Wilkins, Ed.) (Sixth Edit). Philadelphia.

Prise, K. M., & O'Sullivan, J. M. (2009). Radiation-induced bystander signalling in cancer therapy. *Nature Reviews Cancer*, *9*(5), 351–360. https://doi.org/10.1038/nrc2603

Rajendran, S., Harrison, S. H., Thomas, R. A., & Tucker, J. D. (2011). The Role of Mitochondria in the Radiation-Induced Bystander Effect in Human Lymphoblastoid Cells. *Radiation Research*, *175*(2), 159–171. https://doi.org/10.1667/RR2296.1

Raymond, A. K., & Jaffe, N. (2009). Osteosarcoma Multidisciplinary Approach to the Management from the Pathologist's Perspective. In *Cancer Treatment and Research* (Vol. 152, pp. 63–84). Springer, Boston, MA. https://doi.org/10.1007/978-1-4419-0284-9_4

Reed, J. C. (2000). Mechanisms of Apoptosis. *The American Journal of Pathology*, *157*(5), 1415–1430. https://doi.org/http://dx.doi.org/10.1016/S0002-9440(10)64779-7

Ricchetti, M., Tekaia, F., & Dujon, B. (2004). Continued Colonization of the Human Genome by Mitochondrial DNA. *PLoS Biology*, *2*(9), e273. https://doi.org/10.1371/journal.pbio.0020273

Robberson, D. L., Clayton, D. A., & Morrow, J. F. (1974). Cleavage of replicating forms of mitochondrial DNA by EcoRI endonuclease. *Proceedings of the National Academy of Sciences of the United States of America*, *71*(11), 4447–4451. Retrieved from http://www.ncbi.nlm.nih.gov/pubmed/4612520

Rogounovitch, T., Saenko, V., & Yamashita, S. (2004). Mitochondrial DNA and human thyroid diseases. *Endocrine Journal*, *51*(3), 265–77. https://doi.org/10.1507/endocrj.51.265

Rosenberg, I. (2008). Radiation Oncology Physics: A Handbook for Teachers and Students. *British Journal of Cancer*, *98*(5), 1020–1020. https://doi.org/10.1038/sj.bjc.6604224

Russell, R. C., Yuan, H.-X., & Guan, K.-L. (2014). Autophagy regulation by nutrient signaling. *Cell Research*, *24*(1), 42–57. https://doi.org/10.1038/cr.2013.166

Saffran, H. A., Pare, J. M., Corcoran, J. A., Weller, S. K., & Smiley, J. R. (2007). Herpes simplex virus eliminates host mitochondrial DNA. *EMBO Reports*, *8*(2), 188–93. https://doi.org/10.1038/sj.embor.7400878

Santo-Domingo, J., & Demaurex, N. (2010). Calcium uptake mechanisms of mitochondria. *Biochimica et Biophysica Acta (BBA) - Bioenergetics*, *1797*(6–7), 907–912. https://doi.org/10.1016/j.bbabio.2010.01.005

Saris, N.-E. L., & Carafoli, E. (2005). A historical review of cellular calcium handling, with emphasis on mitochondria. *Biochemistry (Moscow)*, *70*(2), 187–194. https://doi.org/10.1007/s10541-005-0100-9

Shao, C., Lyng, F. M., Folkard, M., & Prise, K. M. (2006). Calcium Fluxes Modulate the

Radiation-Induced Bystander Responses in Targeted Glioma and Fibroblast Cells. *Radiation Research*, *166*(3), 479–487. https://doi.org/10.1667/RR3600.1

Shao, C., Stewart, V., Folkard, M., Michael, B. D., & Prise, K. M. (2003). Nitric oxide-mediated signaling in the bystander response of individually targeted glioma cells. *Cancer Research*, *63*(23), 8437–42. Retrieved from http://www.ncbi.nlm.nih.gov/pubmed/14679007

Sherer, T. B., Trimmer, P. A., Parks, J. K., & Tuttle, J. B. (2000). Mitochondrial DNA-depleted neuroblastoma (Rho°) cells exhibit altered calcium signaling. *Biochimica et Biophysica Acta (BBA) - Molecular Cell Research*, *1496*(2–3), 341–355. https://doi.org/10.1016/S0167-4889(00)00027-6

Shiloh, Y. (2001, February). ATM and ATR: Networking cellular responses to DNA damage. *Current Opinion in Genetics and Development*. https://doi.org/10.1016/S0959-437X(00)00159-3

Shiloh, Y. (2006). The ATM-mediated DNA-damage response: taking shape. *Trends in Biochemical Sciences*, *31*(7), 402–410. https://doi.org/10.1016/j.tibs.2006.05.004

Shonai, T., Adachi, M., Sakata, K., Takekawa, M., Endo, T., Imai, K., & Hareyama, M. (2002). MEK/ERK pathway protects ionizing radiation-induced loss of mitochondrial membrane potential and cell death in lymphocytic leukemia cells. *Cell Death and Differentiation*, *9*(9), 963–971. https://doi.org/10.1038/sj.cdd.4401050

Siva, S., MacManus, M. P., Martin, R. F., & Martin, O. A. (2015). Abscopal effects of radiation therapy: a clinical review for the radiobiologist. *Cancer Letters*, *356*(1), 82–90. https://doi.org/10.1016/j.canlet.2013.09.018

Soubannier, V., & McBride, H. M. (2009). Positioning mitochondrial plasticity within cellular signaling cascades. *Biochimica et Biophysica Acta (BBA) - Molecular Cell Research*, *1793*(1), 154–170. https://doi.org/10.1016/j.bbamcr.2008.07.008

Spitkovsky, D. (2004). Activity of complex III of the mitochondrial electron transport chain is essential for early heart muscle cell differentiation. *The FASEB Journal*, *18*(11), 1300–1302. https://doi.org/10.1096/fj.03-0520fje

Strijdom, H., Chamane, N., & Lochner, A. (2009). Nitric oxide in the cardiovascular system: a simple molecule with complex actions. *Cardiovascular Journal of Africa*, *20*(5), 303–10. Retrieved from http://www.ncbi.nlm.nih.gov/pubmed/19907806

Stuurman, N., & Vale, R. D. (2016). Impact of New Camera Technologies on Discoveries in Cell Biology. *The Biological Bulletin*, *231*(1), 5–13. https://doi.org/10.1086/689587

Sykes, P. J. (2016). The ups and downs of low dose ionising radiobiology research. *Australasian Physical & Engineering Sciences in Medicine*, *39*(4), 807–811. https://doi.org/10.1007/s13246-016-0486-2

Taanman, J.-W. (1999). The mitochondrial genome: structure, transcription, translation and

replication. *Biochimica et Biophysica Acta (BBA) - Bioenergetics*, *1410*(2), 103–123. https://doi.org/10.1016/S0005-2728(98)00161-3

Tait, S. W. G., & Green, D. R. (2012). Mitochondria and cell signalling. *Journal of Cell Science*, *125*(4), 807–815. https://doi.org/10.1242/jcs.099234

Taneja, N., Tjalkens, R., Philbert, M. A., & Rehemtulla, A. (2001). Irradiation of mitochondria initiates apoptosis in a cell free system. *Oncogene*, *19*(2), 167–177. https://doi.org/10.1038/sj.onc.1204054

Tartier, L., Gilchrist, S., Burdak-Rothkamm, S., Folkard, M., & Prise, K. M. (2007). Cytoplasmic Irradiation Induces Mitochondrial-Dependent 53BP1 Protein Relocalization in Irradiated and Bystander Cells. *Cancer Research*, *67*(12), 5872–5879. https://doi.org/10.1158/0008-5472.CAN-07-0188

Torre, L. A., Bray, F., Siegel, R. L., Ferlay, J., Lortet-tieulent, J., & Jemal, A. (2015). Global Cancer Statistics, 2012. *CA: A Cancer Journal of Clinicians.*, *65*(2), 87–108. https://doi.org/10.3322/caac.21262.

Upton, A. C. (1992). The first hundred years of radiation research: What have they taught us? *Environmental Research*, *59*(1), 36–48. https://doi.org/10.1016/S0013-9351(05)80224-5

van Gisbergen, M. W., Voets, A. M., Biemans, R., Hoffmann, R. F., Drittij-Reijnders, M.-J., Haenen, G. R. M. M., … Lambin, P. (2017). Distinct radiation responses after in vitro mtDNA depletion are potentially related to oxidative stress. *PLOS ONE*, *12*(8), e0182508. https://doi.org/10.1371/journal.pone.0182508

Vander Heiden, M., Cantley, L., & Thompson, C. (2009). Understanding the Warburg effect: The metabolic Requiremetns of cell proliferation. *Science*, *324*(5930), 1029–1033. https://doi.org/10.1126/science.1160809.Understanding

Vander Heiden, M. G., Cantley, L. C., & Thompson, C. B. (2009). Understanding the Warburg effect: the metabolic requirements of cell proliferation. *Science (New York, N.Y.)*, *324*(5930), 1029–33. https://doi.org/10.1126/science.1160809

Vermes, I., Haanen, C., Steffens-Nakken, H., & Reutellingsperger, C. (1995). A novel assay for apoptosis Flow cytometric detection of phosphatidylserine expression on early apoptotic cells using fluorescein labelled Annexin V. *Journal of Immunological Methods*, *184*(1), 39–51. https://doi.org/10.1016/0022-1759(95)00072-I

Vlassov, A. V., Magdaleno, S., Setterquist, R., & Conrad, R. (2012). Exosomes: Current knowledge of their composition, biological functions, and diagnostic and therapeutic potentials. *Biochimica et Biophysica Acta (BBA) - General Subjects*, *1820*(7), 940–948. https://doi.org/10.1016/j.bbagen.2012.03.017

Vogin, G., & Foray, N. (2013). The law of Bergonié and Tribondeau: A nice formula for a first approximation. *International Journal of Radiation Biology*, *89*(1), 2–8. https://doi.org/10.3109/09553002.2012.717732

Wallace, D. C., & Chalkia, D. (2013). Mitochondrial DNA Genetics and the Heteroplasmy Conundrum in Evolution and Disease. *Cold Spring Harbor Perspectives in Biology*, *5*(11), a021220–a021220. https://doi.org/10.1101/cshperspect.a021220

Whelan, S. P., & Zuckerbraun, B. S. (2013). Mitochondrial Signaling: Forwards, Backwards, and In Between. *Oxidative Medicine and Cellular Longevity*, *2013*, 1–10. https://doi.org/10.1155/2013/351613

Wilkins, H. M., Carl, S. M., & Swerdlow, R. H. (2014). Cytoplasmic hybrid (cybrid) cell lines as a practical model for mitochondriopathies. *Redox Biology*, *2*(1), 619–631. https://doi.org/10.1016/j.redox.2014.03.006

Xue, F., & Hua, Z. (2017). Signaling pathway of mitochondrial stress. *Frontiers in Laboratory Medicine*, *1*(1), 40–42. https://doi.org/10.1016/j.flm.2017.02.009

Yakovlev, V. A. (2015). Role of nitric oxide in the radiation-induced bystander effect. *Redox Biology*, *6*, 396–400. https://doi.org/10.1016/j.redox.2015.08.018

Yamamori, T., Sasagawa, T., Ichii, O., Hiyoshi, M., Bo, T., Yasui, H., … Inanami, O. (2016). Analysis of the mechanism of radiation-induced upregulation of mitochondrial abundance in mouse fibroblasts. *Journal of Radiation Research*, 1–10. https://doi.org/10.1093/jrr/rrw113

Yang, H., Asaad, N., & Held, K. D. (2005). Medium-mediated intercellular communication is involved in bystander responses of X-ray-irradiated normal human fibroblasts. *Oncogene*, *24*(12), 2096–2103. https://doi.org/10.1038/sj.onc.1208439

Yoshida, K., Yamazaki, H., Ozeki, S., Inoue, T., Yoshioka, Y., & Inoue, T. (2000). Role of mitochondrial DNA in radiation exposure. *Radiation Medicine*, *18*(2), 87–91. Retrieved from http://www.ncbi.nlm.nih.gov/pubmed/10888040

Yoshida, T., Goto, S., Kawakatsu, M., Urata, Y., & Li, T. (2012). Mitochondrial dysfunction, a probable cause of persistent oxidative stress after exposure to ionizing radiation. *Free Radical Research*, *46*(2), 147–153. https://doi.org/10.3109/10715762.2011.645207

Appendixes

Appendixes

Appendixes

Supplementary tables

Supplementary Table 1 – Radiobiology Rs and their brief decription. First described to try to explain the differences in the response to irradiation

5Rs of Radiobiology	Brief description
REPAIR	Differences in tumour and normal cells repair after irradiation
REPOPULATION	The repopulation by tumour cells observed after irradiation
REDISTRIBUTION	The redistribution of the cells into the cell cycle phases
REOXYGENATION	The reoxygenation of the tumour cells after irradiation
RADIOSENSIBILITY	Intrinsic radiosensibility of the cells/ndividual irradiated

Supplementary Table 2 – The names of the respiratory chain complexes found on mitochondria

Oxidative Phosphorylation complexes
NADH Dehydrogenase – Complex I
Succinate ubiquinone oxidoreductase – Complex II
Ubiquinol cytochrome c oxidoreductase – Complex III
Cytochorme C Oxidoreductase – Complex IV
ATP Synthase

Image J example

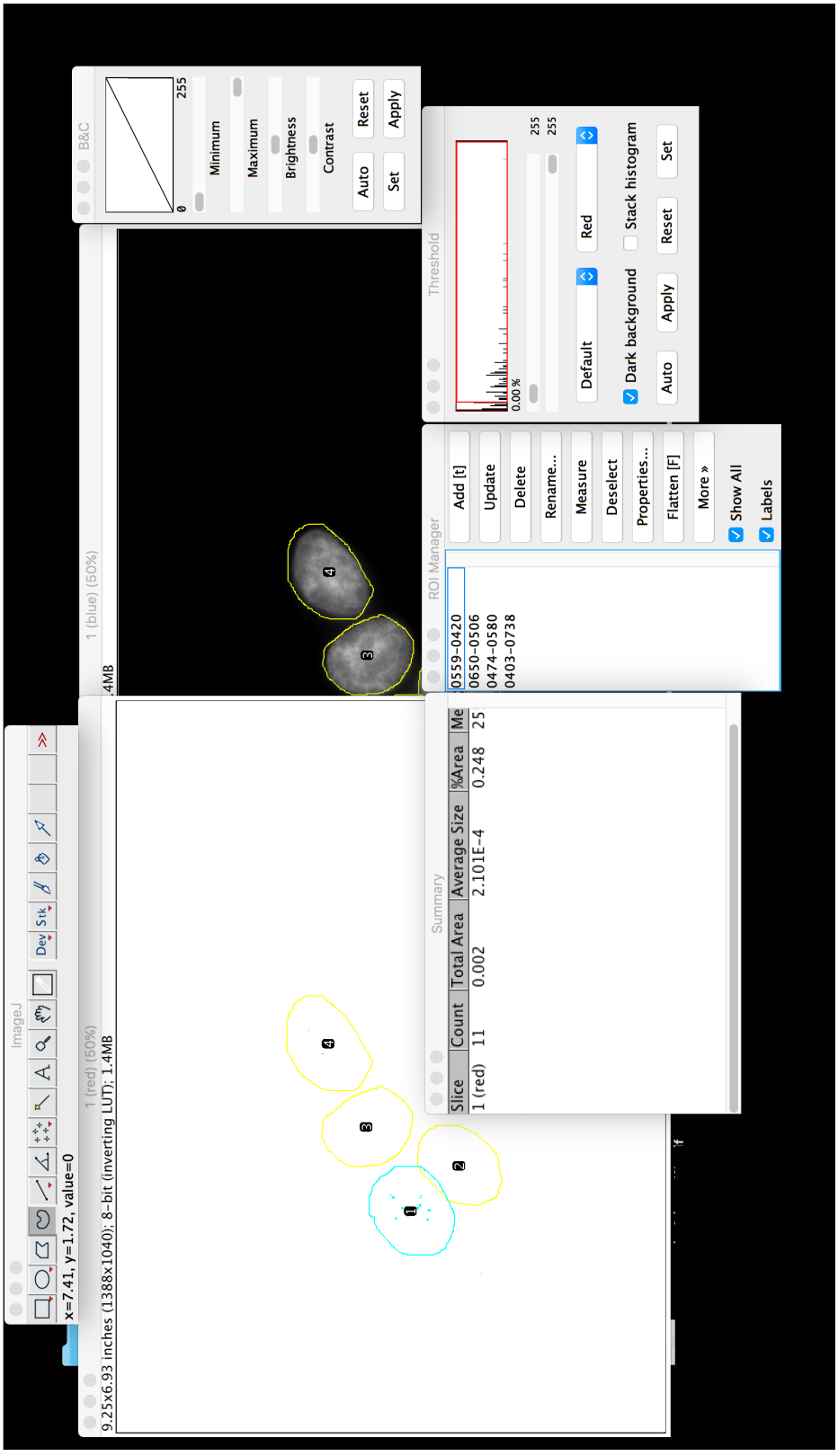

Supplementary figure 1 – Example of the method for counting yH2AX foci using Image J sofware

Supplementary results

DHE titrations

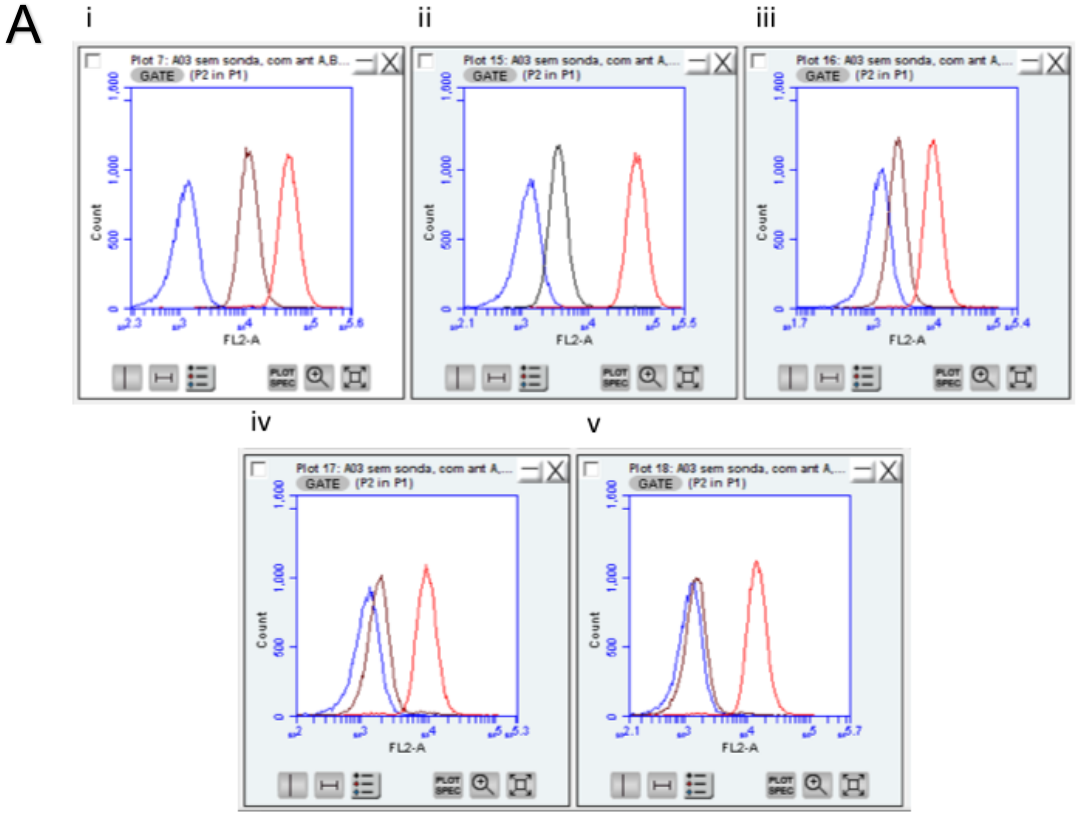

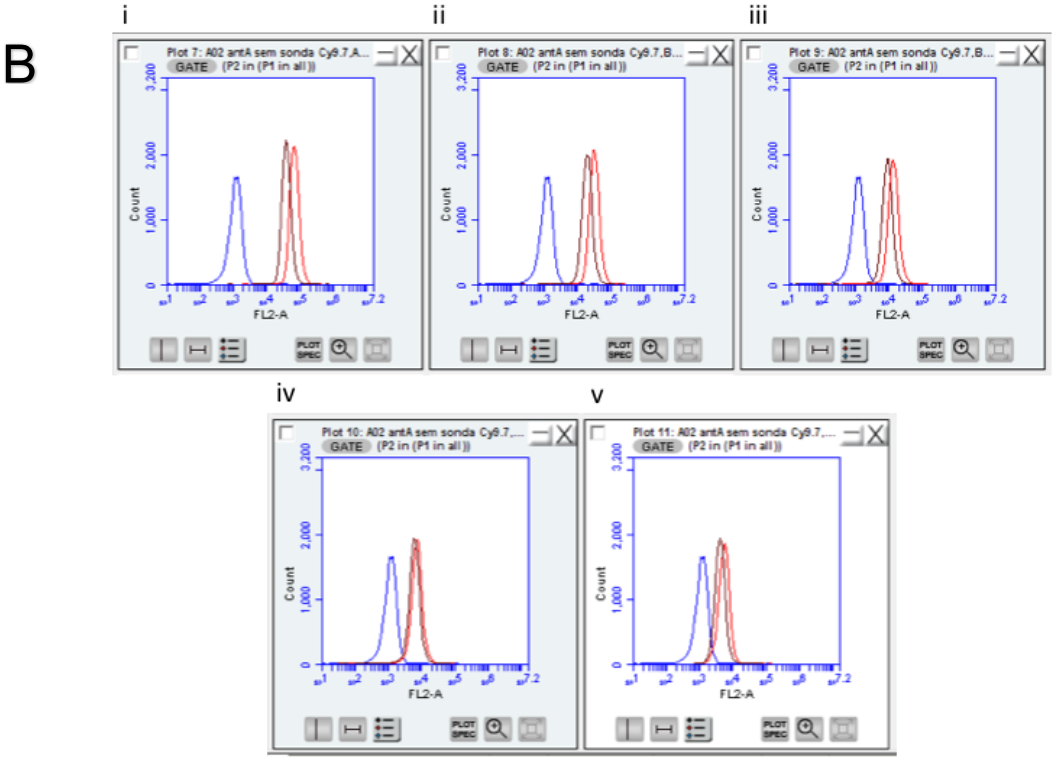

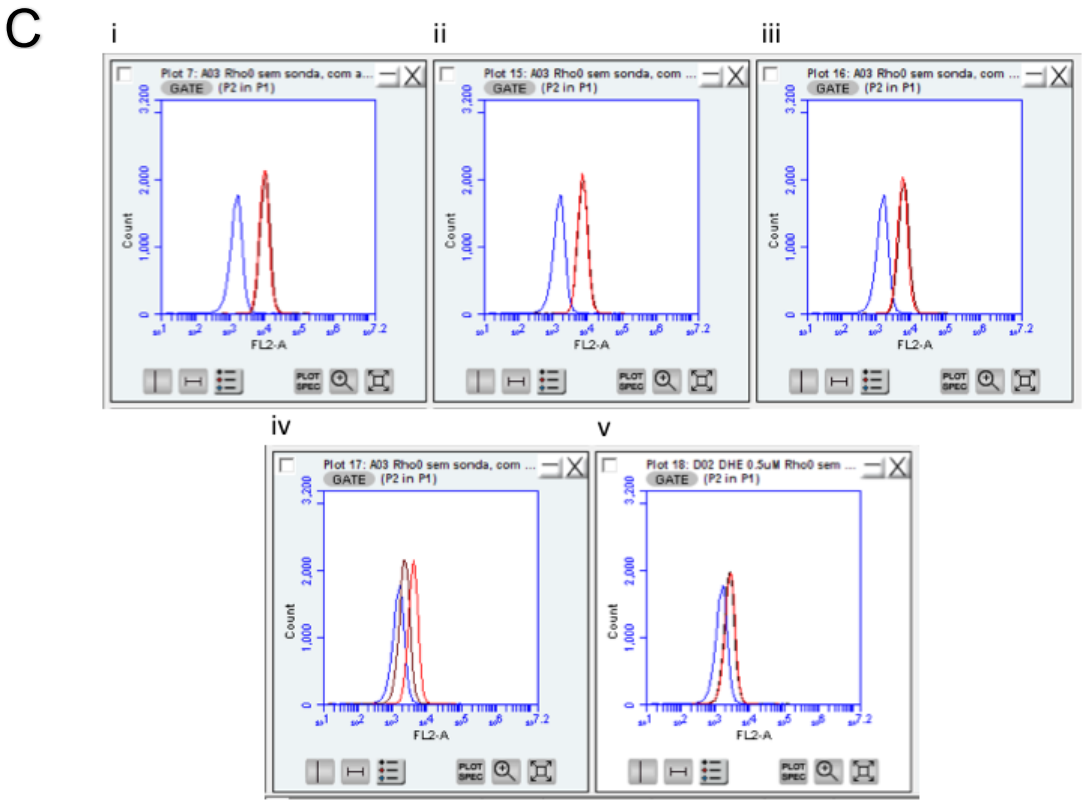

Supplementary figure 2 – Titration of DHE concentrations. A – Cy143Bwt; B – Cy143Bwt; C – 143B-ρ0. i) – 10μM; ii) 5 μM; iii) 2.5 μM; iv) 1 μM; v) 0.5 μM.

Copy rights authorizations

ELSEVIER LICENSE
TERMS AND CONDITIONS

Sep 12, 2017

This Agreement between Miss. Silvana Miranda ("You") and Elsevier ("Elsevier") consists of your license details and the terms and conditions provided by Elsevier and Copyright Clearance Center.

License Number	4186621309788
License date	Sep 12, 2017
Licensed Content Publisher	Elsevier
Licensed Content Publication	Radiotherapy and Oncology
Licensed Content Title	The hazy dawn of brachytherapy
Licensed Content Author	Jean Dutreix,Maurice Tubiana,Bernard Pierquin
Licensed Content Date	Dec 1, 1998
Licensed Content Volume	49
Licensed Content Issue	3
Licensed Content Pages	10
Start Page	223
End Page	232
Type of Use	reuse in a thesis/dissertation
Portion	figures/tables/illustrations
Number of figures/tables /illustrations	1
Format	both print and electronic
Are you the author of this Elsevier article?	No
Will you be translating?	No
Original figure numbers	Figure 1
Title of your thesis/dissertation	The role of mitochondria in the non-targeted effect of ionizing radiation
Expected completion date	Dec 2017
Estimated size (number of pages)	100
Requestor Location	Miss. Silvana Miranda Rua da Barroca 466 1º Matosinhos, Porto 4455-587 Portugal Attn: Miss. Silvana Miranda
Publisher Tax ID	GB 494 6272 12
Total	0.00 USD

Supplementary figure 3 – Permission for Figure 2.

ELSEVIER LICENSE
TERMS AND CONDITIONS

Sep 12, 2017

This Agreement between Miss. Silvana Miranda ("You") and Elsevier ("Elsevier") consists of your license details and the terms and conditions provided by Elsevier and Copyright Clearance Center.

License Number	4186790956431
License date	Sep 12, 2017
Licensed Content Publisher	Elsevier
Licensed Content Publication	The Lancet Oncology
Licensed Content Title	Expanding global access to radiotherapy
Licensed Content Author	Rifat Atun,David A Jaffray,Michael B Barton,Freddie Bray,Michael Baumann,Bhadrasain Vikram,Timothy P Hanna,Felicia M Knaul,Yolande Lievens,Tracey Y M Lui,Michael Milosevic,Brian O'Sullivan,Danielle L Rodin,Eduardo Rosenblatt,Jacob Van Dyk et al.
Licensed Content Date	Sep 1, 2015
Licensed Content Volume	16
Licensed Content Issue	10
Licensed Content Pages	34
Start Page	1153
End Page	1186
Type of Use	reuse in a thesis/dissertation
Portion	figures/tables/illustrations
Number of figures/tables /illustrations	1
Format	both print and electronic
Are you the author of this Elsevier article?	No
Will you be translating?	No
Original figure numbers	Figure 1
Title of your thesis/dissertation	The role of mitochondria in the non-targeted effect of ionizing radiation
Expected completion date	Dec 2017
Estimated size (number of pages)	100
Requestor Location	Miss. Silvana Miranda Rua da Barroca 466 1º Matosinhos, Porto 4455-587 Portugal Attn: Miss. Silvana Miranda

Supplementary figure 4 – Permission for Figure 3.

OXFORD UNIVERSITY PRESS LICENSE
TERMS AND CONDITIONS

Sep 12, 2017

This Agreement between Miss. Silvana Miranda ("You") and Oxford University Press ("Oxford University Press") consists of your license details and the terms and conditions provided by Oxford University Press and Copyright Clearance Center.

License Number	4186800234191
License date	Sep 12, 2017
Licensed content publisher	Oxford University Press
Licensed content publication	Journal of the ICRU
Licensed content title	1. Introduction
Licensed content author	
Licensed content date	Jun 24, 2016
Type of Use	Thesis/Dissertation
Institution name	
Title of your work	The role of mitochondria in the non-targeted effect of ionizing radiation
Publisher of your work	n/a
Expected publication date	Dec 2017
Permissions cost	0.00 USD
Value added tax	0.00 USD
Total	0.00 USD
Requestor Location	Miss. Silvana Miranda Rua da Barroca 466 1º Matosinhos, Porto 4455-587 Portugal Attn: Miss. Silvana Miranda
Publisher Tax ID	GB125506730
Billing Type	Invoice
Billing Address	Miss. Silvana Miranda Rua da Barroca 466 1º Matosinhos, Portugal 4455-587 Attn: Miss. Silvana Miranda
Total	0.00 USD
Terms and Conditions	

STANDARD TERMS AND CONDITIONS FOR REPRODUCTION OF MATERIAL FROM AN OXFORD UNIVERSITY PRESS JOURNAL

Supplementary figure 5 – permission for Figure 5

OXFORD UNIVERSITY PRESS LICENSE
TERMS AND CONDITIONS

Sep 12, 2017

This Agreement between Miss. Silvana Miranda ("You") and Oxford University Press ("Oxford University Press") consists of your license details and the terms and conditions provided by Oxford University Press and Copyright Clearance Center.

License Number	4186800412867
License date	Sep 12, 2017
Licensed content publisher	Oxford University Press
Licensed content publication	Journal of the ICRU
Licensed content title	Report 62
Licensed content author	Landberg, T.; Chavaudra, J.
Licensed content date	Apr 27, 2016
Type of Use	Thesis/Dissertation
Institution name	
Title of your work	The role of mitochondria in the non-targeted effect of ionizing radiation
Publisher of your work	n/a
Expected publication date	Dec 2017
Permissions cost	0.00 USD
Value added tax	0.00 USD
Total	0.00 USD
Requestor Location	Miss. Silvana Miranda Rua da Barroca 466 1º Matosinhos, Porto 4455-587 Portugal Attn: Miss. Silvana Miranda
Publisher Tax ID	GB125506730
Billing Type	Invoice
Billing Address	Miss. Silvana Miranda Rua da Barroca 466 1º Matosinhos, Portugal 4455-587 Attn: Miss. Silvana Miranda
Total	0.00 USD
Terms and Conditions	

STANDARD TERMS AND CONDITIONS FOR REPRODUCTION OF MATERIAL FROM AN OXFORD UNIVERSITY PRESS JOURNAL

Supplementary figure 6 – Permission for Figure 6